Co-funded by the

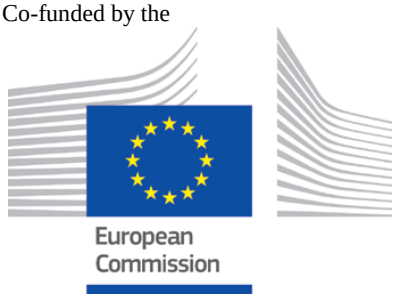

CEBAMA

➢ (Contract Number: 662147)

Deliverable n°D2.03

WP2: State of the Art Report (initial)

Editor: B. GRAMBOW

Date of issue of this report: 02.05.2015

Report number of pages: 103

Start date of project: 01/06/2015 Duration: 48 Months

Project co-funded by the European Commission under the Euratom Research and Training Programme on Nuclear Energy within the Horizon 2020 Framework Programme		
Dissemination Level		
PU	Public	x
PP	Restricted to other programme participants (including the Commission Services)	
RE	Restricted to a group specified by the partners of the CEBAMA project	
CO	Confidential, only for partners of the CEBAMA project	

Tabel of contents

Structural uptake and retention of safety relevant radionuclides in cementitious systems (ULOUGH, JUELICH)

Steve Lange[1)], Guido Deissmann[1)], David Read[2)], Matthew Isaacs[1,2)], Mónica Felipe-Sotelo[2)], Dirk Bosbach[1)]

Affiliation: [1)] Institute of Energy and Climate Research: Nuclear Waste Management and Reactor Safety (IEK-6), Forschungszentrum Jülich GmbH, 52425 Jülich, Germany

[2)] Loughborough University, Epinal Way, Loughborough Leicestershire, UK, LE11 3TU

email: s.lange@fz-juelich.de, g.deissmann@fz-juelich.de, d.read@lboro.ac.uk, M.Isaacs@lboro.ac.uk, d.bosbach@fz-juelich.de

Introduction

Cementitious materials are widely used in radioactive waste management, for example in the solidification of low and intermediate level wastes, or as construction and barrier material in underground and surface repositories. The retention of radionuclides in cement based materials is controlled by radionuclide solubility phenomena, diffusion, and adsorption or incorporation of radionuclides into solids including the formation of solid solutions. Within the frame of CEBAMA WP2, we are studying the uptake of selected long-lived fission and decay products (Ra, Tc, Mo, I, Se, Cl) in cementitious materials and the radionuclide distribution between and within various cement phases on the micro scale, using advanced micro analytical and spectroscopic tools. The objective of these investigations is to enhance mechanistic understanding of the uptake and retention of safety relevant radionuclides in cementitious systems and to assess the relevance of chemical alteration processes, such as carbonation or the solid speciation of radionuclides in aged concrete. In this context, a bottom-up approach is being pursued using synthesised cement phases (model phases) on the one hand and hardened cement pastes with different compositions on the other.

The following sections provide a brief overview on the state of the art with respect to (i) the uptake of the selected radionuclides by cementitious materials and (ii) the synthesis of selected phases present in hydrated cements, namely CSH, ettringite, monosulfate and hydrotalcite. The phases of interest to be studied for this work were selected as they comprise the major phases of a CEM I cement, excluding portlandite, as no significant interaction of the latter and the radionuclides of interest is expected. Calcium silicate hydrate phases, and calcium aluminate (AFm, AFt) phases provide favourable sites for the sorption of radionuclides (Evans, 2008) and as they collectively comprise ~60% of the bulk cementitious material a good understanding of their interaction with radionuclides is vital when building a safety case for a geological disposal facility.

Interaction of the selected radionuclides with cementitious materials

Radium

Radium is a daughter nuclide of ^{238}U, the most abundant uranium isotope, as result of the 4n+2 decay chain. Therefore, with respect to the direct disposal of spent nuclear fuels, ^{226}Ra can be a main contributor to dose in the long term (i.e. after more than

100,000 years) due to the high concentrations of uranium present within the waste inventories (Swedish Nuclear Fuel and Waste Management Co, 2010). In order to demonstrate the long-term safety of a final repository, the retention and release mechanisms of safety relevant radionuclides need to be understood. Studies regarding the uptake of radium (^{226}Ra) by hardened cement paste and solubility studies started in the early 90s. Bayliss et al. (1989) reported that the concentration of radium in cement equilibrated water was up to 10^{-7} mol dm^{-3}. Experimental results indicated that the concentration of Ra remained constant after adding 1 mol dm^{-3} sulphate to the cement-equilibrated solution, in contrast to the thermodynamically predicted solubility limit of $7 \cdot 10^{-8}$ mol dm^{-3} calculated for $RaSO_4$. This phenomenon was explained by the lack of sufficient nucleation sites. The same work by Bayliss et al. (1989) also studied the uptake of radium by a sulphate resistant Portland cement (SRPC) and an ordinary Portland cement (OPC) blended with blast furnace slag (BFS) at a ratio of 1:3 (OPC:BFS). The distribution ratios ranged from 55 $cm^3 \cdot g^{-1}$ to 530 $mL \cdot g^{-1}$ for SRPC and from 900 $cm^3 \cdot g^{-1}$ to 1800 $cm^3 \cdot g^{-1}$ for the OPC/BFS using a time scale of 118 to 160 days for sorption. The higher sorption by OPC/BFS was explained by the formation of $RaSO_4$. Later, Holland and Lee (1992) published their work on the sorption of radium to SRPC/BFS (1:9), SRPC/PFA (1:9), HAC, OPC, SRPC and tobermorite, a CSH surrogate. All experiments ran for 28 days. The distribution ratios or partition coefficients (R_d) obtained in this sorption experiments were highest for the high alumina cement (HAC) ($R_d = 4 \times 10^3$ $dm^3 \cdot kg^{-1}$) and lowest for SRPC ($R_d = 3.7 \times 10^1$ $dm^3 \cdot kg^{-1}$). The sorption of radium to OPC was found to be 5×10^1 $dm^3 \cdot kg^{-1}$. Although these results show that the addition of BFS to SRPC increased the retention of Ra, PFA caused even greater enhancement onto SRPC. The sorption of radium onto tobermorite was studied in different solutions; simulated pore water (pH 13.1), saturated lime (pH 12.6) and SRPC equilibrated water (pH 12.4). The highest distribution ratio of 4.5×10^5 dm^3 kg^{-1} was obtained for saturated lime.

Tits et al. (2006) investigated the interaction of radium with CSH and hydrated cement pastes (HCP). In this study, calcium silicate hydrates with different calcium to silicon ratios were synthesised to represent the composition of the CSH phases expected at different stages of the evolution of cement pastes. The sorption experiments were carried out in batches with water to solid ratio of 50 using 10^{-8} mol dm^{-3} Ra. It was demonstrated that the uptake of radium by CSH is fast and reaches completion within one week of continuously shaking. The speed of uptake showed no differences regarding the calcium to silicon ratio, but the distribution ratios decreased with increasing calcium content of the CSH phases, indicating competitive interaction between calcium and radium. The maximum distribution ratio was found for CSH with Ca:Si = 0.96, approx. 4×10^3 $dm^3 \cdot kg^{-1}$, and decreased to approx. 1.5×10^2 $dm^3 \cdot kg^{-1}$ for CSH with Ca:Si = 1.6. Studies on the liquid to solid ratio used in the batch experiments showed that almost no influence on the distribution of radium was observed between L:S = 50 and L:S = 1000. Tits et al. (2006) also investigated the desorption of radium from the above mentioned phases and observed that radium sorption onto CSH phases is linear and reversible. It was stated that the sorption of radium can be described in terms of a cation exchange model. Furthermore, it was found that, in the case of HCP, the sorption of radium is much slower with fresh HCP, reaching an equilibrium R_d of 400 $dm^3 \cdot kg^{-1}$ after approx. 60 days compared to the very fast uptake of degraded HCP, which reaches equilibrium within one day at a R_d of 140 $dm^3 \cdot kg^{-1}$.

Technetium

Tallent et al. (1987) studied the influence of grout composition on the leachability of

technetium containing cementitious matrices. They demonstrated that leachability decreases with increasing mix ratio, grout fluid density and blast furnace slag content. Later, Gilliam et al. (1990) showed that the effective technetium diffusivity of cement based waste forms decreases by five orders of magnitude on the addition of BFS. A further decrease of the leach coefficient in water and brine (5.2×10^{-16} cm^2 s^{-1}) was achieved by addition of sodium sulphide, as reported by Brodda and Xu (1989) who concluded that technetium seemed to be chemically fixed. The apparent coefficient obtained by leaching a waste containing specimen with Q brine and water was found to be 5.2×10^{-16} cm^2 s^{-1} (Brodda and Xu, 1989).

Thermodynamic calculations carried out by Smith and Walton (1993) suggested that the leachability of the highly mobile anionic species of technetate decreased as a result of oxidation by the sulphur present in BFS and formation of Tc_2S_7. The addition of a limited amount of BFS leads to a significant improvement in the performance, but higher BFS loading only increases the performance marginally. Smith and Walton (1993) concluded by means of technetium speciation modelling studies, that the diffusion of oxygen into concrete would have the opposite effect on technetium immobilisation; the Tc_2S_7 would be oxidised to the highly mobile pertechnetate anion, which can diffuse from the waste form into the environment (Smith and Walton, 1993). Allen et al. (1997) conducted extended X-ray absorption fine structure (EXAFS) studies on the effect of sodium and iron sulphides on technetium speciation. In contrast to the predictions of Smith and Walton (1993), the studies by Allen et al. (1997) demonstrated that the addition of BFS to a cement formulation leads to an in situ partial reduction of pertechnetate anions present, whereas the addition of Na_2S or FeS results in complete reduction to the less mobile Tc(IV). Allen et al. (1997) concluded that sulphide containing species are the active reducing agents in BFS. These findings were in agreement with previous work done by Gilliam et al. (1990). Furthermore, Allen et al. (1997a;b) measured Tc-S and Tc-Tc distances in the presence of Na_2S or FeS, observing bond distances in agreement with an oligomeric structure similar to that found in TcS_2.

Layered double hydroxides (LDHs) have also been suggested as potential host phases for technetium in its anionic form. Berner (1999) suggested that binding and/or incorporation of TcO_4^- into the alumina ferric mono/tri-sulphate (AFm/AFt) phases of cement systems could be also expected, by analogy to other oxo-anions such as SO_4^{2-} or MoO_4^{2-} (and possibly also SeO_3^{2-}). Thus, several minerals are known to incorporate technetium, for example fougerite (green rust) and potassium metal sulphides. A good overview of these potential host phases is given by Luksic et al. (2015).

Molybdenum

The interaction of molybdenum with cementitious materials has received relatively little attention. The immobilization of molybdenum in ordinary Portland cement and single model phases was studied by Kindness et al. (1994), conducting experiments on the uptake of Mo onto OPC, slag cements, C_3S and AFt. The results show that, disregarding starting and cement formulation, the final concentration of molybdenum in these batch experiments ranged between 50 and 80 ppm. Kindness et al. (1994) pointed out that the solubility of molybdenum appears to be controlled by a precipitation mechanism. Further investigations on single model phases demonstrated that two solubility limiting phases could be identified; $CaMoO_4$ isostructural with powellite and a Mo-AFm phase. Solubility studies of powellite demonstrated incongruent dissolution ([Mo] = 2.44×10^{-4} mol dm^{-3}, [Ca] = 1.87×10^{-4} mol dm^{-3}). MoO_4^--AFt could not be synthesized, rather powellite precipitated. Zhang (2000) studied the incorporation of

molybdate by hydrocalumite and ettringite using lower concentrations of molybdate. It was demonstrated that a solid solution of molybdate and hydrocalumite could be synthesized and that molybdate formed a mixed AFm phase with OH^- (Zhang, 2000).

Chlorine

The extent of the interaction of chlorine ions with cement matrices has been shown to depend on several parameters including: (i) the associated cation (Na^+, Ca^{2+}, or Mg^{2+}); (ii) the cement and mineral admixtures; (iii) the ratio of the water to cement, (iv) the curing period and (v) the amount of sulphate in the system (Ogard et al., 1988). Chlorine can react with unhydrated aluminate phases to form new compounds, most commonly Friedel's salt (Birnin-Yauri and Glasser, 1998), which comprises part of the AFm (alumina-ferric oxide mono-) phase in cement. Bulk composition appears to be the most important parameter affecting the chloride binding capacity of cement. The C_3A content determines the amount of the AFm phase produced, whereas silicate phases, such as C_3S and C_2S, determines the amount of calcium silicate hydrogel (CSH) formed upon hydration. The amount of sulphate in the anhydrous cement will determine the composition of the AFm phase, as well as the quantity of AFt phase (Birnin-Yauri and Glasser, 1998).

Several studies have investigated the binding of chloride ions to the CSH phase (Beaudoin et al., 1990; Yu and Kirkpatrick, 2001); they identify four states of chloride: (i) 'free', (ii) surface adsorbed ('chemisorbed'), (iii) interlayer and (iv) lattice-bound. The total chloride chemisorbed is dependent on the H/S and C/S ratios as well as on the surface area. It has been proposed that most of the chloride ions are chemisorbed on the hydrated C_3S phase. Beaudoin et al. (1990) suggested that the chemisorbed and interlayer species may be removed by leaching, whereas lattice-substituted chlorides cannot. Diffusion of ^{36}Cl through Nirex Reference Vault Backfill (NRVB, a cementitious backfill material) was investigated by van Es et al. (2015), reporting significant retardation ^{36}Cl in NRVB. However, the addition of brines to the solution in contact with the cement, approaching seawater salinity, resulted in breakthrough curves similar to those obtained for a conservative tracer (tritiated water, HTO). Autoradiographic and elemental mapping by EDX (energy-dispersive X-ray spectroscopy) suggested that the ^{36}Cl becomes bound to partially hydrated glassy, sulphate-bearing calcium silicate clinker particles. Research by Yu and Kirkpatrick (2001) using ^{35}Cl-NMR relaxation methods (nuclear magnetic resonance) on cement hydrate suspensions indicated that the majority of the chloride adsorbed on the surface of matrix phases, such as calcium hydroxide and jennite ($Ca_9Si_6O_{18}(OH)_6 \cdot 8H_2O$), are in a solid solution environment in rapid exchange with free chloride ions in the pore solution. It was shown that jennite has a limited number of binding sites; however, the number of bound chloride ions exceeds this. This excess is thought to be due primarily to the formation of alkaline metal chloride complexes or ion pairs such as calcium chloride (Yu and Kirkpatrick, 2001).

Iodine

Iodine can be captured in some crystalline cement phases including ettringite and calcium monosulphate, where the IO_3^- or I^- can substitute for OH^-, SO_4^{2-} or CO_3^{2-} (Tanabe et al., 2010). An important aspect of iodine behaviour under repository conditions is its redox chemistry and the differences in mobility for IO_3^- or I^-. Thus, Mattigod et al. (2001) observed a reduction of the leachability of iodine in a cement containing steel fibres. A decrease in the mobility of the iodine was suggest to be due to the reduction of IO_3^- to I^-. In a cementitious repository environment iodine is expected to exist as I^- (Atkins and Glasser, 1992).

A number of studies have been carried out investigating the immobilisation of I^- in cementitious materials using a range of experimental approaches: (i) through-diffusion (Atkinson and Nickerson, 1984; Sarott et al., 1992; Chida and Sugiyama, 2009; Felipe-Sotelo et al., 2014) and (ii) out-diffusion (Mattigod et al., 2001). The rate of diffusion of I^- correlates strongly with the water to cement ratio of the paste and an increase from 0.2 to 0.7 can raise the rate of diffusion by 3 orders of magnitude (Atkinson and Nickerson, 1984). Whilst changes in porosity of the cements at high solid to liquid ratios may account for some of the impact on diffusivity, the authors suggested that other parameters, such as changes in constrictivity could also contribute to the observed differences (Atkinson and Nickerson, 1984).

Iodide sorption onto cement has been shown to increase with increasing Ca:Si ratios in CSH gels in spite of an increased competition from OH^- at sorption sites, suggesting I^- is sorbed electrostatically (Glasser et al., 1989; Pointeau et al., 2008). Accordingly, AFt, which behaves similarly to high Ca:Si ratio CSH, has been shown to remove comparably more I^- from solutions than AFm (Aimoz et al., 2012).

Selenium

A reduction in the mobility of selenium within a cement matrix can occur by means of three mechanisms, namely: precipitation, incorporation and adsorption. Some authors, for example Séby et al. (1998), suggested that precipitation as selenites will play an insignificant role under repository conditions and that only very strongly reducing conditions would be capable of causing the precipitation of Se^0 or selenides, leading to a substantial decrease in selenium mobility. Consequently, relatively few studies have focused on the solubility of selenium under high pH conditions (Pilkington et al., 1988; Felipe-Sotelo et al., 2016). The latter study shows a relation between the concentration of Ca available in the alkaline solutions and the solubility of SeO_3^{2-}, suggesting the formation of $Ca_2SeO_3(OH)_2{\cdot}2H_2O$ as the solubility limiting phase in 95%-saturated $Ca(OH)_2$ and NRVB-equilibrated solutions (Felipe-Sotelo et al., 2016).

Several studies have concluded that adsorption is an unlikely mechanism for immobilisation of anionic species onto cement and have focused investigations on the incorporation of SeO_3^{2-} into cement minerals such as ettringite, monosulphate and calcium silicate hydrate (CSH). Solem-Tishmack et al. (1995) suggested that selenite is retained in cementitious materials more efficiently than selenate by formation of 'selenite-ettringite' in sulphate-rich cement admixtures. Mace et al. (2007) performed batch studies to assess the effect of cement degradation at 70°C on the retention of SeO_3^{2-}. The authors concluded that ettringite plays an important role in the retention of Se(IV), since the formation of ettringite is inhibited at high temperature, causing a corresponding decrease in the proportion of selenium bound. Moreover, the surface area of cement particles decreases at high temperatures owing to crystallization, tending to a further decrease in SeO_3^{2-}uptake (Mace et al., 2007). Although it is usually overlooked, calcite can also contribute to the retention of selenite and other oxyanions in alkaline conditions (Cornelis et al., 2008); the affinity of $SeO_3^{2-}$for calcite surfaces is due to the oxyanion assuming a trigonal pyramid crystal form, similar to CO_3^{2-}.

Conversely, other authors believe that uptake of SeO_3^{2-} by cement is non-specific and is the result of electrostatic or complexation interactions. Johnson et al. (2000) investigated the adsorption of SeO_3^{2-} onto 27 cement formulations in batch studies. They found that the addition of clay to the cement admixtures or variation in the water content had little effect on the adsorption of SeO_3^{2-}. The addition of silica fume was found to decrease the partition coefficient values, presumably due to competition of aqueous silica with selenite for surface sites in the cement. Johnson et al. (2000)

remarked that longer curing times (>28 days) may result in increased R_d values, as the silica fume would react with calcium hydroxide, resulting in additional CSH. The findings agree, in the main, with results reported previously (Rudin, 1996), although the latter attributed the increase in selenium retention not to the chemical properties of the silica fume but to changes in the cement microstructure as a result of the formation of additional tricalcium silicate or physical blockage of the pores with the fine silica particles. Through-diffusion experiments in radial configuration showed higher mobility through a porous backfill cement (NRVB) than through a PFA/OPC cement, which was attributed to the lower porosity of the PFA/OPC grout (Felipe-Sotelo et al., 2016). Baur and Johnson (Baur and Johnson, 2003) carried out batch studies on the uptake of SeO_3^{2-}on individual cement phases, namely ettringite, monosulphate and CSH; on the basis of X-ray diffraction (XRD) data, the authors suggested that binding of SeO_3^{2-} occurs mainly on the surface as a result of surface complexation and surface precipitation with calcium. This hypothesis is supported by extended X-ray absorption fine structure (EXAFS) experiments carried out by Bonhoure et al. (2006) where SeO_3^{2-}bound to the cement appears to show non-specific interaction with the cement minerals, whether CSH, portlandite, ettringite or monosulphate. Although not phase specific, it should be noted that all of these contain calcium and some association between calcium and selenium is an observation common to the majority of the above investigations.

Synthesis of cement model phases

CSH

Several methodologies have been reported for the synthesis of calcium silicate hydrate; for example by co-precipitation of $Ca(NO_3)_2$ + $Si(OH)_4$ or by hydrothermal synthesis (Hartmann et al., 2014; Lachowski et al., 2000). However, the direct method described by Atkins et al. (1992) is the most advantageous because minimal handling of the reagents is required. In general CaO, either obtained by burning of lime or directly obtained as CaO, needs to be calcined prior to use for the removal of remaining carbonates. In terms of silicon oxide, a product is needed with a large surface area to increase the speed of reaction, for example AEROSIL® 300 (SiO_2 specific surface area 300 $m^2\ g^{-1}$). These reagents are simply mixed in the desired ratio of CaO and SiO_2, in a tightly sealed bottle, suspended in decarbonated water and cured for 4 to 8 weeks for reaction; the CSH product is obtained by pozzolanic reaction.

Ettringite

Ettringite can be obtained by the reaction of $Al_2(SO_4)_3{\cdot}18H_2O$ and CaO on a time scale of 2 to 4 weeks (Atkins et al., 1991). Other synthetic routes include using $Ca(NO_3)_2{\cdot}4H_2O$ $Al_2(SO_4)_3{\cdot}18H_2O$ at a constant pH of 11.5, giving a high yield after 1 day and overnight drying (Lo Presti et al., 2013), or a very fast synthesis within 3 hours as described by Terai et al. (2007) using $Ca(OH)_2$, $Al_2(SO_4)_3{\cdot}18H_2O$ and sucrose. Whilst the method described by Atkins et al. (1991) takes the longest amount of time of the synthetic routes, it is generally preferred due to the lack of impurities in the product.

Monosulphate

The synthesis of alumina ferric oxide monosulphate (AFm-SO_4) can be carried out by the reaction of tricalcium aluminate (C_3A) and ettringite; however this route requires the synthesis of C_3A and ettringite of high purity (Atkins et al., 1991). AFm-SO_4 can also be synthesised by the reaction of stoichiometric amounts of $CaSO_4{\cdot}2H_2O$ and C_3A with a rather long curing time of 5 months (Baur et al., 2004). By this method, the

anion can easily be exchanged by simply exchanging $CaSO_4$ for example by $CaCO_3$, CaI_2 or $CaCl_2$ if required (Aimoz et al., 2012).

Hydrotalcite

Co-precipitation methods are common for the synthesis of hydrotalcite (Cavani et al., 1991; Miyata and Kumura, 1973; Sato et al., 1988; Vaccari, 1998, Curtius and Kattilparampil, 2005). A disadvantage of this method is that the concentration of reactants, speed of addition, final pH of the suspension, degree of agitation and the temperature must be carefully controlled. Moreover, the pH can differ in different locations within the suspension leading to formation of very stable agglomerates, resulting in poor reaction yields. This can be avoided by the use of urea, which is decomposed at 90°C to stabilize the pH (Salomao et al., 2014). h work of Long et al.(2014) demonstrated the synthesis of hydrotalcite by a solid state reaction. Aluminium sulphate, magnesium sulphate and sodium carbonate were fully ground in a mortar together with the surfactant polyethylene glycol-400 (PEG-400), stored afterwards at 80°C for 3 hours to give a phase pure product after purification by washing with deionised water, anhydrous ethanol and drying. A microwave synthesis of a phase pure hydrotalcite was reported by Yang et al. (2007) via reaction of magnesium nitrate, aluminium nitrate (Mg/Al = 2:1) and urea at a microwave power of 600W within 1 hour.

References

AIMOZ, L., WIELAND, E., TAVIOT-GUEHO, C., DAHN, R., VESPA, M. & CHURAKOV, S. V. 2012. Structural insight into iodide uptake by AFm phases. *Environ. Sci. Technol.,* 46**,** 3874-3881.

ALLEN, P. G., SHUH, D. K., BUCHER, J. J., EDELSTEIN, N. M., REICH, T., DENECKE, M. A. & NITSCHE, H. 1997a. Chemical speciation studies of radionuclides by XAFS. *J. Phys. IV,* 7**,** 789-792.

ALLEN, P. G., SIEMERING, G. S., SHUH, D. K., BUCHER, J. J., EDELSTEIN, N. M., LANGTON, C. A., CLARK, S. B., REICH, T. & DENECKE, M. A. 1997b. Technetium speciation in cement waste forms determined by X-ray absorption fine structure spectroscopy. *Radiochim. Acta,* 76**,** 77-86.

ATKINS, M. & GLASSER, F. P. 1992. Application of portland cement-based materials to radioactive waste immobilization. *Waste Management,* 12**,** 105-131.

ATKINS, M., GLASSER, F. P. & KINDNESS, A. 1992. Cement hydrate phases: solubility at 25°C. *Cem. Concr. Res.,* 22**,** 241-6.

ATKINS, M., MACPHEE, D., KINDNESS, A. & GLASSER, F. P. 1991. Solubility properties of ternary and quaternary compounds in the calcia-alumina-sulfur trioxide-water system. *Cem. Concr. Res.,* 21**,** 991-8.

ATKINSON, A. & NICKERSON, A. K. 1984. The diffusion of ions through water-saturated cement. *Journal of Materials Science,* 19**,** 3068-3078.

BAUR, I. & JOHNSON, C. A. 2003. Sorption of selenite and selenate to cement minerals. *Environmental Science & Technology,* 37**,** 3442-3447.

BAUR, I., KELLER, P., MAVROCORDATOS, D., WEHRLI, B. & JOHNSON, C. A. 2004. Dissolution-precipitation behaviour of ettringite, monosulfate and calcium silicate hydrate. *Cem. Concr. Res.,* 34**,** 341-348.

BAYLISS, S., EWART, F. T., HOWSE, R. M., LANE, S. A., PILKINGTON, N. J., SMITH-BRIGGS, J. L. & WILLIAMS, S. J. 1989. The solubility and sorption of radium and tin in a cementitious near-field environment. *Mater. Res. Soc. Symp. Proc.,* 127**,** 879-85.

BEAUDOIN, J. J., RAMACHANDRAN, V. S. & FELDMAN, R. F. 1990. Interaction of chloride and CSH. *Cement and Concrete Research,* 20**,** 875-883.

BERNER, U. 1999. Concentration limits in the cement based Swiss repository for long-lived, intermediate-level radioactive wastes (LMA).

BIRNIN-YAURI, U. A. & GLASSER, F. P. 1998. Friedel's salt, Ca2Al(OH)6(Cl,OH)·2H2O: its solid solutions and their role in chloride binding. *Cement and Concrete Research,* 28**,** 1713-1723.

BONHOURE, I., BAUR, I., WIELAND, E., JOHNSON, C. A. & SCHEIDEGGER, A. M. 2006. Uptake of Se(IV/VI) oxyanions by hardened cement paste and cement minerals: An X-ray absorption spectroscopy study. *Cement and Concrete Research,* 36**,** 91-98.

BRODDA, B. G. & XU, M. 1989. Leaching of chlorine, cesium, strontium and technetium from cement-fixed intermediate level liquid waste. *Mater. Res. Soc. Symp. Proc.,* 127**,** 481-7.

CAVANI, F., TRIFIRO, F. & VACCARI, A. 1991. Hydrotalcite-type anionic clays: preparation, properties and applications. *Catal. Today,* 11**,** 173-301.

CHIDA, T. & SUGIYAMA, D. Diffusion behaviour of organic carbon and iodine in low-heat portland cement containing fly ash. Materials Research Society Symposium Proceedings, 2009. 379-384.

CORNELIS, G., JOHNSON, C. A., GERVEN, T. V. & VANDECASTEELE, C. 2008. Leaching mechanisms of oxyanionic metalloid and metal species in alkaline solid wastes: A review. *Applied Geochemistry,* 23**,** 955-976.

CURTIUS, H. & KATTILPARAMPIL, Z. 2005. Sorption of iodine on Mg-Al-layered double hydroxide. *Clay Miner.,* 40**,** 455-461.

EVANS, N. D. M. 2008. Binding mechanisms of radionuclides to cement. *Cement and Concrete Research,* 38**,** 543-553.

FELIPE-SOTELO, M., HINCHLIFF, J., DRURY, D., EVANS, N. D. M., WILLIAMS, S. & READ, D. 2014. Radial diffusion of radiocaesium and radioiodide through cementitious backfill. *Physics and Chemistry of the Earth,* 70-71**,** 60-70.

FELIPE-SOTELO, M., HINCHLIFF, J., EVANS, N. D. M. & READ, D. 2016. Solubility constraints affecting the migration of selenium through the cementitious backfill of a geological disposal facility. *Journal of Hazardous Materials,* 305**,** 21-29.

GILLIAM, T. M., SPENCE, R. D., BOSTICK, W. D. & SHOEMAKER, J. L. 1990. Proceedings of the Gulf Coast Hazardous Substance Research Center Second Annual Symposium: Mechanisms and Applications of Solidification/StabilizationSolidification/stabilization of technetium in cement-based grouts. *Journal of Hazardous Materials,* 24**,** 189-197.

GLASSER, F. P., MACPHEE, D., ATKINS, M., POINTER, C., COWIE, J., WILDING, C. R., MATTINGLEY, N. J. & EVANS, P. A. 1989. Immobilisation of radwaste in cement based matrices.

HARTMANN, A., KHAKHUTOV, M. & BUHL, J. C. 2014. Hydrothermal synthesis of CSH-phases (tobermorite) under influence of Ca-formate. *Materials Research Bulletin,* 51**,** 389-396.

HOLLAND, T. R. & LEE, D. J. 1992. Radionuclide getters in cement. *Cem. Concr. Res.,* 22**,** 247-58.

JOHNSON, E. A., RUDIN, M. J., STEINBERG, S. M. & JOHNSON, W. H. 2000. The sorption of selenite on various cement formulations. *Waste Management,* 20**,** 509-516.

KINDNESS, A., LACHOWSKI, E. E., MINOCHA, A. K. & GLASSER, F. P. 1994. Immobilization and fixation of molybdenum (VI) in portland cement. *Waste Manage. (N. Y.),* 14**,** 97-102.

LACHOWSKI, E. E., HONG, S. Y. & GLASSER, F. P. 2000. Crystallinity in C-S-H gels: influence of preparation and cure conditions. *RILEM Proc.,* PRO 13**,** 215-225.

LO PRESTI, A., CERULLI, T., BIANCARDI, A., MORETTI, E. & SALVIONI, D. 2013. Ettringite: a new synthesis approach. *Proc. Int. Conf. Cem. Microsc.,* 35th**,** 165-177.

LONG, Q., XIA, Y., LIAO, S., LI, Y., WU, W. & HUANG, Y. 2014. Facile synthesis of hydrotalcite and its thermal decomposition kinetics mechanism study with masterplots method. *Thermochim. Acta,* 579**,** 50-55.

LUKSIC, S. A., RILEY, B. J., SCHWEIGER, M. & HRMA, P. 2015. Incorporating technetium in minerals and other solids: A review. *J. Nucl. Mater.,* 466**,** 526-538.

MACE, N., LANDESMAN, C., POINTEAU, I., GRAMBOW, B. & GIFFAUT, E. 2007. Characterisation of thermally altered cement pastes. Influence on selenite sorption. *Advances in Cement Research,* 19**,** 157-165.

MATTIGOD, S. V., WHYAT, G. A., SERNE, R. J., MARTIN, P. F., SCHWAB, K. B. & WOOD, M. I. 2001. Diffusion and leaching of selected radionuclides (Iodine-

129, Technetium-99, and Uranium) through category 3 waste encasement concrete and soil fill material.
MIYATA, S. & KUMURA, T. 1973. Synthesis of new hydrotalcite-like compounds and their physicochemical properties. *Chem. Lett.*, 843-8.
OGARD A, E., THOMPSON J, L., RUNDBERG R, S., WOLFSBERG, K., KUBIK P, W., ELMORE, D. & BENTLEY H, W. 1988. Migration of chlorine-36 and tritium from an underground nuclear test. *Radiochimica Acta,* 44/45(pt.1), 213-217
PILKINGTON, N. J., SHADBOLT, P. J. & WILKINS, J. D. 1988. Experimental measurements of the solubilities of selected long-lived fission products, activation products and actinide daughters under high pH conditions.
POINTEAU, I., COREAU, N. & REILLER, P. E. 2008. Uptake of anionic radionuclides onto degraded cement pastes and competing effect of organic ligands. *Radiochimica Acta,* 96**,** 367-374.
RUDIN, M. J. 1996. Leaching of selenium from cement-based matrices. *Waste Management,* 16**,** 305-311.
SALOMAO, R., DIAS, I. M. M. & ARRUDA, C. C. Hydrotalcite (Mg6Al2(OH)16(CO3).4H2O): a potentially useful raw material for refractories. 2014. John Wiley & Sons, Inc., 1151-1156.
SAROTT, F. A., BRADBURY, M. H., PANDOLFO, P. & SPIELER, P. 1992. Special Double Issue Proceedings of Symposium D of the E-MRS Fall Meeting 1991 Diffusion and adsorption studies on hardened cement paste and the effect of carbonation on diffusion rates. *Cement and Concrete Research,* 22**,** 439-444.
SATO, T., FUJITA, H., ENDO, T., SHIMADA, M. & TSUNASHIMA, A. 1988. Synthesis of hydrotalcite-like compounds and their physico-chemical properties. *React. Solids,* 5**,** 219-28.
SÉBY, F., POTIN-GAUTIER, M., GIFFAUT, E. & DONARD, O., F.X. 1998. Assessing the speciation and the biogeochemical processes affecting the mobility of selenium from a geological repository of radioactive wastes to the biosphere. *Analusis*, 26 5 (1998) 193-198
SMITH, R. W. & WALTON, J. C. 1993. The role of oxygen diffusion in the release of technetium from reducing cementitious waste forms. *Mater. Res. Soc. Symp. Proc.,* 294**,** 247-53.
SOLEM-TISHMACK, J. K., MCCARTHY, G. J., DOCKTOR, B., EYLANDS, K. E., THOMPSON, J. S. & HASSETT, D. J. 1995. High-calcium coal combustion by-products: Engineering properties, ettringite formation, and potential application in solidification and stabilization of selenium and boron. *Cement and Concrete Research,* 25**,** 658-670.
SWEDISH NUCLEAR FUEL AND WASTE MANAGEMENT CO 2010. Radionuclide transport report for the safety assessment SR-Site. Swedish Nuclear Fuel and Waste Management Co.
TALLENT, O. K., MCDANIEL, E. W., CUL, G. D. D., DODSON, K. E. & TROTTER, D. R. 1987. Immobilization of technetium and nitrate in cement-based materials. *MRS Online Proceedings Library Archive,* 112.
TANABE, H., SAKURAGI, T., YAMAGUCHI, K., SATO, T. & OWADA, H. 2010. Development of new waste forms to immobilize iodine-129 released from a spent fuel reprocessing plant. *Advances in science and technology,* 73**,** 158-170.
TERAI, T., MIKUNI, A., NAKAMURA, Y. & IKEDA, K. 2007. Synthesis of ettringite from portlandite suspensions at various Ca/Al ratios. *Inorg. Mater.,* 43**,** 786-792.

TITS, J., IIJIMA, K., WIELAND, E. & KAMEI, G. 2006. The uptake of radium by calcium silicate hydrates and hardened cement paste. *Radiochim. Acta,* 94**,** 637-643.

VACCARI, A. 1998. Preparation and catalytic properties of cationic and anionic clays. *Catal. Today,* 41**,** 53-71.

VAN ES, E., HINCHLIFF, J., FELIPE-SOTELO, M., MILODOWSKI, A. E., FIELD, L. P., EVANS, N. D. M. & READ, D. 2015. Retention of chlorine-36 by a cementitious backfill. *Mineralogical Magazine,* 79**,** 1297-1305.

YANG, Z., CHOI, K.-M., JIANG, N. & PARK, S.-E. 2007. Microwave synthesis of hydrotalcite by urea hydrolysis. *Bulletin of the Korean Chemical Society,* 28**,** 2029-2033.

YU, P. & KIRKPATRICK, R. J. 2001. 35Cl NMR relaxation study of cement hydrate suspensions. *Cement and Concrete Research,* 31**,** 1479-1485.

ZHANG, M. 2000. Incorporation of oxyanionic boron, chromium, molybdenum, and selenium into hydrocalumite and ettringite: application to cementitious systems.

A structural and thermodynamic study of the intercalation of iodine, selenium, and sulfur in AFm-phases (EMPA, PSI)

Jan Tits, Barbara Lothenbach, Latina Nedyalkova, Erich Wieland

Introduction

Safety assessment studies for low- and intermediate level nuclear waste (L/ILW) repositories have shown that selenium-75 and iodine-129 are important dose-determining radionuclides due to their long half-lives and their presence in the anionic form resulting in weak retention by many common near- and far field minerals having negatively charged surfaces (NAGRA, 2002). However, such predictions ignore the potential uptake by positively charged anion exchangers present in the cementitious near-field of a L/ILW repository, such as AFm-phases, a group of Ca,Al layered double hydroxides. AFm phases consist of positively charged calcium-aluminium hydroxide layers having a fixed Ca^{2+}:Al^{3+} ratio of 2:1, separated by interlayers containing anions and H_2O molecules. The type of anions forming the interlayers depends on the composition of the starting cement clinker materials and on the composition of the supplementary cementitious materials (SCM) added to the cements. Typical anions frequently found in AFm phases are OH^-, SO_4^{2-} and CO_3^{2-} forming hydroxyl-AFm, monosulfoaluminate, hemi- and monocarboaluminates, respectively. In addition, under reducing conditions, HS^- originating from the reduction of SO_4^{2-} might also be present as competitive anion in significant quantities. The mobility of ^{75}Se- and ^{129}I-anions present in radioactive waste may be reduced significantly through uptake reactions involving substitution in the AFm interlayers.

The present PhD proposal aims at investigating the intercalation of selenium (Se), iodine(I) and sulfur (S) by AFm phases under repository redox conditions.

Conditions expected in the cementitious near-field of a radioactive waste repository

It is generally assumed that after closure, the available oxygen in an ILW repository will be depleted rapidly (within 100 years) and conditions will become reducing (Wersin et al., 2003). The redox potential will mainly be controlled by the Fe^{3+}/Fe^{2+} redox couple due to the corrosion of steel resulting in the formation of magnetite as the major corrosion product (Berner, 2003; Wersin et al., 2003). Based on this assumption, Wersin et al (2003) estimated the redox potential in the cementitious near-field of the planned Swiss L/ILW repository to be between -750mV and -230 mV (SHE).

Selenium and iodine speciation under repository conditions

Thermodynamic calculations with the code Medusa (Puigdomenech, 1983) using the NEA thermodynamic database for Se indicate that under the alkaline reducing conditions expected in the cementitious near-field, Se(IV), Se(0) and Se(-II) are the predominant redox states and the aqueous Se speciation is dominated by anionic species SeO_3^{2-}, HSe^- and a series of polyselenides (Se_x^{2-}), mainly Se_2^{2-}, Se_3^{2-} and Se_4^{2-} (Olin et al., 2005) (Figure 1a). The stability field of the polyselenide species strongly

depends on the total Se concentration: At high total Se concentrations, the polyselenide stability fields are very large at the expense of SeO_3^{2-} and HSe^-, whereas at very low total Se concentrations, the Se speciation under reducing conditions is mainly dominated by SeO_3^{2-} and HSe^-.

Thermodynamic calculations suggest that HS^- is the dominating sulfur species under alkaline, reducing conditions (Hummel et al., 2002). However, due to kinetic effects, in reality, $S^{IV}O_3^{2-}$ may dominate the sulfur speciation under moderately reducing conditions, whereas under more strongly reducing conditions, $S^{II}{}_2O_3^{2-}$, HS^- and a series of polysulfides will be dominant (e.g., Gruskovnjak et al., 2006).

Iodide (I^-) is the thermodynamically stable phase under alkaline and reducing repository near-field conditions (Thoenen et al., 2014) (Figure 1b).

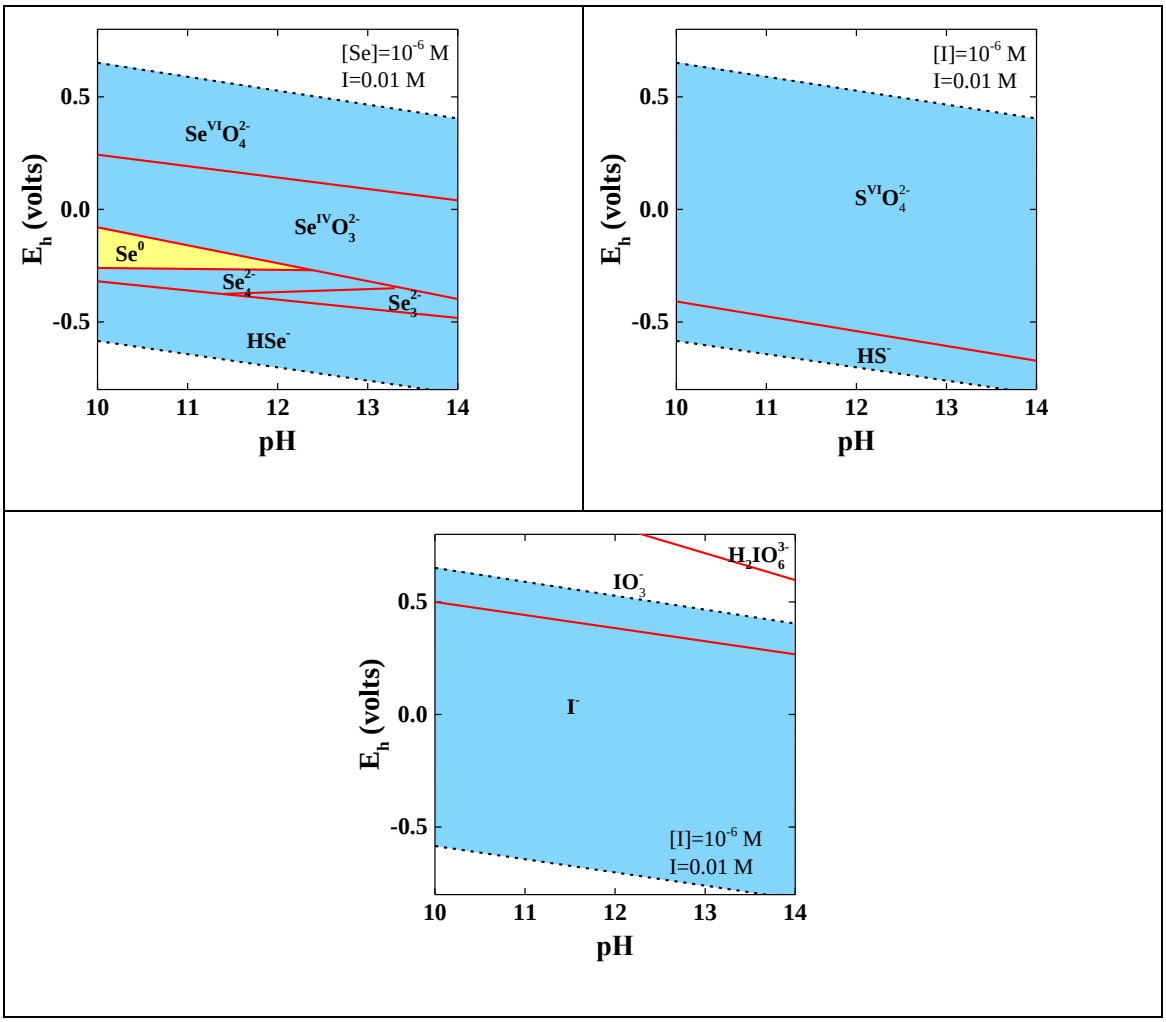

Figure 1: Predominance diagrams of Se, S and I in the pH and E_h regions relevant for the cementitious near field of a level/ILW nuclear waste repository calculated for a total radionuclide concentration of 10^{-6} M. Calculations were performed using the code Medusa (Puigdomenech, 1983) with thermodynamic data for Se included in the NEA thermodynamic database and with thermodynamic data for I included in the PSI thermodynamic database (Thoenen et al., 2014).

Cement composition

During the cement hydration process, various hydrated cement phases are formed. Among them, calcium silicate hydrate phases (C-S-H phases) and calcium aluminates phases (AFt and AFm phases) exhibit favourable radionuclide sorption properties (e.g., Chen et al., 2009). They make up approximately 46% and 17 % of the hardened cement paste (HCP) respectively (e.g., Lothenbach and Wieland, 2006).

C–S–H phases are characterized by strong negative surface charge density originating from the ionization of silanol (=Si-O-H) and silandiol ($=Si(OH)_2$) groups on the particle surfaces and in the interlayers (e.g., Churakov et al., 2014; Labbez et al., 2006; Pointeau et al., 2006b). This negative surface charge explains the low affinity of this cement component for anions in spite of their extremely large surface area. Recent studies however suggest increased anion sorption in the presence of high Ca^{2+} concentrations due to overcompensation of the negative charge on the C-S-H surfaces (Plusquellec et al., 2012).

A high anion exchange capacity resulting from a permanent structural negative charge on surfaces and in flexible interlayers, make AFm phases very promising cement phases for the retention of radioactive anions. The different types of AFm phases differ mainly in their interlayer composition, their interlayer distance and their solubilities (aqueous composition in equilibrium with each AFm phase). Typical anions frequently found in AFm phases are OH^-, SO_4^{2-} and CO_3^{2-} and under reducing conditions possibly $S_2O_3^{2-}$ and HS^-. The interlayer distance depends on the type of anions present in the interlayer and on the number of H_2O molecules. The strongly bound CO_3^{2-} anions and the water molecules in the interlayers of AFm-CO_3 firmly connect the main layers resulting in a rigid, narrow interlayer (basal spacing = 7.55 Å, hindering diffusion of other anions into the interlayers (Baquerizo et al., 2015; Francois et al., 1998). The weakly bound $[OH(CO_3^{2-})_{0.5}]^{2-}$ and SO_4^{2-} anions in AFm-OH-CO_3 and AFm-SO_4 on the other hand give rise to much larger, more flexible interlayers (basal spacing = 8.17 Å and 8.93 Å, respectively (Allmann, 1977; Balonis and Glasser, 2009)) allowing easy access to other anions. Dissolution – re-precipitation reactions may provide a further mechanism for other anions to become incorporated in AFm structures.

Immobilisation of selenium and iodine by AFm phases under reducing conditions

Retention processes on cementitious materials have an essential impact on the migration of ^{75}Se and ^{129}I from the waste canisters through the near-field to the host rock. Retention may occur through reactions on the mineral surfaces (inner-, outer sphere complexation, anion exchange, surface precipitation) or by structural incorporation into mineral phases via co-precipitation or recrystallization processes. In the case of I and Se anions in an alkaline, cementitious environment, complexation processes with surface functional groups are expected to be of minor importance because such processes mainly occur in the acidic to neutral pH range (e.g., Stumm and Morgan, 1996). Under alkaline conditions, anion sorption will mainly occur via anion exchange processes on surfaces of minerals carrying a positive charge (e.g. AFm-phases), intercalation in AFm interlayers through substitution of the typical AFm

anions (i.e., OH^-, SO_4^{2-} and CO_3^{2-}) or dissolution of the primary AFm phases and re-precipitation of a new AFm phases containing Se(IV), Se(-II) or I(-I).

Selenium

Under moderately reducing conditions, $Se^{IV}O_3^{2-}$ will dominate the Se speciation whereas under more strongly reducing conditions, HSe^- and a series of polyselenides will be dominant.

In the last two decades, several studies on the uptake of Se(IV) by cement materials have been published e.g., Baur and Johnson, 2003; Bonhoure et al., 2006; Macé et al., 2007; Pointeau et al., 2006a; Pointeau et al., 2008). Moderately strong uptake was observed on the main cement phases with R_d values of 180 L kg^{-1}, 380 L kg^{-1} and 210 L kg^{-1} on ettringite, C-S-H phases and AFm phases, respectively (Baur and Johnson, 2003; Bonhoure et al., 2006). Recent in-house sorption experiments on different cement phases show a slightly different picture (Rojo et al., 2015, pers. comm.). Rojo et al. found similar R_d values for C-S-H phases of 300 L kg^{-1} at low loadings (10^{-5} mol kg^{-1}) but much higher R_d values for AFm phases ranging from 10^3 L kg^{-1} to $2 \cdot 10^4$ L kg^{-1} (loading = 10^{-5} mol kg^{-1}). Furthermore, they found SeO_3^{2-} sorption onto AFm phases to depend strongly on the type of anions present in the interlayers (and thus on the interlayer distance): AFm-OH-CO_3 exhibited a strong affinity for Se(IV) ($R_d = 10^4$ L kg^{-1}) whereas the affinity of AFm-CO_3 for this anion was found to be significantly lower ($R_d = 10^3$ L kg^{-1}).

Several Se(IV) sorption studies onto hydrated cement pastes (HCP) showed that the degradation state of the cement has a strong impact on the uptake of this anion (Pointeau et al., 2006a; Pointeau et al., 2008). The stronger sorption on degraded HCP appeared to be inversely proportional to the sulphate concentration suggesting that either ettringite or AFm-SO_4 are involved in the Se(IV) sorption process.

The knowledge obtained from these earlier studies clearly indicates that AFm phases play a key role in the immobilization of Se(IV) in cementitious environments and that exchange with anions in the AFm phases is the mechanism controlling the $Se^{IV}O_3^{2-}$ uptake. This is no surprise. knowing that AFm phases belong to the family of the layered double hydroxides (LDH's) a group of minerals well known for their excellent anion exchange properties (e.g., Goh et al., 2008).

Under strongly reducing conditions, the HSe^- and polyselenides are the Se species dominating the redox speciation. Studies concerning the sorption of Se(-II) on cementitious materials are completely inexistent up to date as it is very difficult to maintain Se in the (-II) redox state during sorption experiments. First attempts to measure the sorption of Se(-II) onto cement phases have been carried out in house by Rojo et al. (pers. comm.). In these experiments, hydrazine was used in an attempt to stabilize the Se(-II) redox state. It was shown that the (–II) redox state was maintained for the Se sorbed onto the cement phases, but that the Se remaining in the aqueous phase was oxidized during the sorption experiments. Therefore, R_d values for Se(-II) sorption could not be derived from these experiments.

Sulfur

The binding of sulfate (S(VI)) in AFm and AFt phases is well investigated (e.g., Matschei et al., 2007). At high sulfate concentrations as predominant in the presence of gypsum, the formation of ettringite is observed. At lower sulfate concentrations ettringite can be destabilised to form AFm-SO_4.

The formation of sulphide containing AFm-phases (AFm-S: $3(CaO)\cdot Al_2O_3\cdot CaS\cdot 13H_2O$ and disulfurooaluminate: $3(CaO)\cdot Al_2O_3\cdot 2(CaS)\cdot 10H_2O$) has been suggested by Vernet (Vernet, 1982). Unfortunately, no further characterisation or experimentally derived solubility data are available for these or any other sulphide bearing AFm or AFt phase.

The different redox species of sulfur and selenium are isostructural although the ions have somewhat different sizes. Thus a strong influence of sulfur on the selenium binding is expected.

Iodine

The recent literature contains numerous studies on the retention of I^- by cementitious materials. Recent comprehensive literature overviews can be found in the review report of Wang et al (Wang et al., 2009) and the paper of Evans (2008). These authors concluded that the main uptake processes for I^- in cement include surface complexation onto C-S-H phases as well as structural incorporation into AFm phases. Ochs et al. (Ochs et al., 2010) compared the I^- sorption onto different cement minerals and reported sorption values to decrease following the order AFm > C-S-H with high C/S ratio ~ AFt > C-S-H with low C/S ratio. I^- incorporation into AFm interlayers has been studied by Brown and Grutzeck (1985), Toyohara et al. (2002) and Aimoz et al. (2011, 2012a, 2012b). These studies proved the existence of mono-iodide as a stable phase and unravelled its structure. Furthermore evidence was provided that the intercalation of I^- in AFm interlayers depends on the type of competing anion: i.e., AFm-SO_4 is capable of taking up I^- forming a solid solution whereas the presence of CO_3^{2-} or Cl^- prevented I^- intercalation. The I^- uptake by AFm-OH-CO_3 was not included in these studies.

Objectives

Although Se and I uptake by AFm phase has already been the subject of several studies, sorption data for Se(-II) under strongly reducing conditions, as well as an atomic scale understanding of the uptake processes of Se(IV), Se(-II) and I^- and thermodynamic models describing the uptake, are still largely missing. Such models are essential for predicting the fate of selenium in the cementitious near-field of a L/ILW repository. Furthermore, presently no data exist on the fate of sulfur in AFm phases under reducing conditions and on the competition between reduced sulfur species and Se(-II) or I(-I) for ion exchange sites in AFm phases.

The aims of the present PhD thesis are

1) To compare the Se and I sorption data from co-precipitation experiments and sorption experiments with different AFm phases

2) to construct thermodynamic models able to predict the uptake of Se(IV) and I(-I) by different types of AFm phases,

3) to investigate the interaction of Se(-II) and reduced sulfur species (S(IV), S(II) and S(-II)) with AFm phases and to construct thermodynamic models describing these interactions

The main experimental challenge of the present project is the development of experimental procedures to synthesize AFm phases containing reduced Se and S species under highly alkaline conditions and to characterize them with advanced spectroscopic techniques (ESEM, TG, IR, XRD and Rietveld refinement, XAS, acid digestion) without re-oxidation of the samples. To our knowledge, studies on the interaction of Se(-II) and S(-II) by cement minerals have never been published so far, mainly due to the experimental difficulties associated with the stabilization of the Se(-II) and S(-II) redox states. To overcome this problem, either the use of electrochemical cells or chemical reducing agents are envisaged. In the past, sorption studies with Np(IV), a highly oxygen-sensitive actinide, have been carried out by our research group (Gaona et al., 2011). The experience obtained during this study will be very helpful in the present PhD project.

References

Aimoz, L., Taviot-Gueho, C., Churakov, S.V., Chukalina, M., Daehn, R., Curti, E., Bordet, P. and Vespa, M. (2011) Anion and cation order in iodide-bearing Mg/Zn−Al layered double hydroxides. J. Phys. Chem. C. 116, 5460-5475.

Aimoz, L., Kulik, D.A., Wieland, E., Curti, E., Lothenbach, B. and Maeder, U. (2012a) Thermodynamics of AFm-(I_2, SO_4) solid solution and of its end-members in aqueous media. Appl. Geochem. 27, 2117-2129.

Aimoz, L., Wieland, E., Taviot-Gueho, C., Daehn, R., Vespa, M. and Churakov, S.V. (2012b) Structural insight into iodide uptake by AFm phases. Environ. Sci. Technol. 46, 3874-3881.

Allmann, R. (1977) Refinement of the hybrid layer structure $[Ca_2Al(OH)_6)]^+ \cdot [1/2SO_4 \cdot 3H_2O]^-$. Neues Jb. Mineral. Monatsh. 3, 136-144.

Balonis, M. and Glasser, F.P. (2009) The density of cement phases. Cem. Concr. res. 39, 733-739.

Baquerizo, L.G., Matschei, T., Scrivener, K.L., Saeidpour, M. and Wadsö, L. (2015) Hydration states of AFm cement phases. Cem. Concr. res. 73, 143-157.

Baur, I. and Johnson, C.A. (2003) Sorption of selenite and selenate to cement materials. Environ. Sci. Technol. 37, 3442-3447.

Berner, U. (2003) Project Opalinus Clay: Radionuclide Concentration Limits in the Cementitious Near-Field of an ILW Repository, PSI Bericht Nr. 02-26, Paul Scherrer institut, Villigen, Switzerland and Nagra Technical report NTB 02-22, Wettingen, Switzerland.

Bonhoure, I., Baur, I., Wieland, E., Johnson, C.A. and Scheidegger, A.M. (2006) Uptake of Se(IV/VI) oxyanions by hardened cement paste and cement minerals: An X-ray absorption spectroscopy study. Cem. Concr. res. 36, 91-98.

Brown, D.R. and Grutzeck, M.W. (1985) The synthesis and characterization of calcium aluminate monoiodide. Cem. Concr. res. 15, 1068-1078.

Chen, Q.I., Tyrer, M., Hills, C.D., Yang, X.M. and Carey, P. (2009) Immobilisation of heavy metal in cement-based solidification/stabilisation: A review. Waste Manag. 29, 390-403.

Churakov, S.V., Labbez, C., Pegado, L. and Sulpiyi, M. (2014) Intrinsic Acidity of Surface Sites in Calcium Silicate Hydrates and Its Implication to Their Electrokinetic Properties. J. Phys. Chem. C. 118, 11752-11762.

Evans, N.D.M. (2008) Binding mechanisms of radionuclides to cement. Cem. Concr. res. 38, 543-553.

Francois, M., Renaudin, G. and Evrard, O. (1998) A Cementitious Compound with Composition $3CaO.Al_2O_3.CaCO_3.11H_2O$. Acta Cryst. C54, 1214-1217.

Gaona, X., Dähn, R., Tits, J., Scheinost, A. and Wieland, E. (2011) Uptake of Np(IV) by C-S-H phases and cement paste: an EXAFS study. Environ. Sci. Technol. 45, 8765-8771.

Goh, K.-H., Lim, T.-T. and Dong, Z. (2008) Application of layered double hydroxides for removal of oxyanions: A review. Water Research 42, 1343-1368.

Gruskovnjak, A., Lothenbach, B., Holyer, L., Figi, R. and Winnefeld, F. (2006) Hydration of alkali-activated slag: comparison with ordinary Portland cement. Advances in Cement Research 18, 119-128.

Hummel, W., Berner, U.R., Curti, E., Pearson Jr, F.J. and Thoenen, T. (2002) Nagra-PSI chemical thermodynamic database, version 01/01. Universal Publishers / Upubl.com, New York.

Labbez, C., Jönnson, B., Pochard, I., Nonat, A. and Cabane, B. (2006) Surface Charge Density and Electrokinetic Potential of Highly Charged Minerals: Experiments and Monte Carlo Simulations on Calcium Silicate Hydrate. J. Phys. Chem. B. 110, 9219-9230.

Lothenbach, B. and Wieland, E. (2006) A thermodynamic approach to the hydration of sulphate-resistent Portland cement. Waste Manage. 26, 706-719.

Macé, N., Landesman, C., Pointeau, I., Grambow, B. and Giffaut, E. (2007) Characterisation of thermally altered cement pastes. Influence on selenite sorption. Adv. Cem. Res. 19, 157-165.

Matschei, T., Lothenbach, B. and Glasser, F.P. (2007) The AFm phase in Portland cement. Cem. Concr. Res. 37, 118-130.

NAGRA (2002) Project Opalinus Clay. Safety report. Demonstration of disposal feasibility for spent fuel, vitrified high-level waste and long-lived intermediate level waste (Entsorgungsnachweis), Nagra Technical Report, NTB 02-05, Nagra, Wettingen, Switzerland.

Ochs, M., Vielle-Petit, L., Wang, D., Mallants, D. and Leterne, B. (2010) Additional sorption parameters for the cementitious barriers of a near-surface repository. ONDRAF/NIRAS, Brussels, Belgium.

Olin, Å., Noläng, B., Osadchii, E.G., Öhman, L.-O. and Rosén, E. (2005) Chemical thermodynamics of Selenium. Elsevier, Amsterdam.

Plusquellec, G., Nonat, A. and Pochard, I. (2012) Anion uptake by calcium silicate hydrate in: Russell, M.I., Basheer, M.P.A. (Eds.), 32nd Cement and Concrete Science Conference, Queen's University Belfast, Belfast, Nordern Ireland.

Pointeau, I., Coreau, N. and Reiller, P.E. (2008) Uptake of anionic radionuclides onto degraded cement pastes and competing effect of organic ligands. Radiochimica acta 96, 367-374.

Pointeau, I., Hainos, D., Coreau, N. and Reiller, P. (2006a) Effect of organics on selenite uptake by cementitious materials. Waste Manag. 26, 733-740.

Pointeau, I., Reiller, P., Macé, N., Landesman, C. and Coreau, N. (2006b) Measurement and modeling of the surface potential evolution of hydrated cement pastes as a function of degradation. J. Colloid Interface Sci. 300, 33-44.

Puigdomenech, I., 1983. INPUT, SED, and PREDOM: Computer programs drawing equilibrium diagrams; TRITA-OOK-3010. Royal Institute of Technology (KTH), Dept. Inorg. Chemistry, Stockholm (Sweden).

Stumm, W. and Morgan, J.J. (1996) Aquatic Chemistry, Third Edition. John Wiley & Sons, inc., New-York.

Thoenen, T., Hummel., W., Berner, U. and Curti, E. (2014) The PSI/Nagra Chemical Thermodynamic Database 12/07, PSI Bericht Nr. 14-04. Paul Scherrer institut, Villigen PSI, Switzerland.

Toyohara, M., Kaneko, N., Mitsutsuka, H., Hujihara, H., Saito, N. and Murase, T. (2002) Contribution to understanding iodine sorption mechanism onto mixed solid alumina cement and calcium compounds. J. Nucl. Sci. Technol. 39, 950-956.

Vernet, C. (1982) Comportement de l'ion S^{--} au cours de l'hydratation des ciments riche en laitier (CLK). Silicates industriels 47, 85-89.

Wang, L., Martens, E., Jacques, D., De Canniere, P., Berry, J. and Mallants, D. (2009) Review of sorption values for the cementitious near field of a near surface radioactive waste disposal facility. ONDRAF / NIRAS.

Wersin, P., Johnson, L.H., Schwyn, B., Berner, U. and Curti, E. (2003) Redox Conditions in the Near Field of a Repository for SF/HLW and ILW in Opalinus Clay, Nagra Technical Report NTB 02-13, Wettingen, Switzerland.

Solubility, hydrolysis, carbonate complexation and uptake of beryllium in cementitious systems (KIT)

Xavier Gaona, Melanie Böttle, Thomas Rabung, Marcus Altmaier

Affiliation: Institute for Nuclear Waste Disposal, Karlsruhe Institute of Technology, Germany

e-mail: xavier.gaona@kit.edu

Abstract

Beryllium is a highly chemotoxic element expected in certain waste forms to be disposed of in repositories for radioactive waste disposal. The amphoteric behaviour of Be(II) is widely accepted in the literature, although the number of experimental studies reporting the formation of anionic hydrolysis species ($Be(OH)_3^-$ and $Be(OH)_4^{2-}$) under alkaline to hyperalkaline conditions is very scarce. Be(II) forms also strong complexes with carbonate, but so far most of the available studies investigating this interaction have focused on acidic to weakly alkaline pH conditions. In spite of the lack of dedicated studies assessing the uptake of Be(II) by cementitious materials, a weak sorption is conservatively predicted based on the formation of negatively charged species in the aqueous phase. This contribution summarizes the state of the art on the solubility, hydrolysis and sorption of Be(II) in the alkaline to hyperalkaline pH conditions relevant in cementitious systems.

Introduction

This state of the art report summarizes the main publications available in the literature investigating the chemistry of Be(II) in alkaline to hyperalkaline pH conditions relevant in cementitious systems. The report is divided in two main sections, namely "*Solubility, hydrolysis and carbonate complexation of Be in alkaline to hyperalkaline pH conditions*" and "*Sorption of Be in cementitious systems*". Focus has been given to the quantitative description of Be(II) behavior in this systems, *e.g.* to the availability of thermodynamic data, distribution coefficients and/or surface complexation models. Publications dealing with Be(II) aqueous speciation and solid phase characterization under alkaline to hyperalkaline pH conditions but providing no quantitative description of these systems are shortly summarized in the report. The final section entitled "*Summary and outlook*" provides the link between this state of the art report and the activities on Be(II) chemistry planned at KIT–INE within the CEBAMA project.

Solubility, hydrolysis and carbonate complexation of Be in alkaline to hyperalkaline pH conditions

This section summarizes those experimental studies investigating the solubility, hydrolysis and carbonate complexation of Be(II) in alkaline to hyperalkaline pH conditions. A larger number of publications have dealt with the chemistry of Be(II) under acidic to near-neutral pH conditions, but these are out of the scope of this report and are consequently not discussed in the following.

Gilbert and Garrett (1956) conducted a comprehensive solubility study with α-$Be(OH)_2$(cr) in weakly acidic ($4.8 \leq pH \leq 5.3$) and hyperalkaline pH conditions ($0.02\ m \leq [NaOH] \leq 0.71\ m$). In the case of alkaline samples, the authors worked with nitrogen-

filled flasks to avoid carbonate contamination. Solubility samples were equilibrated for one week. Phase separation was achieved by sedimentation for at least seven days. Experimental data collected in NaOH solutions (see Figure 1) were interpreted by the authors with the formation of $Be(OH)_3^-$ and $Be(OH)_4^{2-}$ according with the equilibrium reactions (1) and (2). Hydrolysis constants for these species recalculated in Baes and Mesmer (1976) and Bruno (1987) from experimental solubility data in Gilbert and Garrett (1956) and using estimated corrections for activity coefficients variation are summarized in Table 1:

$$\alpha\text{-}Be(OH)_2(cr) + OH^- \Leftrightarrow Be(OH)_3^- \quad (1)$$

$$\alpha\text{-}Be(OH)_2(cr) + 2\ OH^- \Leftrightarrow Be(OH)_4^{2-} \quad (2)$$

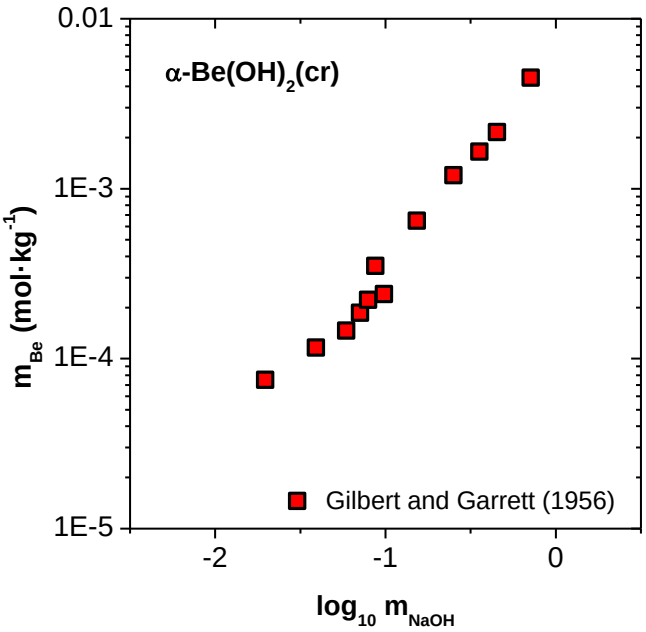

Figure 1. Experimental solubility data reported in Gilbert and Garrett (1956) for α-$Be(OH)_2(cr)$ in 0.02 m ≤ [NaOH] ≤ 0.71 m.

Green and Alexander (1963, 1965) performed solvent extraction experiments with $^7Be(II)$ within $5 \leq pH \leq 13$ using *N*-n-butylsalicylideneimine dissolved in toluene as extractant system. Concentration of $^7Be(II)$ in the organic and aqueous phase was quantified by γ-spectroscopy. The authors interpreted their extraction data according with the chemical reactions (3) and (4), although acknowledging that the decrease in the distribution coefficients observed at pH > 9 (assigned to the formation of $Be(OH)_3^-$) could be attributed also to the decomposition of *N*-n-butylsalicylideneimine. The stability constant reported in Green and Alexander (1965) for the chemical reaction (4) is summarized in Table 1.

$$Be(H_2O)_4^{2+} \Leftrightarrow Be(H_2O)_2(OH)_2(aq) + 2\ H^+ \quad (3)$$

$$Be(H_2O)_4^{2+} \Leftrightarrow Be(H_2O)(OH)_3^- + 3\ H^+ \quad (4)$$

Table 1. Summary of thermodynamic data reported in the literature for the solubility and hydrolysis of Be(II). Only aqueous species forming in alkaline to hyperalkaline pH conditions are reported.

Reference	Method	Medium	T (°C)	$\log_{10} K$	$\log_{10} K°$
α-$Be(OH)_2(cr) + 2\ H^+ \Leftrightarrow Be^{2+} + 2\ H_2O(l)$					
Gilbert and Garrett (1956)	solubility	$HCl / HClO_4$	25		(6.86 ± 0.05) (6.69 ± 0.02)[a] (6.87 ± 0.05)[b]
β-$Be(OH)_2(cr) + 2\ H^+ \Leftrightarrow Be^{2+} + 2\ H_2O(l)$					
Bruno et al. (1987)	solubility	3.0 M $NaClO_4$	25	(6.18 ± 0.03)	(5.9 ± 0.1)
α-$BeO(cr) + H_2O(l) + OH– \Leftrightarrow Be(OH)_3^-$					
Soboleva et al. (1977)	solubility	NaOH	25[c]	3.60	
			150	(2.95 ± 0.2)	
			200	(2.7 ± 0.3)	
			250	(2.4 ± 0.3)	
$Be^{2+} + 3\ H_2O(l) \Leftrightarrow Be(OH)_3^- + 3\ H^+$					
Gilbert and Garrett (1956)	solubility	NaOH	25		$-(23.26 \pm 0.04)$[a] $-(23.46 \pm 0.05)$[b]
Green and Alexandre (1965)	sol. extr.	NaOH	25	$-(24.11 \pm 0.03)$	
$Be^{2+} + 4\ H_2O(l) \Leftrightarrow Be(OH)_4^{2-} + 4\ H^+$					
Gilbert and Garrett (1956)	solubility	NaOH	25		$-(37.4 \pm 0.2)$[a] $-(37.59 \pm 0.05)$[b]

a. recalculated in Baes and Mesmer (1976); b. recalculated in Bruno (1987); c. extrapolated in Soboleva et al. (1977) from experimental results at T = 150, 200 and 250°C

Sengupta (1964) studied the formation of basic beryllium carbonate compounds. The author precipitated from beryllium carbonate solutions at pH ≥ 10 a number of solid phases with the generic formula $M_6[Be_4O(CO_3)_6](cr)$, where $M^+ = 1/3[Co(NH_3)_6]^{3+}$, K^+, Na^+ and NH_4^+. No thermodynamic data is available so far in the literature for these solid phases.

Soboleva et al. (1977) investigated the solubility of α-BeO(cr) in acidic to hyperalkaline pH conditions at 150, 200 and 250°C. The authors explained their experimental observations with the equilibrium reactions (5) to (7). The experimentally determined $\log_{10} K_{s,(1,x)}$ (with x = 1–3, T = 150, 200 and 250°C) and the accordingly extrapolated constants at T = 25°C are summarized in Table 1.

$$\alpha\text{-}BeO(cr) + H^+ \Leftrightarrow BeOH^+ \quad (5)$$

$$\alpha\text{-}BeO(cr) + H_2O(l) \Leftrightarrow Be(OH)_2(aq) \quad (6)$$

$$\alpha\text{-}BeO(cr) + H_2O(l) + OH^- \Leftrightarrow Be(OH)_3^- \quad (7)$$

Bruno et al. (1987a, 1987b) performed the most comprehensive investigation available to date on the system Be(II)–H_2O–CO_2(g). The authors used a combination of e.m.f. measurements and solubility experiments in the range $2.0 \le -\log_{10}[H^+] \le 8.5$ at partial pressures of CO_2(g) of 0.01 to 0.95 atm. Bruno and co-workers quantified the solubility product of the crystalline phase β-$Be(OH)_2(cr)$ (Table 1) and determined the stoichiometry and stability of a number of ternary Be(II)–OH–CO_3 aqueous species (Table 2).

Table 2. Complexation constants of Be(II) with carbonate as reported in Bruno et al. (1987a, 1987b). All constants reported in 3.0 M $NaClO_4$.

Reaction[a]	$\log_{10} K$	Reference
$3\ Be^{2+} + 3\ H_2O(l) + CO_2(g) \Leftrightarrow [Be_3(OH)_3(CO_2)]^{3+} + 3\ H^+$	$-(8.90 \pm 0.02)$	Bruno et al. (1987a)
$5\ Be^{2+} + 6\ H_2O(l) + CO_2(g) \Leftrightarrow [Be_5(OH)_6(CO_2)]^{4+} + 6\ H^+$	$-(17.24 \pm 0.04)$	Bruno et al. (1987a)
$6\ Be^{2+} + 9\ H_2O(l) + 2\ CO_2(g) \Leftrightarrow [Be_6(OH)_9(CO_2)_2]^{3+} + 9\ H^+$	$-(29.46 \pm 0.06)$	Bruno et al. (1987a)
$Be^{2+} + 2\ H_2O(l) + CO_2(g) \Leftrightarrow Be(OH)_2(CO_2)(aq) + 2\ H^+$	$-(10.4 \pm 0.1)$	Bruno et al. (1987a)
	$-(10.12 \pm 0.06)$	Bruno et al. (1987b)
$Be^{2+} + 3\ H_2O(l) + CO_2(g) \Leftrightarrow Be(OH)_3(CO_2)(aq) + 3\ H^+$	$-(16.82 \pm 0.02)$[b]	Bruno et al. (1987b)
	$-(16.68 \pm 0.08)$[c]	Bruno et al. (1987b)
$Be^{2+} + 4\ H_2O(l) + CO_2(g) \Leftrightarrow Be(OH)_4(CO_2)(aq) + 4\ H^+$	$-(24.2 \pm 0.1)$[b]	Bruno et al. (1987b)
	$-(24.22 \pm 0.04)$[c]	Bruno et al. (1987b)
$3\ Be^{2+} + 9\ H_2O(l) + 3\ CO_2(g) \Leftrightarrow [Be_3(OH)_9(CO_2)_3]^{3-} + 9\ H^+$	$-(45.5 \pm 0.5)$	Bruno et al. (1987b)
$3\ Be^{2+} + 10\ H_2O(l) + 3\ CO_2(g) \Leftrightarrow [Be_3(OH)_{10}(CO_2)_3]^{4-} + 10\ H^+$	$-(52.0 \pm 0.5)$	Bruno et al. (1987b)

a. stoichiometry of the complexes (1,2,1), (1,4,1), (3,3,1), (3,9,3), (3,10,3) suggested by Raman as $BeCO_3(aq)$, $[Be_3(OH)_2(HCO_3)]^{3+}$, $[Be_3(OH)_3(CO_3)_3]^{3-}$, $[Be_3(OH)_4(CO_3)_3]^{4-}$, $[Be_5(OH)_4(CO_3)]^{4+}$; b. determined by solubility experiments; c. determined by e.m.f measurements

Figure 2 exemplarily shows the solubility curves of α-$Be(OH)_2$(cr) and β-$Be(OH)_2$(cr) calculated using the thermodynamic data provided in Table A1 of the Appendix. The same set of constants are used in solid and dashed curves, except for the species $Be(OH)_2$(aq), for which $\log_{10} K°_{1,2} = -13.76$ (solid line, as reported in Baes and Mesmer, 1976) and $\log_{10} K°_{1,2} = -11.00$ (dashed line, as reported in Bruno 1987) are used. Differences in the aqueous speciation underlying the solubility curve of α-$Be(OH)_2$(cr) are shown in the fraction diagram in Figure 3. The relevant disagreement between both sets of constants basically arises from the lack of experimental studies in the near-neutral to weakly alkaline pH-range. With regard to cementitious systems, these uncertainties have a direct impact on the calculated solubility of Be(II) within $10 \leq pH \leq 12$, where differences of up to 2 $\log_{10}$-units are observed. Note further that all calculations shown in Figures 2 and 3 have been performed at $I = 0$ due to the lack of reliable SIT ion interaction coefficients for those species forming under alkaline to hyperalkaline pH conditions.

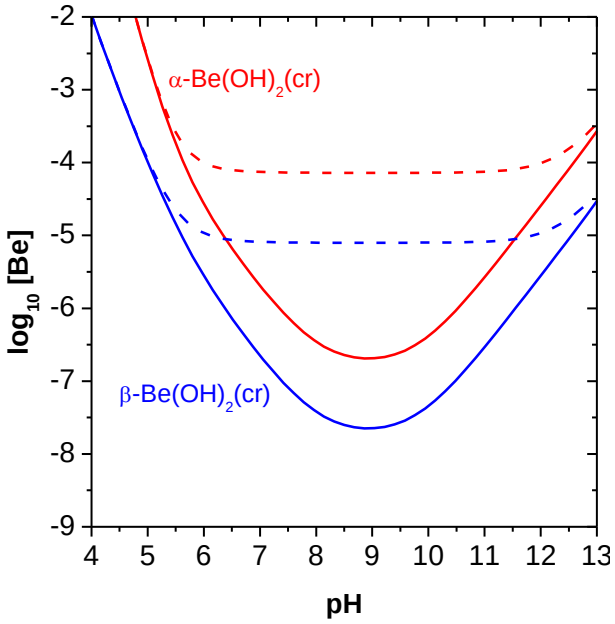

Figure 2. Solubility of α-$Be(OH)_2$(cr) and β-$Be(OH)_2$(cr) as calculated using the thermodynamic data summarized in Table A1. Solid lines calculated using $\log_{10} K°_{1,2}$ = –13.76 as reported in Baes and Mesmer (1976). Dashed lines calculated using $\log_{10} K°_{1,2}$ = –11.00 as reported in Bruno (1987). All calculations performed at I = 0.

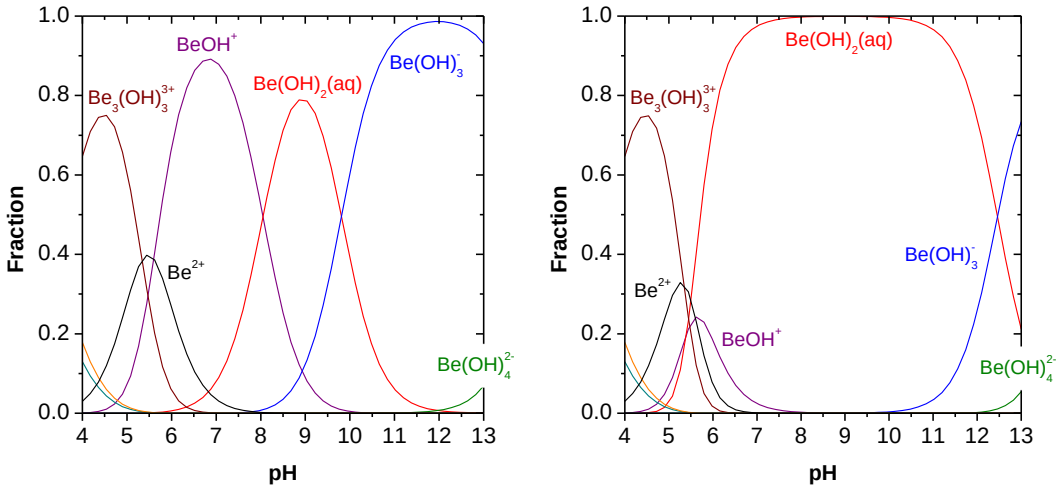

Figure 2. Fraction diagrams of Be(II) underlying the solubility curve of α-$Be(OH)_2$(cr) calculated using the thermodynamic data summarized in Table A1. Left diagram calculated with $\log_{10} K°_{1,2}$ = –13.76 as reported in Baes and Mesmer (1976). Right diagram calculated using $\log_{10} K°_{1,2}$ = –11.00 as reported in Bruno (1987). All calculations performed at I = 0.

Renders and Anderson (1987) investigated the solubility of kaolinite ($Al_2Si_2O_5(OH)_4$) and beryl ($Be_3Al_2Si_6O_{18}$) in the temperature range 363 ≤ T [K] ≤ 573. In order to interpret their solubility data at elevated temperatures, the authors estimated the enthalpy and entropy of step-wise hydrolysis reactions of Be(II) based on the

correlations previously described in Baes and Mesmer (1981). Values of $\Delta_r H°$ and $\Delta_r S°$ estimated in Renders and Anderson (1987) for the step-wise hydrolysis reactions of Be(II), in combination with the corresponding $\log_{10} K°$ reported in Baes and Mesmer (1976) are summarized in Table 3.

Table 3. Enthalpy and entropy data estimated in Renders and Anderson (1987) for the step-wise hydrolysis reactions of Be(II). Stability constants $\log_{10} K°$ as reported in Baes and Mesmer (1976).

Reaction	$\Delta_r H°$ (kJ·mol^{-1})	$\Delta_r S°$ (J·mol^{-1}·mol^{-1})	$\log_{10} K°$
$Be^{2+} + H_2O(l) \Leftrightarrow BeOH^+ + H^+$	47.7	54.4	–5.387
$BeOH^+ + H_2O(l) \Leftrightarrow Be(OH)_2(aq) + H^+$	48.5	4.6	–8.267
$Be(OH)_2(aq) + H_2O(l) \Leftrightarrow Be(OH)_3^- + H^+$	40.6	–46.0	–9.621

A number of experimental studies in the 60's investigated the formation of ternary M–Be(II)–OH solid phases (with M = Na^+, Ca^{2+}, Sr^{2+} and Ba^{2+}) under hyperalkaline pH conditions (Everest et al., 1962; Scholder et al., 1968; among others). The structural definition of these solid phases was based on the predominant role of the anion $Be(OH)_4^{2-}$ (i.e. $Na_2[Be(OH)_4](cr)$, $Ca[Be(OH)_4](cr)$, etc.), although no proof of concept other than quantitative chemical analysis was provided in that publications. Later studies have demonstrated that the structure of these solid phases is more complex than originally proposed (Schmidbaur et al., 1998; Schmidt et al., 1998; Schmidbaur, 2001), and contains polyatomic moieties of Be(II) as those forming under acidic pH conditions. Hence, the compound $Na_2[Be_4(OH)_{10}]\cdot 5H_2O(cr)$ was reported to form in concentrated NaOH solutions (Schmidbaur et al., 1998), whereas the solid phase $Ca_2[Be_2(OH)_7][H_3O_2]\cdot 2H_2O(cr)$ was observed in alkaline $CaCl_2$ solutions. Note that the latter structure contains the hydrated OH^- ion, $H_3O_2^-$, which was previously reported in the literature (Ruf et al., 1996; Tuckerman et al., 1997, among others). The role of these polyatomic Be(II) moieties in the aqueous phase and the corresponding equilibria with the monomeric $Be(OH)_4^{2-}$ species and solid phases remain so far unknown:

$$2\ Be(OH)_4^{2-} \Leftrightarrow [Be_2(OH)_7]^{3-} + OH^- \quad (8)$$

$$4\ Be(OH)_4^{2-} \Leftrightarrow [Be_4(OH)_{10}]^{2-} + 6\ OH^- \quad (9)$$

High level nuclear waste resulting from plutonium production is stored in more than 170 tanks in the Hanford Site, WA (USA). Most of these wastes are characterized by high pH (12–13.5) and the presence of concentrated salts ($NaNO_3$, $NaNO_2$, etc.). As a result of its use as a component of the Zircaloy 2 fuel cladding processed in the PUREX plant and as a feed constituent in the plutonium finishing plant (PFP), beryllium is found in both solid and liquid phases of the Hanford waste (Reynolds, 2013). Although with a very heterogeneous distribution, Be(II) concentrations of up to 180 ppm and 3 ppm ($\approx 3.3\cdot 10^{-4}$ M) are found in solid and liquid wastes, respectively. Provided the high concentration of carbonate and fluoride in the alkaline wastes, Reynolds speculated on the possible predominance of the species $Be(OH)_2CO_3^{2-}$ and $BeF_y(OH)_m^{2-y-m}$ in the aqueous phase of the Hanford tanks.

^{9}Be NMR and DFT calculations have been also used in the literature to assess the aqueous speciation of Be(II) (Chinea et al., 1997; Alderighi et al., 1998; Rozmanov et al., 2004, among others). So far most of these studies have focused in the acidic to near-neutral pH range where cationic hydrolysis species prevail, but may also prove to be helpful in the assessment of Be(II) aqueous speciation under alkaline to hyperalkaline pH conditions where anionic hydrolysis species are known to form.

Sorption of Be in cementitious systems

No experimental studies investigating the uptake of Be(II) by cement and cementitious materials are available in the literature. Due to the high charge-to-size ratio of Be^{2+} (z/d = 1.21, with $d = r_{Be^{2+}} + r_{OH^-}$) caused by its very small size ($r_{Be^{2+}} = 0.27$ Å), Wieland and Van Loon (2003) speculated on the moderate sorption to be expected in hardened cement paste (HCP). In spite of this, the authors conservatively proposed a $R_d = 0$ accounting for the predominance of negatively charged hydrolysis species $Be(OH)_3^-$ and $Be(OH)_4^{2-}$ in the pore water conditions expected in cement systems (Wieland and Van Loon, 2003; Wieland, 2014). A similar approach was proposed in the recent review work by Ochs and co-workers (Ochs et al., 2016).

Summary and outlook

This state of the art report highlights the relevant limitations affecting the knowledge of Be(II) chemistry under alkaline to hyperalkaline pH conditions, both in the absence and presence of carbonate. Hence, important uncertainties arise with regard to the aqueous species of Be(II) prevailing in this pH-range and absence of carbonate. The formation of ternary Na/Ca–Be(II)–OH solid phases has been described in a number of experimental studies, but no thermodynamic data is available so far in the literature. The possible role of these solid phases in controlling the solubility of Be(II) in cementitious systems remains unclear. Large uncertainties arise also on the solubility of α/β-$Be(OH)_2$(cr) within $10 \leq pH \leq 12$, mostly due to the lack of experimental studies within this pH-range and the very discrepant values provided for the second hydrolysis constant of Be(II). This pH-range is particularly relevant in the later degradation steps of cement, and thus dedicated studies with Be(II) targeting this pH-region are greatly needed. Similarly as for hydrolysis, most comprehensive experimental studies investigating Be(II) complexation by carbonate have focused on acidic to weakly alkaline pH conditions. Because of the very strong hydrolysis of Be(II), ternary Be(II)–OH–CO_3 complexes were already reported at $-\log_{10} [H^+] \leq 8.5$. A large collection of ternary complexes (both mono- and polynuclear) and solid phases is consequently expected under hyperalkaline conditions.

No experimental studies are available so far on the uptake of Be(II) by cement or cementitious materials. R_d estimates provided in the literature are largely conservative and can be significantly improved by a dedicated experimental program.

The uncertainties identified within this state of the art report are in line with the motivation of KIT–INE to investigate the chemistry of Be(II) in cementitious systems within WP2 of the CEBAMA project. In a first step, KIT–INE will investigate the solubility and hydrolysis of Be(II) in dilute to concentrated NaCl and $CaCl_2$ solutions within $5 \leq pH_m \leq 14$ (with $pH_m = -\log_{10} [H^+]$). The near neutral pH range is considered for a more accurate characterization of $\log_{10} K°_{s,0}$ of the solid phases investigated, whereas the use of dilute to concentrated salt systems aims at a better extrapolation of conditional constants to the reference state ($I = 0$) and the simultaneous determination

of the (SIT) activity model parameters for calculating activity coefficients. Experimental focus will be given to (undersaturation) solubility experiments complemented with extensive solid phase characterization (XRD, SEM–EDS, quantitative chemical analysis, XPS). The aqueous phase will be also investigated by ^{9}Be NMR, although the KIT–INE team is aware of the limitations of this technique/system under hyperalkaline pH conditions. The final goal of this part of the study is to derive complete and accurate chemical, thermodynamic and activity models for the system Be^{2+}–Na^{+}–Ca^{2+}–OH^{-}–Cl^{-}–H_2O(l). Although it is expected that the thermodynamic models and chemical speciation schemes derived for NaCl systems can be adopted for the modeling of the largely analogous KCl systems relevant during certain evolution stages of cement degradation, work will include selected solubility studies to validate this analogy and related chemical thermodynamics. Based upon the studies to investigate Be(II) solubility in the absence of carbonate, latter studies will include experiments to assess the influence of carbonate. Focus will be put on the systems under absence of carbonate for which comprehensive chemical and thermodynamic models will be developed.

In a second step, the uptake of Be(II) by ordinary Portland cement (OPC, fresh) and C–S–H phases with different Ca:Si ratio will be investigated. Sorption isotherms with increasing [Be] will be quantified with these materials. In the case of C–S–H phases, different pH conditions ($10.0 \leq pH \leq 13.3$) will be investigated as imposed by the corresponding Ca:Si ratio. The preparation of these solid phases will be conducted in close co-operation with BRGM, PSI–LES and EMPA. The main goal of this part of the study is the quantification of Be(II) uptake by cementitious materials within different degradation stages of cement. Modelling of the sorption data will be also attempted, either as surface complexation or as solid solution models.

References

Alderighi, L., Bianchi, A., Mederos, A., Midollini, S., Rodriguez, A., Vacca, A. 1998, *Thermodynamic and multinuclear NMR study of beryllium(II) hydrolysis and beryllium(II) complex formation with oxalate, malonate, and succinate anions in aqueous solution*. Eur. J. Inorg. Chem., 1209–1215.

Baes, C. F., Mesmer, R. E. 1976, *The hydrolysis of cations*. Wiley.

Baes, C. F., Mesmer, R. E. 1981, *The thermodynamics of cations hydrolysis*. Am. J. Sci., **281**: 953–962.

Bruno, J. 1987, *Beryllium(II) hydrolysis in 3.0 mol dm^{-3} perchlorate*. J. Chem. Soc. Dalton Trans., 2431–2437.

Bruno, J., Grenthe, I., Sandström, M., Ferri, D. 1987a, *Studies of metal carbonate equilibria. Part 15. The beryllium(II)–water–carbon dioxide(g) system in acidic 3.0 mol dm^{-3} perchlorate media*. J. Chem. Soc. Dalton Trans., 2439–2444.

Bruno, J., Grenthe, I., Munoz, M. 1987b, *Studies of metal carbonate equilibria. Part 16. The beryllium(II)–water–carbon dioxide(g) system in neutral-to-alkaline 3.0 mol dm^{-3} perchlorate media at 25°C*. J. Chem. Soc. Dalton Trans., 2445–2449.

Chinea, E., Dominguez, S., Mederos, A., Brito, F., Sanchez, A., Ienco, A., Vacca, A. 1997, *Hydrolysis of beryllium(II) in DMSO:H_2O*. Main Group Metal Chemistry, **20**: 11–17.

Everest, D. A., Mercer, R. A., Miller, R. P., Milward, G. L. 1962, *The chemical nature of sodium beryllate solutions*. J. Inorg. Nucl. Chem., **24**: 525–534.

Green, R. W., Alexander, P. W. 1963, *Hydrolysis of bis-(acetylacetonato)-beryllium(II)*. J. Phys. Chem., **67**: 905–907.

Green, R. W., Alexander, P. W. 1965, *Schiff base equilibria. II. Beryllium complexes of N-n-butylsalicylideneimine and the hydrolysis of the Be^{2+} ion*. Austr. J. Chem., **18**: 651–658.

Gilbert, R. A., Garrett, A. B. 1956, *The equilibria of the metastable crystalline form of beryllium hydroxide. $Be(OH)_2$ in hydrochloric acid, perchloric acid and sodium hydroxide solutions at 25°*. J. Am. Chem. Soc., **78**: 5501–5505.

Ochs, M., Mallants, D., Wang, L. 2016, *Radionuclide and Metal Sorption on Cement and Concrete*. Springer International Publishing.

Reynolds, J. G. 2013, *The concentration and distribution of beryllium in Hanford high-level waste*. Proceedings of the IHLRWMC, Albuquerque, NM, April-May, 2013.

Renders, P. J., Anderson, G. M. 1987, *Solubility of kaolinite and beryl to 573 K*. Applied Geochemistry, **2**: 193–203.

Rozmanov, D. A., Sizova, O., Burkov, K. A. 2004, *Ab initio studies of beryllium aquahydroxocomplexes*. Journal of Molecular Structure: THEOCHEM, **712**: 123–130.

Ruf, M., Weis, K., Vahrenkamp, H. 1996, *$Zn{-}O_2H_3{-}Zn$: a coordination mode of the hydrolytic zinc−aqua function and a possible structural motif for oligozinc enzymes*. J. Am. Chem. Soc., **118**: 9288–9294.

Schmidbaur, H. 2001, *Recent contributions to the aqueous coordination chemistry of beryllium*. Coordination Chemistry Reviews, **215**: 223–242.

Schmidbaur, H., Schmidt, M., Schier, A., Riede, J., Tamm, T., Pyykkö, P. 1998, *Identification and structural characterization of the predominant species present in alkaline hydroxyberyllate solutions*. J. Am. Chem. Soc., **120**: 2967–2968.

Schmidt, M., Schier, A., Riede, J., Schmidbaur, H. 1998, *The novel binuclear hydroxyberyllate species $[Be_2(OH)_7]^{3-}$ and the hydroxide hydrate anion $[H_3O_2]^-$ as components of beryllate equilibria*. Inorg. Chem., **37**: 3452–3453.

Scholder, R., Hund, H., Schwarz, H. 1968, *Über Hydroxoberyllate des Natriums und der Erdalkalimetalle*. Zeitschrift für anorganische und allgemeine Chemie, **361**: 284–294 (in German).

Schwarzenbach, G., Wenger, H. 1969, *Die Deprotonierung von Metall-Aquoionen I.: $Be\cdot_{aq}^{2+}$ Solvatations-Isomerie*. Helv. Chim. Acta, **52**: 644–665 (in German).

Sengupta, A. K. 1964, *Basic beryllium complex carbonates*. J. Inorg. Nucl. Chem., **26**: 1823–1828.

Soboleva, G. I., Tugarinov, I. A., Kalinina, V. F., Khodakovskiy, I. L. 1977, *Investigation of equilibria in the system $BeO–NaOH–HNO_3–H_2O$ in the temperature interval 25°–250°C*. Geokhimiya, **7**: 1013–1024 (in Russian).

Tuckerman, M. E., Marx, D., Klein, M. L., Parrinello, M. 1997, *On the quantum nature of the shared proton in hydrogen bonds*. Science, **275**: 817–820.

Wieland, E., Van Loon, L. R. 2003, *Cementitious near-field sorption data base for performance assessment of an ILW repository in opalinus clay*. PSI report 03-06.

Wieland, E. 2014, *Sorption Data Base for the Cementitious Near Field of L/ILW and ILW Repositories for Provisional Safety Analyses for SGT-E2*. NAGRA Technical report 14-08.

Appendix

Table A1. Solubility and hydrolysis constants of Be(II) reported in the literature and considered in the present work for thermodynamic calculations.

Reaction	$\log_{10} K°$	Reference
α-$Be(OH)_2(cr) + 2\ H^+ \Leftrightarrow Be^{2+} + 2\ H_2O(l)$	(6.86 ± 0.05)	Gilbert and Garrett (1956)[a]
β-$Be(OH)_2(cr) + 2\ H^+ \Leftrightarrow Be^{2+} + 2\ H_2O(l)$	(5.9 ± 0.1)	Bruno et al. (1987)
α-$BeO(cr) + 2\ H^+ \Leftrightarrow Be^{2+} + H_2O(l)$	(5.0 ± 0.1)	Soboleva et al. (1977)
$Be^{2+} + H_2O(l) \Leftrightarrow BeOH^+ + H^+$	$-(5.6 \pm 0.1)$	Schwarzenbach and Wenger (1969); Bruno (1987)
$Be^{2+} + 2\ H_2O(l) \Leftrightarrow Be(OH)_2(aq) + 2\ H^+$	*$-(13.65 \pm 0.05)$*	*Baes and Mesmer (1976)*
	$-(11.00 \pm 0.05)$	*Bruno (1987)*
$Be^{2+} + 3\ H_2O(l) \Leftrightarrow Be(OH)_3^- + 3\ H^+$	$-(23.46 \pm 0.05)$	Gilbert and Garrett (1956)[a]
$Be^{2+} + 4\ H_2O(l) \Leftrightarrow Be(OH)_4^{2-} + 4\ H^+$	$-(37.59 \pm 0.05)$	Gilbert and Garrett (1956)[a]
$2\ Be^{2+} + H_2O(l) \Leftrightarrow [Be_2OH]^{3+} + H^+$	$-(3.47 \pm 0.05)$	Bruno (1987)
$3\ Be^{2+} + 3\ H_2O(l) \Leftrightarrow [Be_3(OH)_3]^{3+} + 3\ H^+$	$-(8.86 \pm 0.05)$	Bruno (1987)
$5\ Be^{2+} + 6\ H_2O(l) \Leftrightarrow [Be_5(OH)_6]^{4+} + 6\ H^+$	$-(19.5 \pm 0.1)$	Bruno (1987)
$6\ Be^{2+} + 8\ H_2O(l) \Leftrightarrow [Be_6(OH)_8]^{4+} + 8\ H^+$	$-(26.3 \pm 0.1)$	Bruno (1987)

a. recalculated in Bruno (1987)

Molybdenum behaviour in cementitious materials (AMPHOS)

Grivé, M., Olmeda, J.

Affiliation: Amphos 21 Consulting

e-mail: mireia.grive@amphos21.com

Abstract

Molybdenum-93, an activation product from the steel with a half-life of 4,000 years, supposes a threat to LILW disposal safety as it is able to form highly mobile and thermodynamically stable molybdate anions in cementitious porewaters. In general, there is a lack of experimental information in the literature to gain insight into this element behaviour under different conditions. Initially, ettringite (AFt-SO_4) and monosulphate (AFm-SO_4) have been proposed as viable cement constituents for oxyanion immobilization via sulphate substitution. Experimental evidences point out that ettringite has the potential to accommodate oxyanions from a solely thermodynamic point of view, although this phase uptake strongly depends on size and charge similarities between sulphate and substituting oxyanions. Oxyanion-substituted ettringites can be easily converted into sulphate ones if they are exposed to sulphate influx. Monosulphate is more suitable than ettringite for oxyanion immobilization as it is not as restricted as ettringite with regard structural charge and size. AFm-SO_4 phase is reported to be the major host phase for anion immobilization at pH above 12, being able at the same time to control oxyanion solubility to lower levels than ettringite. There is a general lack of thermodynamic parameters which difficult the development of efficient models to predict molybdenum behaviour at repository conditions. C-S-H gels binding mechanisms for oxyanion depends on surface zeta potential, two C-S-H phases with C/S ratio of 0.8 and 1.1 has been suggested to be studied as they show clear opposite ζ values.

Introduction

The chemical processes occurring within the near-field due to metal corrosion and concrete degradation, as well as interactions with groundwater flowing through the facility, will determine the long-term chemical evolution of the repository near-field.

Two crucial parameters characterizing the chemical system are both pH and the redox potential, the latter being important as it governs aqueous speciation of some redox-sensitive radionuclides. This in turn, defines the source term for these radionuclides from the near-field into the geosphere and subsequently to the biosphere. This is the case of molybdenum-93, an activation product from the steel with a half-life of 4000 years. Mo is a redox-sensitive element, whose aqueous speciation is dominated by the thermodynamically highly stable molybdate (MoO_4^{2-}) - Molybdates of the alkali metals and ammonium are quite soluble in water. This species is typically considered to dominate even under moderately reducing conditions. However, even though the most common oxidation state of Mo is +VI, its reduction to Mo +IV can be envisaged considering strongly reducing redox conditions developed in the near-field under high pH conditions imposed by cementitious surroundings.

Besides the groundwater flow barrier function, concrete is included in the repository design to condition the near-field pore water to a high pH for long periods of time and to provide abundant microstructural surfaces for the sorption of radioelements. The high pH pore water ensures an environment in which the solubility of many radioelements is lower than under circum-neutral pH conditions.

Under the cementitious conditions (pH>9), Powellite ($CaMoO_4$(s)) becomes the solubility-controlling phase under all the states of cement degradation. In this case, molybdenum solubility is very sensitive to differences in calcium concentrations.

Therefore, the main parameters that may control molybdenum solubility are pH, Eh and calcium concentration. Under cementitious conditions, Mo released from the waste could be controlled either by $CaMoO_4$(s) (Mo(VI)) or MoO_2(s) (Mo(IV)) – depending on the redox potential and dissolved Ca concentrations.

However, given large amounts of dissolving/precipitating cementitious phases, Mo dissolved concentrations are expected to be further reduced by additional processes, such as surface complexation and ion-exchange. The most representative phases responsible for molybdate immobilization in cement environment are reported to be AFt and AFm phases.

Apart of AFt and AFm phases, even though no specific studies have been focused on C-S-H capacities for molybdate immobilization, experimental data obtained from other anions such as CrO_4^{2-} and AsO_4^{3-} suggest that C-S-H gels might be also important cementitious phases to retain MoO_4^{2-}.

On the other hand, Mo uptake in cement-based materials might be strongly reduced by the presence of some other anions such as $B(OH)_4^-$ or CrO_4^{2-}, SeO_4^{2-}, SO_4^{2-}, OH^- and CO_3^{2-} in the system.

Further experimental work would be of interest to fully understand the behavior of Mo under cementitious environments. The most important uncertainty concerning molybdenum is the scarcity of thermodynamic data available in the literature. Although the chemical behavior of this element is assumed to be alike to Selenium (under alkaline conditions) due to structural and electric equivalences, there are still a rather large uncertainties and insufficient information on the redox phenomena, reaction kinetics, changes in solubility and speciation, release mechanisms and solid solution formation.

Objectives

The overall objectives of WP2 corresponding to CEBAMA framework are to study radionuclide retention processes in high pH concrete environments on relevant hydrated cement phases and alteration products. In this context, Amphos 21 in collaboration with ANDRA will focus on **molybdenum retention to contribute to the acquisition of data and understanding the retention mechanisms of molybdenum in cement.**

The Amphos 21 objectives include:

- Study of the kinetic evolution of the anionic substitution of Mo on cement pastes as well as on pure phases.
- Develop a bottom-up description of Mo retention mechanisms and the parameters affecting its potential release to solution.

The main expected outcome is the acquisition and the understanding of the mobility/retention processes of Mo through the different cementitious barriers. The information and models derived within WP2 of CEBAMA can be applied for high level waste disposal scenarios, but also offer the possibility to assess several aspects of low and intermediate level waste disposal on a significantly improved scientific and technical basis.

The general methodology to fulfil the objectives comprises a set of successive specific objectives or tasks. These tasks will be subsequently carried out jointly to complete the abovementioned overall objectives.

Specific objective of task 1

Task 1 will involve a literature review and pre-experimental thermodynamic calculations. The details of these sub-tasks are explained as follows:

Literature review: An in-depth revision of related literature on the latest available data of interest. The study will focus on the necessary parameters to help experimental design and modeling with special attention to:

- Molybdenum chemical behavior in alkaline environments (pH > 11) including thermodynamic data.
- All the parameters potentially affecting R_d of Mo and its kinetics onto cement pastes and pure cementitious phases.
- Stability fields and solubility of cementitious phases presumed to be study.
- Experimental data reporting zeta potential of cementitious systems and its influence towards anions retention.
- Experimental data from AFt and AFm analogues substituted with other anions (e.g. SeO_4^{2-}, CrO_4^{2-}).

Thermodynamic calculations: Based on information and parameters gathered in the literature review, this task will focus on the modeling of these parameters in order to identify gaps of information and sensitive parameters and assumptions as well as their experimental accessibility.

This methodological (desk) study will define and scope the experimental approach and will aid to identify the most interesting conditions to be studied (e.g. define type of experimental setup and solid phases to be studied, i.e. CEM V type, AFm and AFt phases, etc.).

Literature review

Sources of Molybdenum within the near-field

Typical molybdenum radionuclides in LILW are Mo-99 and Mo-93. While the former has a half-life of $4.52 \cdot 10^{-3}$ years, the latter (Mo-93) in turn is a synthetic radioisotope with a half-life of 4000 years formed by irradiation with thermal neutrons and fast neutrons (Lindgren et al. 2007). Sources for Mo-93 are metallic materials (steels and zircaloy in the core region), and activation of molybdenum in dissolved form or as corrosion particles in the coolant (Figure 1). The release of activation products in the core components is controlled by the corrosion of steel and stainless steel.

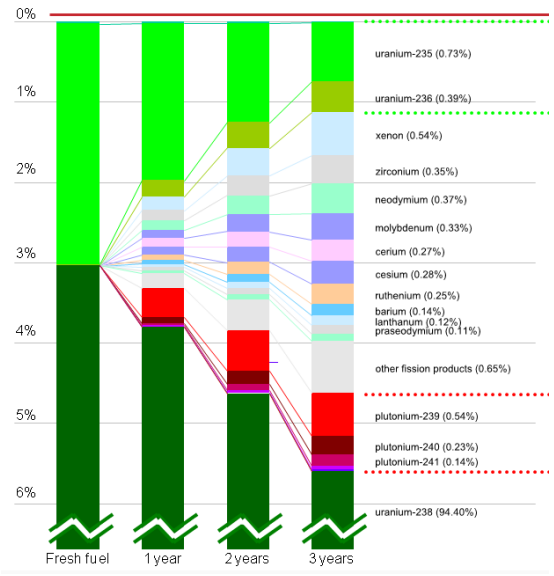

Figure 1. Evolution with time of the composition of a conventional nuclear fuel (from fresh fuel to 3-year irradiation). Source: Thorium: Reduce, Reuse, Recycle, (n.d.)

Solubility and speciation of Molybdenum

Molybdenum is redox-sensitive with broad range of oxidation states, the most common are +IV and +VI. Under anoxic/sulphidic (euxinic) conditions, Molybdenite ($Mo^{IV}S_2$) is the most common mineral and the main commercial source of molybdenum, however, Mo is predicted to exist in its most oxidized state in oxic waters as tetrahedrally coordinated molybdate anion ($Mo^{VI}O_4^{2-}$ - Figure 2).

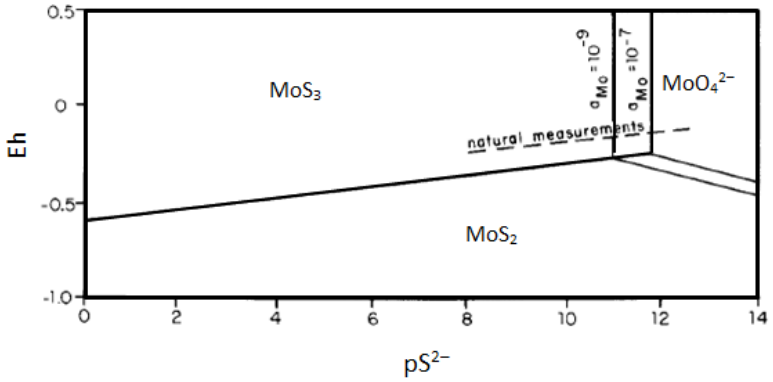

Figure 2. Redox potential – pS diagram for molybdenum in water at 25 °C and pH = 8. Dashed line stands for natural measurements after Berner (1964). Source: Bertine (1972)

Solubility of the common alkali and alkali earth salts of molybdate are usually high, the most water soluble compounds of Mo (VI) include ammonium, sodium, potassium and magnesium salts (Scadden, 1960). However, molybdenum compounds show in general low solubility in water, forming rather insoluble compounds with Hg^{2+}, Pb^{2+}, Sr^{2+} or Th^{4+} (Table 1).

Table 1. Insoluble compounds of molybdenum. Source: Scadden (1960) and others.

Reagent	Precipitate	Water solubility (g/100g of water)
Ag^{+}	Ag_2MoO_4	$4.4 \cdot 10^{-3}$ (25 °C)
Ba^{2+}	$BaMoO_4$	$5.8 \cdot 10^{-3}$ (23 °C)
Bi^{3+}	$Bi_2(MoO_4)_3$	$2.0 \cdot 10^{-2}$
Ca^{2+}	$CaMoO_4$	$4.1 \cdot 10^{-3}$ (20 °C)
Cd^{2+}	$CdMoO_4$	sl. soluble
Hg_2^{2+}	Hg_2MoO_4	insoluble
Pr^{3+}	$Pr_2(MoO_4)_3$	$1.2 \cdot 10^{-3}$ (20 °C)
Pb^{2+}	$PbMoO_4$	$1.2 \cdot 10^{-5}$ (20 °C)
Sr^{2+}	$SrMoO_4$	$1.1 \cdot 10^{-2}$ (20 °C)
Th^{4+}	$Th(MoO_4)_2$	insoluble

When Mo is found at high concentration in solution and pH < 7, this metal oxyanions tend to condense to form polymolybdate ions, however the principal Mo species existing at alkaline conditions is the mononuclear molybdate ion MoO_4^{2-}.

Furthermore, molybdenum has a strong capacity to form complex anions such as heteropoly acids, peroxy-molybdates, complexes with halides, cyanide, thiocyanate, etc., as well as complexes with organic substances such as oxalic, citric acids, EDTA (a reduction factor of 1 is proposed for molybdenum in the presence of organic ligands based on the work performed by Colàs et al. (2014). See sorption section for more details).

Solubility and speciation of Mo under alkaline/cementitious conditions

The main parameters affecting molybdenum solubility are the pH, the redox potential of the system and calcium concentrations present in contacting waters. At the conditions imposed by cementitious media (strong alkaline pH), molybdate anion is soluble and thermodynamically stable even under highly reducing conditions (Figure 3a). This can be observed in Figure 3b, where maximum molybdate dissolved concentration is unaffected in a wider pe range for higher pH.

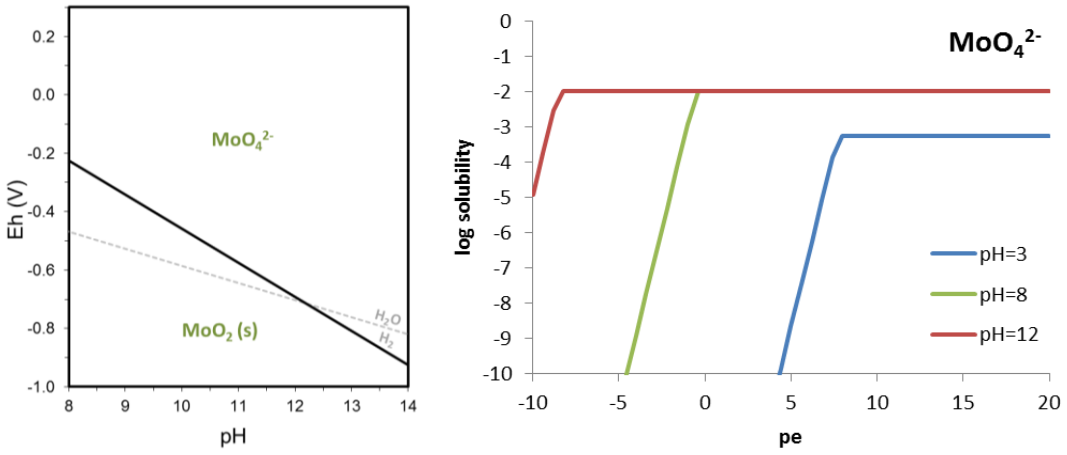

(a) (b)

Figure 3. (a) Predominance Eh/pH diagram of Mo at 25 ºC (Phase-controlled environment) $[Mo(VI)]_{tot} = 2 \cdot 10^{-6}$ M; $[Ca(II)]_{tot} = 2 \cdot 10^{-2}$ ML; (b) Solubility of Mo versus pe at different system pH $[Mo]_0 = 10^{-2}$ M (***Diagrams calculated in the present work with Spana v3 using ThermoChimie database v9b0***).

Under cementitious conditions, $CaMoO_4$(s) could be the solubility-controlling phase depending on the redox potential and dissolved Ca concentrations. As can be observed in Figure 4 performed in the present work with TC database v9b0, at 10^{-2} M of dissolved calcium concentration, the area where Powellite might precipitate covers a wide range of pH and Eh, suggesting the great stability of this phase at cementitious-related conditions. Only at advanced degradation states of cement, dissolved Mo solubility could be controlled by MoO_2(s) at moderate reducing conditions. Note that Figure 4 only depicts a ternary system where Ca, Mo and H_2O have been considered; so in a more complex system, e.g. in composite cements containing Blast Furnace Slags (BFS) (e.g. CEM III, CEM V), sufficient sulphide content might be present so as to form other compounds such as MoS_2. Furthermore, as Kindness et al. (1994) suggested, a more complex system will involve the inclusion of Mo in any hydrated cement phase which will modify its solubility at these conditions (see sorption section).

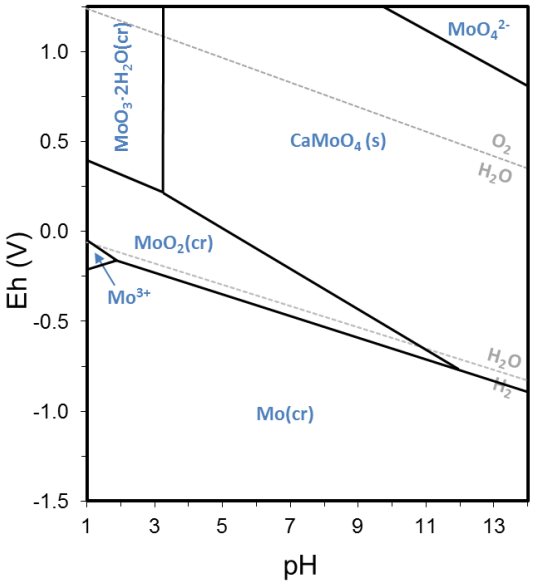

Figure 4. Predominance Eh/pH diagram of the system Mo-Ca-H_2O at 25 °C. [Ca(II)]=10^{-2} M; [Mo(VI)]=10^{-3} M. (***Diagram calculated in the present work with Spana v3 using ThermoChimie database v9b0 (*****https://www.***thermochimie-**tdb.com*****)***

From the calculations carried out with ThermoChimie database v7b by Ochs et al. (2015), the authors also suggested Powellite as the only solid phase relevant to control the dissolved Mo concentration. They also indicate that this phase solubility is pH-dependent as Powellite precipitation is favoured at lower pH which means that molybdate activity (i.e. the solubility) decreases with decreasing pH as is controlled by equation 10:

$$CaMoO_4(s) + 2H_2O \rightarrow Ca(OH)_2(s) + MoO_4^{2-} + 2H^+ \quad [\log K = -30.7] \qquad \text{eq. 10}$$

Kindness et al. (1994) studied molybdenum solubility in OPC and reported a dissolved Mo concentration of $6 \cdot 10^{-5}$ M after 30 days of experiment. The solid phases identified were Powellite ($CaMoO_4$(s)) and Mo-substituted cementitious phases. Berner (2002) conducted solubility and speciation calculations in cementitious pore waters using the Nagra/PSI Chemical Thermodynamic Data Base for Mo. He established the total dissolved concentration of this element in $2.6 \cdot 10^{-5}$ M at -230 mV with $CaMoO_4$(s) resulting as the stable solid (MoO_2(s) was only stable below -750 mV). The underlying

aqueous speciation was dominated by molybdate ion. From his calculations, solubility increased to $1.6 \cdot 10^{-3}$ M at pH 13.44, which was assumed to be the upper limit.

More recently, Berner (2014) performed a new set of solubility calculations with the most recent version of GEMS/PSI (GEMS3.2 v.890) using the PSI/Nagra Chemical Thermodynamic Data Base 12/07 with data for hydrated cement phases from CEMDATA07 and with data from the literature concerning Mo. The calculated Powellite solubility was established at $7.2 \cdot 10^{-6}$ [mol/kg H_2O], which was reported as the recommended value. Table 2 displays the recommended and upper limit values as well as speciation obtained by this author latest calculation.

Table 2. Recommended and upper limit molybdenum solubility and corresponding underlying speciation calculated by Berner (2014).

Limiting phase – $CaMoO_4$(s)	Calculated solubility (mol/kg H_2O)	Speciation
Recommended	$7.2 \cdot 10^{-6}$	MoO_4^{2-} (82.9%) $CaMoO_4$(aq) (17.1%)
Upper limit	$2.0 \cdot 10^{-5}$	MoO_4^{2-} (60.5%) $CaMoO_4$(aq) (39.5%)

In alkaline porewaters of Maqarin, the measured concentrations of molybdenum are in the order of 10^{-6} M (Linklater, 1998). Based on these experimental data from natural analogues and solubility calculations, Grivé et al. (2012) performed a solubility assessment of different radionuclides and indicated the Mo most likely concentrations at alkaline conditions (Figure 5). The upper limit of the solubility range is given by the highest solubility of $CaMoO_4$(s) ($3 \cdot 10^{-4}$ M) whereas the lower limit are defined by the lower concentration measured in Natural Analogues groundwater (10^{-6} M). The author indicated that these smaller values would include the effect of sorption processes in Mo retention.

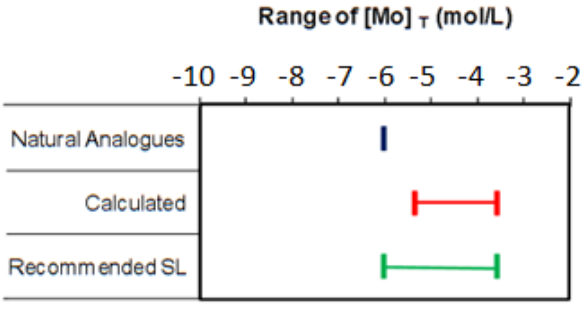

Figure 5. Mo solubility limits analysed in Natural Analogues and calculated. On the basis of these data, recommended range of Mo concentration is also given. Source: Grivé et al. (2012).

Ochs et al. (2015) plotted the solubility of $CaMoO_4$(s) with changing Ca concentration to simulate the fate of this phase along an eventual cement degradation represented by Ca dissolved concentration in the porewater. As can be observed in Figure 6, where dissolved calcium and molybdenum concentration are shown, when cement porewater is fresh (state I - pH = 13.5), alkali concentration is limiting Portlandite solubility by common ion effect, so Mo dissolved concentration is high. As alkali content has being removed from solution (state II - pH = 12.5), dissolved Mo concentration follows a steady decrease, reaching its lowest value in solution with $2 \cdot 10^{-6}$ mol/kg when the system is governed by Portlandite equilibrium. Once Portlandite has dissolved (pH <

12.5), Mo aqueous content suffers a constant increase in state III which is associated with a decrease of Ca concentration. At these degradation states (III and IV), Ca dissolved content is regulated by the solubility of C-S-H phases and varies as function of pH, and therefore the solubility of $CaMoO_4$(s) will be affected.

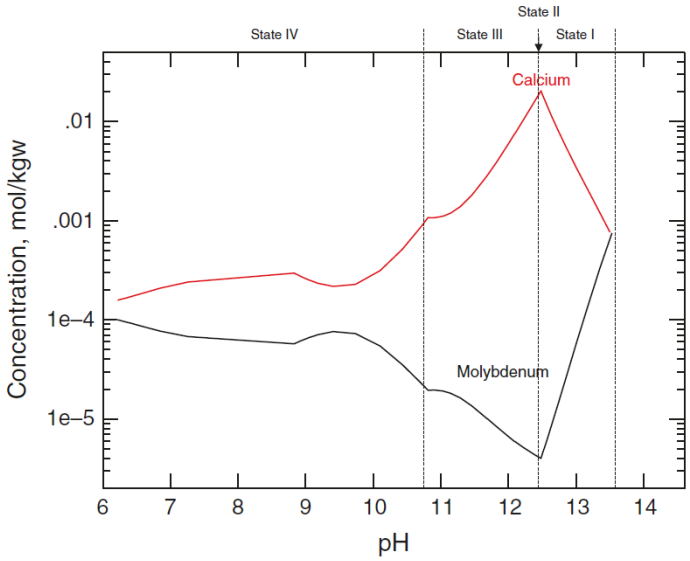

Figure 6. Solubility of $CaMoO_4$(s) in a system where the concentration of calcium is controlled by the solubility of portlandite at State I–II (pH 13.5–12.5), at State III C-S-H_1.6 to pH ~ 12.1, C-S-H_1.2 to pH ~ 11.7, and C-S-H_0.8 to pH = 10.8. Source: Ochs et al. (2015).

These results are in agreement with the ones experimentally acquired by Kindness et al. (1994), where the solubility of Powellite in distilled water, saturated $Ca(OH)_2$ and saturated $Ca(OH)_2$ in 0.1 M NaOH was determined at 25°C (Table 3).

Table 3. Experimentally determined $CaMoO_4$(s) solubility at 25 °C in different media. Source: Kindness et al. (1994)

$CaMoO_4$(s) solubility	**Mo concentration (ppm)**	
	ICP/MS	AAS
Distilled water	21.46	25.40
Saturated $Ca(OH)_2$	25.69	30.81
Saturated $Ca(OH)_2$ in 0.1 NaOH	35.10	39.10

Solubility calculations carried out in the present work

Calculations performed with ThermoChimie v.9.0 suggest that, under cementitious conditions, Powellite ($CaMoO_4$(s)) could be the solubility-controlling phase with a solubility of ~$2.9 \cdot 10^{-4}$ m. The underlying speciation is completely dominated by MoO_2^{4-} (Figure 7). Under eventual cement degradation, molybdenum concentration in solution is still controlled by Powellite in all degradation states, i.e. alkali-free (state II), portlandite-free (state III) and totally degraded (state IV) (Figure 7).

Solubility of this phase is strongly associated to calcium availability in solution, and therefore Powellite solubility follows a symmetrical trend as Calcium dissolved concentration (see Figure 6 and 7), i.e. at state I, the presence of alkalis limits Ca content in solution and thus Powellite solubility shows a maximum (orange dots in Figure 7); from state I to state II, calcium concentrations increase in solution (blue dots) and promotes Powellite precipitation (State II, Figure 7); from this degradation state

onwards, as the cement is undergoing a progressive de-calcification, Ca decreases in solution and slightly enhances Powellite dissolution (States III and IV, Figure 7). Therefore, Powellite solubility covering the conditions resulting from the degradation of cement is within the range $5.52 \cdot 10^{-6}$ and $2.92 \cdot 10^{-4}$ mol/kgw, which in turn assumes a pH range from 13.29 to 9.96 and a redox potential of -278.48 to +15.80 mV. It is noteworthy to mention that molybdenum aqueous speciation is entirely governed by MoO_4^{2-} ion at every studied degradation state.

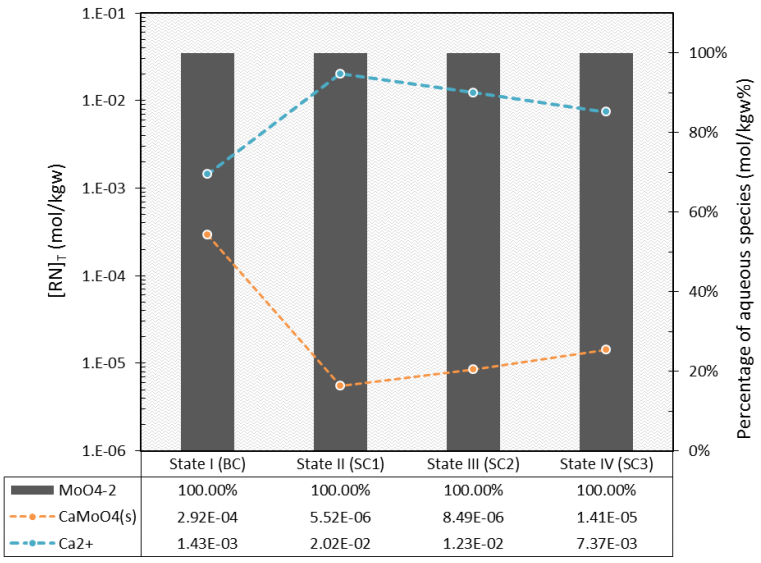

Figure 7. Calculated Powellite solubility and dissolved calcium concentration against cement degradation states. Left axis stands for Mo(VI) total concentration ($mol \cdot kgw^{-1}$) in equilibrium with the selected solubility-limiting phase (orange dashed line) and Ca(II) total concentration (blue dashed line). Right axis stands for molal percentage of predominant Mo aqueous species (>5%) in the studied conditions (grey bars).

The effect of calcium on Mo solubility is shown in Figure 8. Differences in Powellite solubility correspond to up to 2 orders of magnitude when calcium concentration in solution increases from 10^{-4} to 10^{-2} mol/l (the limits of Ca concentration range expected to be encountered under cementitious environment are between 10^{-3} and 10^{-2} mol/l). In this case, molybdenum solubility is very sensitive to differences in calcium concentrations.

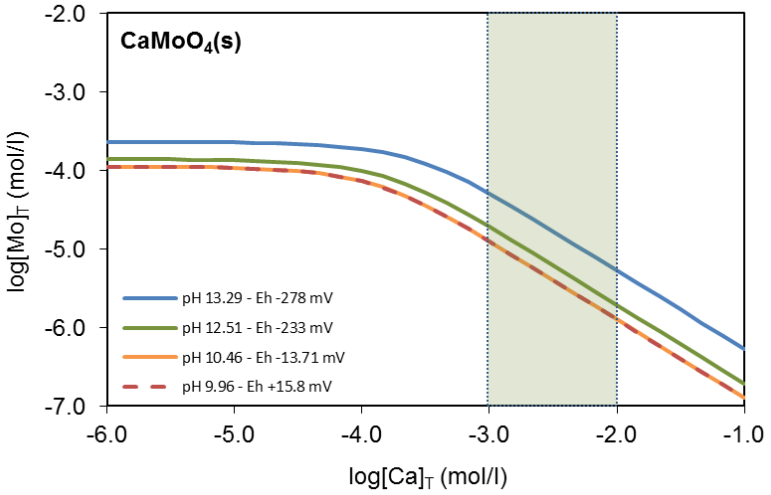

Figure 8. Influence of calcium concentration on the solubility of $CaMoO_4$(s) under cementitious conditions at different pH and Eh. Green area stands for Ca concentration found in cementitious media.

Although molybdenum is a redox-sensitive element, the Eh of the system does not influence Mo concentrations in solution under the abovementioned circumstances (Table 4). Scoping calculations performed herein suggest that under this environment, only the conditions imposed by a system ruled by anaerobic/reducing steel corrosion (very low Eh) could be able to reduce molybdenum from Mo (+VI) to Mo (+IV) and thus the solubility of this element would be then controlled by MoO_2 (s).

Table 4. Solubility-controlling phase, solubility limits and aqueous speciation for Mo under cementitious media calculated in this report.

Cement porewater (-278.48 < Eh (mV) < +15.80)			
Solid phase	**State**	**Concentration (mol/kgw)**	**Speciation**
$CaMoO_4$(s)	State I	$2.92 \cdot 10^{-4}$	MoO_4^{2-} (100%)
	State II	$5.52 \cdot 10^{-6}$	
	State III	$8.49 \cdot 10^{-6}$	
	State IV	$1.41 \cdot 10^{-5}$	

Thermodynamic data

There are several databases including data for this element although they are not complete.

Thermodynamic data selection for molybdenum compounds was based on data available in the open literature (e.g. Aveston et al., 1964; Sasaki and Sillén, 1968a; 1968b; O`Hare et al., 1974; O`Hare, 1974, etc.) and gathered different thermodynamic parameters, including stability constants for formation reactions and standard molar Gibbs energy of formation (ΔG_f^0) (http://www.thermochimie-tdb.com/).

The value for molybdate anion was acquired after the review on solubility and thermochemistry data performed by O´Hare et al. (1974). In turn, the value of the constant for molybdate hydrolysis ($HMoO_4^-$) was selected according to the studies conducted by Aveston et al. (1964), Sasaki et al. (1968) and Sasaki and Sillén (1968). Apart of thermodynamic values for molybdate aqueous species (e.g. MoO_4^{2-}, $HMoO_4^-$) and solid molybdates (e.g. $CaMoO_4$(s), $BaMoO_4$(s), $PbMoO_4$ (s), etc.), the selection also included molybdenum oxides and sulphides

Thermoddem database V1.10 only contains thermodynamic information of the aqueous species MoO_4^{2-} and $HMoO_4^-$.

In turn, PSI/Nagra Chemical Thermodynamic Data Base (12/07) (Thoenen et al., 2014) includes information of Mo(s), Mo(cr), Molybdite and MoO_3(s), not including any aqueous species.

As far as the present literature review has revealed, there is only one work that gathers extensive thermodynamic information with respect to molybdenum compounds, the one conducted by Dellien et al. (1976). The authors performed a critical review on the thermodynamic properties of compounds and aqueous ions of molybdenum (among others). They stablished a data selection based on available experimental information as well as on recalculated published data.

Sorption mechanisms and reported sorption values

The analysis of expected Mo dissolved concentrations under cementitious conditions presented in the previous section considers pure mineral solubility as the only occurring process. However, given large amounts of various materials (cement phases, corrosion products or bentonite) present in the system, Mo dissolved concentrations are presumed to be further reduced by additional processes, such as surface complexation or ion-exchange mechanisms.

The main molybdenum species relevant for the repository conditions is the molybdate ion, which is referred to have low sorption capacity on matrix cement mineral,s as it is negatively charged. Kato et al. (2002) conducted batch sorption measurements on hydrated Ordinary Portland Cement (OPC) paste at pH of about 12.1 - 12.5 to test different Mo(VI) concentrations and solid-to-liquid ratios. The R_d values obtained at low initial Mo concentrations (low enough so the formation of Powellite is unlikely) ranged between 30 and 100 l/kg and resulted to be in good agreement with the values reported by Lothenbach et al. (1999) for selenate (SeO_4^{2-}) (Figure 9).

Due to similarities with regards chemical properties (both oxyanions are isostructural and the central atoms (+VI) have the same charge), and in the absence of significant available experimental data for Mo, some authors have referred to selenate as a chemical analogue for molybdate and thus assumed the sorption of molybdate in cementitious matrices to be the same as the one corresponding to selenate, i.e. related to the presence of ettringite (Kato et al., 2002; Ochs et al., 2011).

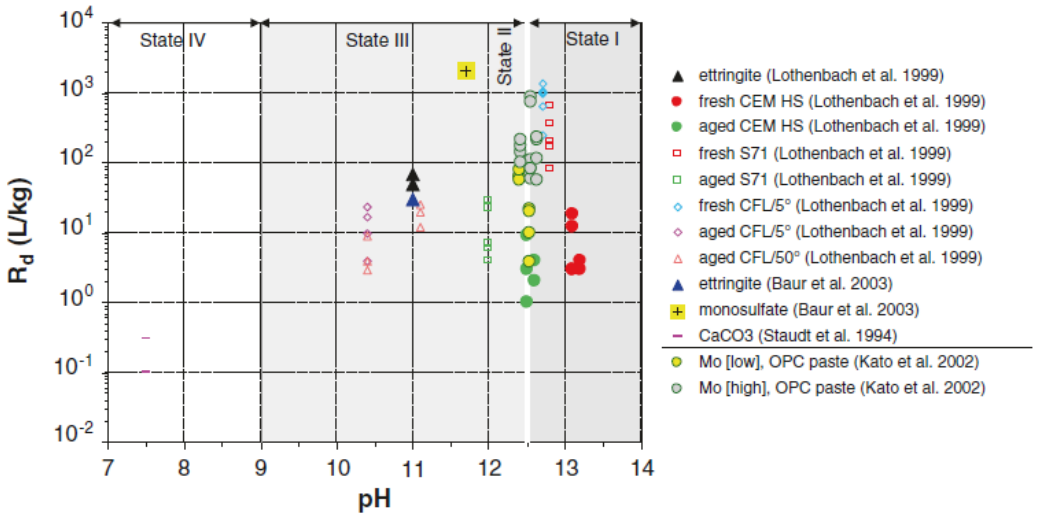

Figure 9. Distribution ratio (R_d) of Se(VI) and Mo(VI) in cementitious systems as a function of pH. The values for calcite are a range estimated by Ochs et al. (2001). CEM HS refers to sulphate resisting Portland cement. Mo [low] refers to an initial Mo concentration of 5 - $7.5 \cdot 10^{-7}$ mol/l; Mo [high] to a range of ca. $4 \cdot 10^{-6}$ to $6 \cdot 10^{-5}$ mol/l.

In this context, Keller (2002) investigated the sorption of selenite and selenate to ettringite, monosulphate and C-S-H obtaining associated distribution ratios (Table 5). A weak selenate sorption was observed onto ettringite and no significant sorption to C-S-H, whereas sorption to monosulphate was strong. The author suggested substitution of sulphate as the relevant process, indicating a more efficiently selenate sorption by monosulphate-rich cement.

Table 5. Distribution ratios for selenite and selenate on ettringite, monosulphate and C-S-H(I) at varying liquid to solid ratio. n.s. indicates no significant uptake. Source: Keller (2002)

Distribution ratio - R_d (l/kg)	Ettringite	Monosulphate	C-S-H(I)
Selenite			
LS52	0.09 ± 0.01		
LS260	0.07 ± 0.02		
LS520	0.18 ± 0.08	0.38 ± 0.09	0.21 ± 0.07
Selenate			
LS520	0.03 ± 0.03	2.06 ± 0.59	n.s.

Kindness et al. (1994) studied the potential immobilization of cement systems for molybdenum using commercial Portland cements (OPC and blended cement) and single phase mixtures (C_3S, C_3A, $C_3A + CaSO_4.2H_2O$ and ettringite).

From the tests with pure phases they observed a rapid decrease of Mo concentration in solution over the first 12 days and thereafter remained steady. Final soluble Mo concentrations were in the range 40-50 ppm after 46 days of test. These values resulted to be very similar to those obtained by reaction of Mo with actual cement systems (Table 6) which were in the range 54-80 ppm after 28 days. The difference between

both results was attributed to the higher alkali content in the cement porewaters which reduces soluble Ca concentration.

Table 6. Mo dissolved concentrations in OPC and slag cement porewaters at different temperature and curing time. Source: Kindness et al. (1994)

	20 °C		55 °C	
OPC	7 days	28 days	7 days	28 days
0.05 mg Mo/g cement	70	60	67	59
0.5 mg Mo/g cement	360	76	300	80
Slag cement (9:1)	7 days	28 days	7 days	28 days
0.05 mg Mo/g cement	58	57	59	58
0.5 mg Mo/g cement	240	54	225	58

More recently, Vollpracht and Brameshuber (2016) conducted an experimental study to investigate the binding of several trace elements in different types of cements. Although molybdenum concentration in the porewater differed from one another cement, they observed a reduction of Mo dissolved content with the hydration time, which was associated with a sulphate replacement in ettringite (Figure *10*a). The same conclusion was attained by Engelsen and Van der Sloot (2010) from their leaching and modelling studies, although the model of Mo binding to ettringite was not in fair agreement with experimental data. Finally, from the leaching tests, Vollpracht and Brameshuber (2016) indicate that molybdate release from cement matrix is controlled by diffusion processes (Figure 10b).

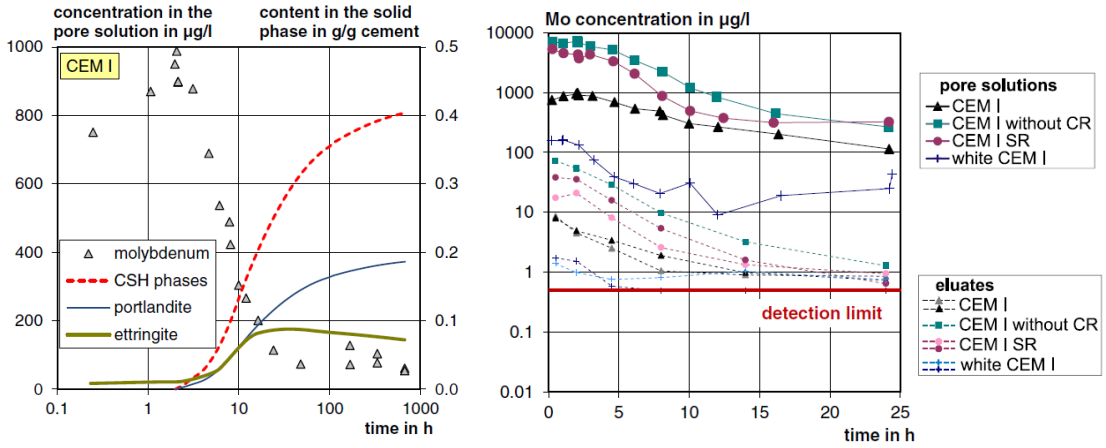

(a) (b)

Figure 10. (a) Decrease of Mo concentrations in the pore solution during cement hydration; (b) Comparison of Mo concentrations in the leaching tests to pore solution concentrations of fresh cement paste. Source: Vollpracht and Brameshuber (2016)

Zhang (2000) studied Mo (among others) retention in pure ettringite- and hydrocalumite-water systems. He observed almost a complete removal of this oxyanion from solution when hydrocalumite was present. However, incorporation into ettringite was not as strong as the one observed with other anions. Maximum uptake values reported in the literature for different anions are listed in Table 7.

Table 7. Maximum uptake capacity (MUC) of some anions by hydrocalumite and ettringite. Source: Zhang (2000).

	Oxyanion	MUC ($x10^3$ mg/kg)	Reference

Hydrocalumite	B	18.7	Wenda and Kuzel (1986)
	Cr	74.7	Perkins (2000)
	Mo	133	Kindness et al. (1994)
	Se	-	-
Ettringite	B	33.8	Pollman et al. (1993)
	Cr	119	Kumarathasan et al. (1990)
	Mo	-	-
	Se	170	Hassett et al. (1990)

When $Ca_3AI_2O_6{\cdot}CaSO_4{\cdot}13H_2O$ (AFm-type phase) was mixed with Na_2MoO_4 at 25 °C during 14 days of curing, Kindness and co-workers observed the presence of three phases: Powellite, Mo-AFm and ettringite. Analysis of the products by AEM revealed that the ettringite did not contain any significant quantity of Mo. Therefore they concluded that Mo concentration in this system appears to be controlled by precipitation mechanisms, being identified two main solubility-limiting phases, i.e. an isostructural $CaMoO_4$ with the naturally occurring mineral Powellite and an AFm-type phase.

It is noteworthy to point out that whereas Kindness et al. (1994) found much stronger bonding of Mo onto AFm relative to AFt, Ochs et al. (2015) indicated that the bonding of Se into AFt phases is reported to be stronger and attributed this disagreement to a conservative data acquisition for Se/AFt compared to Mo. However, as previously seen in Table 2, sorption experiments conducted by Keller (2002) also revealed a weak selenate adsorption to ettringite (R_d = 0.03 m^3/kg) compared to monosulphate (R_d = 2.06 m^3/kg), indicating that Se(VI) has a higher tendency to sorb in a monosulphate-rich cement.

The best estimates and associated upper and lower limits for Mo adsorption according to Ochs and co-workers are listed in Table 8. The approach proposed for selenate has been adopted for molybdate, with R_d being strongly related to the presence (and the amount) of ettringite in the system. As ettringite is assumed to be present during states I, II and the first part of state III, the adopted values by Ochs and co-workers are 3 l/kg in all these cases (Table 8). On the other hand, the presence of ettringite is not clearly established for the second part of state III (and it is also not likely that a large amount of calcite will be present). Therefore, very low sorption value has been assigned for molybdate in these states.

Similarly, Colàs et al. (2014) used data reported for selenate (SKB, 2014a; SKB, 2014b) to attain a reduction factor of -1 for molybdenum in the presence of organic ligands.

Table 8. Selected best estimate, upper and lower limit R_d values for molybdenum. Source: Ochs et al. (2015)

pH state	Best estimate R_d (l/kg)	Upper limit R_d (l/kg)	Lower limit R_d (l/kg)
State I	3	33	0.3
State II	3	33	0.3
State III – ett. present[a]	3	33	0.3
State III – ett. absent	0.1	0.3	0.01
State IV	0.1	0.3	0.01

The condition "ettringite present" is valid up to ~pH 11.3; below this value, ettringite is exhausted ("ettringite absent"). [a]Rd may also be obtained by considering a functional relationship with the amount of ettringite and its evolution (Rd would not be a fixed number but variable). A value corresponding to pure ettringite present would be 50 l/kg

The data reported by Ochs et al. (2015) must be referred as tentative and taken with caution as there are many reports available in the literature that point out an oxyanion immobilization favored by incorporation into hydrocalumite structures. From the in-depth revision carried out by Chrysochoou and Dermatas (2006), the authors state that ettringite exhibits an immobilization potential which only exists under strictly controlled conditions, being sulphate substitution by oxyanions in the monophases (AFm) more pronounced at lower anion concentrations.

Cementitious phases

AFt and AFm phases

AFt phases have the general formula $[Ca_3(Al,Fe)(OH)_6 \cdot 12H_2O]_2 \cdot X_3 \cdot xH_2O$, where X normally represents one divalent anion (or, in some cases, two monovalent anions). The most important AFt phase is ettringite, $[Ca_3Al(OH)_6 \cdot 12H_2O]_2 \cdot (SO_4)_3 \cdot 2H_2O]$ (Taylor 1997) and it forms quite rapidly during cement hydration.

AFt phases are formed under broadly similar conditions to AFm phases, but at higher ratios of CaX to $C_3(A,F)$. AFt can decompose to form AFm phases depending on sulphate and carbonate activity. In blended cements ettringite does not show systematic changes in composition, it seems to form a solid solution between Al – Fe and an incomplete solid solution between CO_3^{2-} – SO_4^{2-} (Möschner et al., 2009; Matschei and Glasser, 2010).

Naturally occurring **AFm** phases (also known as SO_4-hydrocalumite) are double-layered hydroxides with variable composition. Taylor (1997) adopted the term hydrocalumite to refer to any calcium aluminate with the formula $Ca_4Al_2(OH)_{12} \cdot X_2 \cdot nH_2O$, thus, AFm can be named as SO_4-hydrocalumite as well as Friedel´s salt as Cl-hydrocalumite. According to Zhang and Reardon (2003), monosulphate (AFm - SO_4^{2-}) or its hydroxide analogue (AFm - OH^-) are referred to as the major host mineral studied for oxyanions. In this regard, as mentioned in section 0, Kindness et al. (1994) proposed monosulphate as the controlling mineral phase for molybdate in cement from solubility studies using PhreeqC (eq. 11).

$$Ca_4[Al(OH)_6]_2 \cdot MoO_4 \cdot 10H_2O + 12H^+ = 4Ca^{2+} + 2Al^{3+} + MoO_4^{2-} + 22H_2O \quad [\log K = 71.66] \qquad \text{eq. 11}$$

Structure and derived properties

Both AFt and AFm phases have shown to play an important role on the fate of oxyanions in cement environment by means of sorption/incorporation mechanisms. These phases' capacities are strongly dependent on their crystallographic structure, including crystal size and nature of the layer charge (e.g., isomorphic substitutions, vacancies). AFm crystal structure is composed of brucite-like octahedral layers with Ca^{2+} occupying 6-fold coordination with hydroxyl anions (Figure 11(a)). One third of Ca^{2+} sites are occupied by Al^{3+} generating a positive net charge in the octahedral layers which enables anion incorporation to achieve charge balance.

Ettringite, like other AFt phases, forms hexagonal prismatic crystals with columns of positive-charged chemical units with a composition of $Ca_6[Al(OH)_6 \cdot 12H_2O]_2^{6+}$. Anions ($SO_4^{2-}$ in the case of ettringite) and water molecules are located in channels between columns in each unit cell (Figure 11(b)).

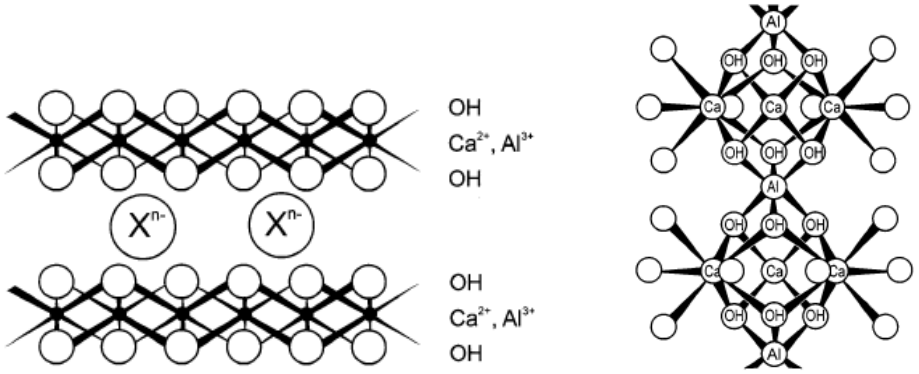

(a) (b)

Figure 11. Schematic representation of (a) hydrocalumite structure; (b) single column of ettringite projected parallel to c-axis (Blank circles stand for H_2O molecules).

The columns consist of $AI(OH)_6$ octahedra alternating with triangular groups of edge-sharing CaO_8 polyhedra. The column alignment is along the c-axis of the trigonal-hexagonal unit cell. Eight oxygen atoms in the polyhedra come from the Ca^{2+} coordination with four OH^- ions shared with the $AI(OH)_6$ octahedra and from the coordination with four H_2O molecules. The hydrogen atoms from the molecules of water are forming the cylindrical surface of the columns. The channels contain four sites per formula unit of the column structure which contains six calcium atoms. Three of these sites are occupied by SO_4^{2-} and one by two H_2O molecules (Taylor, 1997 - Figure 11(b)).

Mechanism of anion uptake

There is a general consensus that the two main mechanisms identified for oxyanion uptake in these types of cementitious phases are:

a) Adsorption onto the surfaces

b) Direct partial/complete substitution for SO_4^{2-}/OH^- in the interlayer regions of these phases (Figure 12 (a-b)).

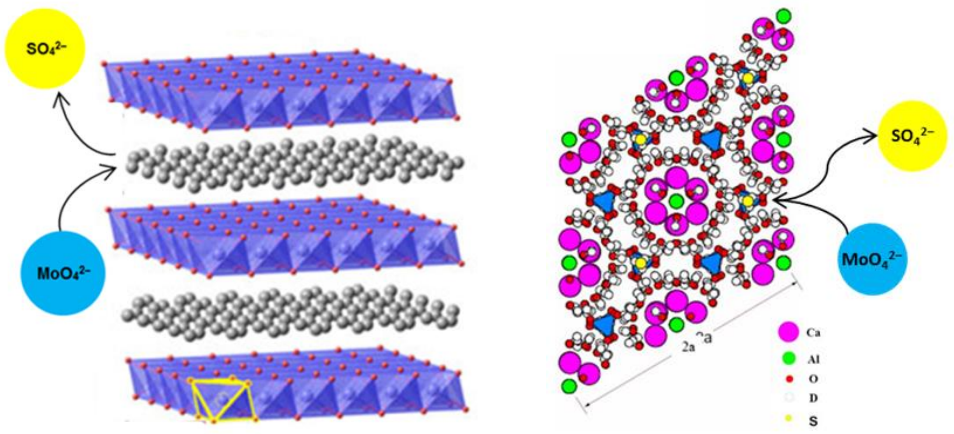

(a) (b)

Figure 12. (a) 3D image of a hydrocalumite-type structure (AFm if the outgoing anion is sulphate) (b) Ettringite structure (cross section view – parallel to c-axis). Fixation mechanisms of molybdenum in these phases by anion exchange process.

Stability fields

The following solid phases are likely to form at 25 °C in the system $CaO–Al_2O_3–SO_3–H_2O$:

- Ettringite (AFt): $3CaO·Al_2O_3·3CaSO_4·32H_2O$
- Monosulphoaluminate or Monosulphate (AFm): $3CaO·Al_2O_3·CaSO_4·12H_2O$
- Gypsum: $CaSO_4·2H_2O$
- Hydrogarnet (C_3AH_6): $3CaO·Al_2O_3·6H_2O$ (other calcium alumina hydrates are also possible but they are metastable with respect to hydrogarnet);
- Portlandite (CH): $Ca(OH)_2$
- Gibbsite (AH_3): $Al(OH)_3$

According to the stability field diagram corresponding to the system $CaO–Al_2O_3–SO_3–H_2O$ established by Hampson and Bailey (1983), ettringite increases its stability as the activity of sulphate also increases (Figure 13). The range of pH where this phase is stable widens as SO_4^{2-} concentration grows up to a certain level in which high sulphate concentrations favours gypsum stabilization instead.

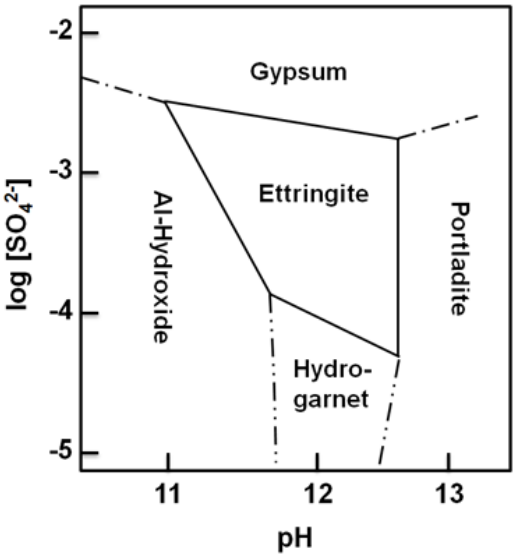

Figure 13. Stability fields of compatible phases for the system $CaO-Al_2O_3-CaSO_4-H_2O$ as a function of sulphate concentration and pH. Source: Hampson and Bailey (1983).

Damidot and Glasser (1995a) conducted thermodynamic investigations of the same system at 25 °C and observed similar results to experimental data. They indicate that ettringite formation is compatible with all the phases, being only stable when sulphate concentration is between 0.015 and 15 mM. Below that range of concentration the stable phases are hydrogarnet, portlandite and gibbsite; whereas above that range the phases prone to form are gibbsite and gypsum (Figure 14 and Table 9).

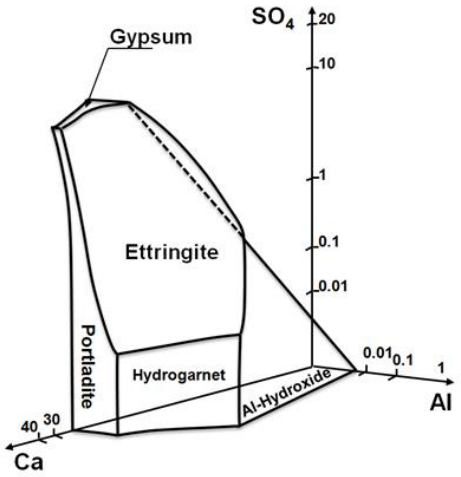

Figure 14. 3D representation of the stability fields of compatible phases for the system CaO-Al2O3-CaSO4-H2O as a function of sulphate, aluminium and calcium concentration in solution. Source: Damidot and Glasser (1995).

The same authors also studied the $CaO\text{-}Al_2O_3\text{-}CaSO_4\text{-}H_2O$ system with different additions of Na_2O. They observed that the presence of a cation other than calcium enables to have a greater concentration of soluble sulphate when aluminate concentration and pH are very low (Table 9). When Na_2O concentration is increased from 0.025 to 0.125 M, the ranges of sulphate and aluminate concentrations are increased while that of calcium is reduced as observed in presence of Na_2O 0.025 M.

Table 9. Invariant points where ettringite is stable for the system $CaO\text{-}Al_2O_3\text{-}CaSO_4\text{-}H_2O$ with and without Na_2O additions. Source: Damidot and Glasser (1995a).

System	Invariant point (Phases in equilibrium)	Ca (mM)	Al (mM)	S(VI) (mM)	pH
$CaO\text{-}Al_2O_3\text{-}CaSO_4\text{-}H_2O$	1.C_3AH_6-AH_3-ett	5.04	0.3860	0.03	11.92
	2.C_3AH_6-CH-ett	21.25	0.01	0.015	12.52
	3.gypsum-AH_3-ett	15.17	0.001	15.0	10.43
	4.gypsum-CH-ett	31.30	0.0003	11.4	12.47
$CaO\text{-}Al_2O_3\text{-}CaSO_4\text{-}H_2O$ + Na_2O 0.025 M	1.C_3AH_6-AH_3-ett	0.425	1.84	0.7	12.58
	2.C_3AH_6-CH-ett	8.12	0.0134	0.04	12.71
	3.gypsum-AH_3-ett	11.12	0.0143	35.8	10.66
	4.gypsum-CH-ett	21.5	0.0007	20.78	12.57
$CaO\text{-}Al_2O_3\text{-}CaSO_4\text{-}H_2O$ + Na_2O 0.125 M	1.C_3AH_6-AH_3-ett	0.05	9.545	12.4	13.16
	2.C_3AH_6-CH-ett	1.45	0.045	0.8	13.23
	3.gypsum-AH_3-ett	10.29	0.042	135	10.53
	4.gypsum-CH-ett	13.85	0.0007	91	12.79

Variation of hydroxyl concentration is important and therefore alkali concentration is relevant as it contributes to OH^- content in cement porewaters. The stability field of ettringite at incremental Na_2O concentrations is represented in Figure 15. The lower limit of pH is similar with or without Na_2O and close to 10.5. This pH value is quite close to the value of 10.7 given by Gabrisova et al. (1991) for the minimal pH value at which ettringite is stable. On the contrary, the upper limit of pH increases with the increase of Na_2O content and corresponds to the maximum pH value that can be reached by the system. Ettringite is stable on a wide range of pH but not for all

solutions having such pH; the composition of the solution should belong to the surface of equilibrium of ettringite.

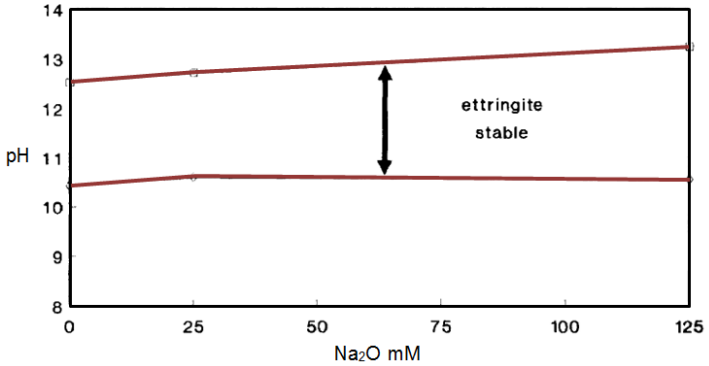

Figure 15. Range of pH at which ettringite can be stable depending on Na_2O concentration. Source: Damidot and Glasser (1995a).

The CaO-Al_2O_3-$CaSO_4$-$CaCO_3$-H_2O closed system at 25 °C was also investigated through thermodynamic calculations by Damidot and Glasser (1995b). Eight isothermally invariant points were determined and eight stable phases were also defined in the system, i.e. ettringite, portlandite, gibbsite, gypsum, hydrogarnet, hemicarboaluminate, monocarboaluminate and calcite. In all of these points, ettringite resulted to be stable having a limiting carbonate concentration of $8.39 \cdot 10^{-6}$ M (Figure 16). From this concentration upwards ettringite will decompose to form calcite, gypsum and gibbsite. Sulphate dissolved concentration promotes ettringite formation avoiding its decomposition to hemicarboaluminate or monocarboaluminate phases, the range of sulphate content in solution of which ettringite is stable stands between a lower limit of $7.60 \cdot 10^{-3}$ mM and an upper limit of 15.2 mM. Under these circumstances, the range of pH where this phase remains stable is not too different from previously seen in the system CaO-Al_2O_3-$CaSO_4$-H_2O, i.e. $10.25 < pH < 12.52$.

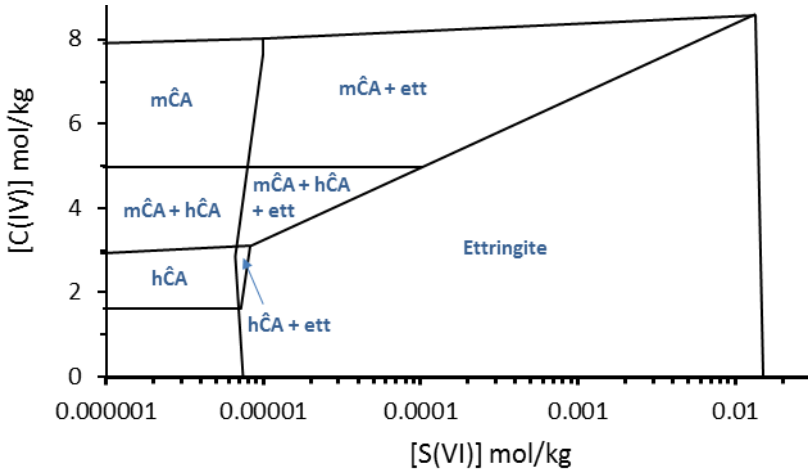

Figure 16. Stability fields of compatible phases for the system CaO-Al_2O_3-$CaSO_4$-$CaCO_3$-H_2O as a function of sulphate and carbonate concentrations. Source: Damidot and Glasser (1995b).

Analysis of stability field of ettringite in a system containing silica (i.e. $CaO\text{-}SiO_2\text{-}Al_2O_3\text{-}CaSO_4\text{-}H_2O$) is detailed in section 0.

C-S-H phases

The term C-S-H phase comprises a group of more than 30 identified phases that are poorly ordered (Taylor, 2002). Due to the poorly crystalline structure of C-S-H gels, no real crystal substitution reactions can occur, however, its irregular stacking of the layers, each 10-100 nm, creates a large specific surface area available for sorption (Glasser, 1993). At C/S ratios > 1.2 these C-S-H gels are positively charged, and thus might have the potential to adsorb oxyanions.

Structure and derived properties

The structure of a C-S-H phase is amorphous in nature, but it can maintain to some extent a certain level of order within a short range. A successful structural model is based on *Dreierketten*, which consist on three silicate tetrahedra which are defined basing on the structure of 1.4-nm tobermorite (Figure 17). In this case two tetrahedra share two oxygen atoms with a Ca-O layer and are called "bridging tetrahedra". The third tetrahedron shares only one oxygen atom with the Ca-O layer. Bridging tetrahedra may be missing and the periodicity of the building units is variable, these variations affect the composition of the solid, resulting in different calcium-to-silica ratios (C/S ratios are found to range from 3 to 0.6). In the model proposed by Taylor (1986), C-S-H structure was based on layers of 14-nm tobermorite (5-link chain) with jennite (2-link chain) placed the inter-layer, however, in a recent work by Grangeon et al. (2013), it has been proven that C-S-H structure remains based on tobermorite structure even at C/S ratio close or slighlty higher than that of jennite (Figure 17).

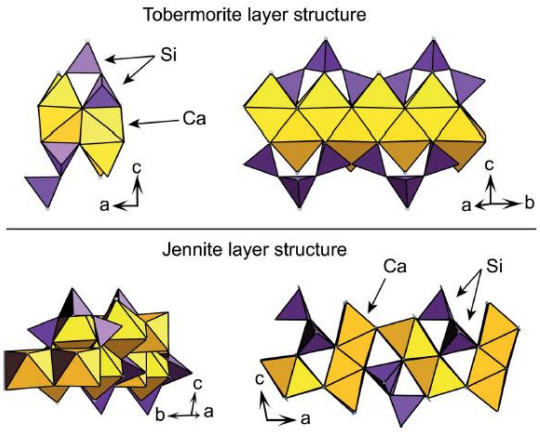

Figure 17. Tobermorite and jennite layer structures. Interlayer water and calcium are omitted for clarity. Source: Grangeon et al. (2013).

The large specific surface of C-S-H gels creates a strong potential for ion adsorption. Calcium-rich C-S-H has a positive surface area potential and tends to adsorb anions although it has been reported that the performance for trace elements adsorption is weak due to the strong interaction of highly abundant anions (e.g. OH^-, SO_4^{2-}, Cl^-) in cement pore water. On the contrary, the surface becomes negatively charged at C/S ratios below 1.2, thereby favouring cation adsorption.

Nonetheless, adsorption is not the only mechanism of C-S-H gels for RN retention, incorporation into C-S-H structure from ion-exchange mechanisms may also be important under certain circumstances. Both substitutions for silicate and calcium, as well as adsorption to the large interlayer surfaces have been suggested by several

authors as the most relevant binding mechanisms of C-S-H gels (Beaudoin et al., 1990; Richardson and Groves, 1993; Pointeau et al., 2004; Tits et al., 2006; Papadokostaki and Savidou 2009).

Stability fields

Martínez-Ramírez and Blanco-Varela (2009) studied the thermodynamic stability of different hydrated phases of cement (C-S-H, gypsum, ettringite and $Ca(OH)_2$) in the $CaO\text{-}SiO_2\text{-}Al_2O_3\text{-}CaSO_4\text{-}H_2O$ closed system at 25 °C, determining the range of several ion concentration and pH at which these phases are stable.

The $CaO\text{-}SiO_2\text{-}Al_2O_3\text{-}CaSO_4\text{-}H_2O$ system is reported to have 12 stable phases at 25 °C:

- C-S-H (C/S = 0.8): $Ca_{0.8}SiO_{2.8}{:}H_2O$
- C-S-H (C/S = 1.1): $Ca_{1.1}SiO_{3.1}{:}H_2O$
- C-S-H (C/S = 1.8): $Ca_{1.8}SiO_{3.8}{:}H_2O$
- H_4SiO_4 (SH)
- Hydrogrossular with low Si content (HGSi low): $Ca_3Al_2Si_{0.3}O_{6.6}{\cdot}5.4H_2O$
- Hydrogrossular with high Si content (HGSi high): $Ca_3Al_2Si_{0.8}O_{7.6}{\cdot}4.4H_2O$
- Strätlingite (C_2ASH_8): $Ca_2Al_2SiO_7{\cdot}8H_2O$
- Ettringite (AFt): $3CaO{\cdot}Al_2O_3{\cdot}3CaSO_4{\cdot}32H_2O$
- Gypsum: $CaSO_4{\cdot}2H_2O$
- Hydrogarnet (C_3AH_6): $3CaO{\cdot}Al_2O_3{\cdot}6H_2O$
- Portlandite (CH): $Ca(OH)_2$
- Gibbsite (AH_3): $Al(OH)_3$

Table 10 comprises the fifteen invariant points resulted from this system, as can be observed, there is no more than four compatible phases at each point. The C-S-H gel decomposes when sulphate concentration reaches 14.98 mM for the $CaO\text{-}SiO_2\text{-}CaSO_4\text{-}H_2O$ system (Aguilera, 2003), whereas its stability increases up to $[SO_4^{2-}]$ = 15.40 mM in the $CaO\text{-}SiO_2\text{-}Al_2O_3\text{-}CaSO_4\text{-}H_2O$ system, which indicates that the presence of aluminium produces a C-S-H stabilization with respect to sulphate concentration (Table 10). In turn, the stability field of C-S-H gels increases in the presence of sulphates, being stable across a broader range of silicon concentrations (up to 3.87 mM) in the $CaO\text{-}SiO_2\text{-}Al_2O_3\text{-}CaSO_4\text{-}H_2O$ than in a sulphate-free system. It requires a higher calcium concentration though (i.e. 16.2 versus 5.74 mM in the absence of sulphates) (Martínez-Ramírez and Blanco-Varela, 2009). The pH in which C-S-H gels of different C/S are stable ranges from 12.47 to 9.75 (Table 10).

With respect to ettringite, an analysis of system variation showed that this phase begins to stabilize when sulphate concentration reaches $7.64{\cdot}10^{-3}$ mM, being the only stable sulphate-containing phase until the concentration is of about $1.23{\cdot}10^{-2}$ mM, when gypsum also precipitates (Table 10). For high sulphate concentrations, $15.4 > [SO_4^{2-}] >$ 12.3 mM, compatible ettringite and gypsum appear in four invariant points where low aluminium and high calcium or silicon concentrations are present (up to 1.38 mM of this latter phase) (Martínez-Ramírez and Blanco-Varela, 2009).

Table 10. Invariant points for the system $CaO-SiO_2-Al_2O_3-CaSO_4-H_2O$. Source: Martínez-Ramírez and Blanco-Varela (2009).

Invariant point (Phases in equilibrium)	Ca (mM)	Si (mM)	Al (mM)	S(VI) (mM)	pH
1. C_3AH_6-ett-HGSi low-CH	20.4	0.00169	0.01	0.00764	12.47
2. CSH1.8-ett-HGSi low-CH	20.4	0.00249	0.00946	0.00794	12.47
3. CSH1.1-CSH1.8-ett-HGSi low	17.9	0.00366	0.0121	0.0086	12.42
4. C_3AH_6-ett-AH_3-HGSi low	5.56	0.000383	0.372	0.0112	11.95
5. CSH1.1-ett-HGSi high-HGSi low	6.87	0.0167	0.115	0.0147	12.05
6. C_2ASH_8-ett-AH_3-HGSi low	4.96	0.00686	0.333	0.0158	11.91
7. C_2ASH_8-ett-HGSi high-HGSi low	5.65	0.0135	0.205	0.0158	11.97
8. C_2ASH_8-CSH1.1-ett-HGSi high	5.84	0.0224	0.153	0.0177	11.98
9. C_2ASH_8-CSH1.1-ett-AH_3	2.76	0.0988	0.178	0.11	11.64
10. CSH0.8-CSH1.1-ett-AH_3	5.74	1.00	0.02	4.99	10.68
11. CSH1.8-ett-gyp-CH	31.7	0.00231	1.34E-7	12.3	12.43
12. CSH1.1-CSH1.8-ett-gyp	29.5	0.00335	1.85E-7	12.5	12.37
13. CSH0.8-AH_3-gyp-SH	16.2	3.87	0.00249	15.2	9.75
14. CSH0.8-CSH1.1-ett-gyp	16.0	0.782	0.00173	15.4	10.54
15. CSH0.8-ett-AH_3-gyp	16.0	1.38	0.00734	15.4	10.22

Data from analogues of hydrated cementitious phases

Dissolution–precipitation rates

The binding of RN can occur by ion exchange, by adsorption-desorption, or, in the case of ion substitution, by dissolution-precipitation processes. The rates of these different processes vary from one another, i.e. ion exchange and adsorption-desorption reactions usually occur within minutes to hours (Keller, 2002); in contrast, dissolution-precipitation processes tend to be much slower. According to these considerations, known dissolution-precipitation rates would be a helpful tool to obtain a better interpretation of data obtained from sorption studies. In this framework, Keller (2002) investigated the dissolution and precipitation behaviour of pure ettringite, monosulphate and C-S-H(I) phases at saturation, the results are listed in Table 11.

According to the author, dissolution-precipitation rates obtained for ettringite and monosulphate can facilitate the distinction of ion substitution in sorption studies from comparably fast reactions, such as surface complexation and ion exchange. The case of C-S-H(I) resulted to be different because of its semi-crystalline structure and its variable C/S ratio without changing the main structure or properties. This structural flexibility has been shown to allow the incorporation of Zn^{2+} into interlayers or internal surfaces without Ca^{2+} release, at a slow, diffusion controlled rate (Ziegler et al., 2001). Such a diffusion process would be difficult to discern from the dissolution-precipitation reaction rate for C-S-H(I).

Table 11. Determined tracer uptake rates ($k_{i,2}$) and dissolution-precipitation rates ($k_{i,1}$) at first (1) and second (2) series of experiments. Source: Keller (2002).

Phases	i	$K_{i,2}$ (10^{-3} d^{-1})	log $k_{i,1}$ (mol/m^2s)
Ettringite	Ca(1)	3.26	-12.15
	Ca(2)	6.60	-11.86
	SO_4(1)	9.38	-11.65
	SO_4(1)	3.25	-12.12
Monosulphate	Ca(1)	5.31	-11.17
	Ca(2)	4.65	-11.23
C-S-H(I)	Si(2)	3.23	-11.56

It is important to note that for a contaminant to be built into a crystal structure as a consequence of dissolution-precipitation processes, the resulting mineral must be thermodynamically more stable than the original cement mineral. Therefore both kinetic and thermodynamic approaches must be considered for each contaminant species in order to understand its binding mechanism.

Cementitious phases substituted with other anions

Substitution of Cr(III) for Al(III) and CrO_4^{2-} for SO_4^{2-} in the ettringite structure has been widely studied and resulted to be an important way of chromium immobilization in alkaline environments (Kumarathasan et al., 1990; Poellman et al., 1993; Myneni, 1995; Palmer, 2000; Chrysochoou and Dermatas, 2006). In this context, Perkins (2000) investigated ettringite and its chromium analogues to determine the solubility product (K_{SP}) and thermodynamic properties via dissolution and precipitation experiments between pH 10 and 13. The solubility product and free energy of formation for $Ca_6[Al(OH)_6]_2(CrO_4)_3 \cdot 26H_2O$ were calculated to be log $K_{SP,298}$ = –41.46 ± 0.30 and $\Delta G°_{f,298}$ = −15130 ± 19 kJ/mol. Obtained and calculated results are comprised in Table 12.

Likewise, Perkins (2000) studied the solubility of monosulphate (AFm) analogue in order to determine its solubility product and associated thermodynamic properties as a way to obtain information concerning Cr retention in mature cements (in absence of ettringite). The solubility product of $3CaO \cdot Al_2O_3 \cdot CaCrO_4 \cdot 15H_2O$ at 25 °C was calculated to be –30.38 ± 0.28. The whole set of results for monochromate is listed in Table 12.

Table 12. Measured and calculated thermodynamic data of $Ca_6[Al(OH)_6]_2(CrO_4)_3 \cdot 26H_2O$ and $3CaO \cdot Al_2O_3 \cdot CaCrO_4 \cdot 15H_2O$ at 25 °C. Source: Perkins (2000).

Phase	Log K_{SP}	ΔH_f^0 kJ/mol	ΔG_f^0 kJ/mol	S_f^0 J/mol·K	ΔH_r^0 kJ/mol	ΔS_r^0 J/mol·K
$Ca_6[Al(OH)_6]_2(CrO_4)_3 \cdot 26H_2O$	–41.46 ± 0.30	-17330 ± 15	−15131 ± 19	2190 ± 110	77.5 ± 9.5	-533 ± 87
$3CaO \cdot Al_2O_3 \cdot CaCrO_4 \cdot 15H_2O$	–30.38 ± 0.28	–11303 ± 8.3	–9905 ± 16	1439 ± 89	39.1 ±3.2	450 ± 10

Kindness et al. (1994) prepared a Mo analogue of the AFm phase by reacting C_3A and $CaMoO_4$(s) in distilled water at 25 °C for 5 days. Identified phases were

$Ca_3AI_2O_6CaMoO_4 \cdot 10H_2O$ and $Ca_3AI_2O_6CaMoO_4 \cdot 14H_2O$, which the X-ray pattern of the 10-hydrate phase was reported to be similar to AFm pattern. According to the authors, Mo-AFm phase dissolves incongruently since the sulphate concentration was approximately two orders of magnitude lower than the expected from congruent dissolution. The solubility was determined to be Ca = 5.02 mM, Al = 3.09 mM, Mo = 0.101 mM and pH = 12.19. Cornelis et al. (2008) used these data to calculate Mo-AFm solubility product (log K_{SP} ($Ca_4[Al(OH)_6]_2MoO_4$) = 71.66) which results to be lower than the ones corresponding to Se-AFm (73.40 – Baur and Johnson, 2003) and SO_4-AFm included in TC (73.70 – Blanc et al., 2010).

In the study performed by Zhang (2000) on the behaviour of B, Cr, Mo and Se in pure ettringite- and hydrocalumite-water systems, residual solution concentration of all oxyanions were below detection limits after incorporation into hydrocalumite, and the B concentration were below detection after incorporation into ettringite. The anion preference by the latter resulted to be $B(OH)_4^- > SeO_4^{2-} > CrO_4^{2-} > MoO_4^{2-}$, being molybdate anion the least preferred by ettringite to uptake.

Additionally, Zhang (2000) synthesised different hydrocalumite solid solutions to investigate the effect of those oxyanions on mineral phase solubility and stability in the system $CaO\text{-}Al_2O_3\text{-}XO_3/Y_2O_3\text{-}H_2O$ (where X = Cr(VI), Mo(VI), Se(VI); Y = B(III)). The results indicate that, with the exception of molybdate, all the solid solutions containing different anions showed similar trend, i.e. hydrocalumite is the dominant phase throughout the whole set of solid solutions. At low anion content solid solution, hydrogarnet and portlandite (only if sulphate is present) are also found; however, with increasing anion concentration hydrocalumite gains domain. Only at higher anion content, ettringite forms alongside hydrocalumite as the only phase assemblage (not in the case of Se, where HG and CH coexist with HC and Ett).

Clear differences where reported for molybdate solid solution:

i. Hydrogarnet persists the entire solid solution series regardless Mo(VI) concentration.
ii. Powellite ($CaMoO_4$(s)) is identified on most of the samples.
iii. Although the presence of molybdate in the structure favours hydrocalumite stabilization, the stability field of this solid solution is much more limited than with other oxyanions.

The results of this study on Mo showed that large quantity of MoO_4^{2-} is needed (over 80%) to form a stable solid solution. Zhang (2000) attributed this to the incompatibility between molybdate and hydroxyl anions plus the presence of powellite. As a result, high amount and persistence of hydrogarnet take place in the system. Due to the low solubility of powellite, the initial precipitates consist of OH-rich solid solution. If molybdate does not enter the structure to stabilize OH-hydrocalumite, this phase eventaully turns into hydrogarnet. Once this phase is formed, the unreacted powellite is less prone to give rise to Mo-hydrocalumite. And a long-term condition is then maintained.

From these results, free energy of formation was determined for borate hydrocalumite end-member ($Ca_4Al_2(OH)_{12}(HBO_3) \cdot 5.5H_2O$ - $\Delta G°_{f,298}$ = −7750.42 ± 1.20 kJ/mol) as well as for borate ettringite ($Ca_6Al_2(OH)_{12}(B(OH)_4)_4[OH]_2 \cdot 24H_2O$ - $\Delta G°_{f,298}$ = −17408.22 ± 4.34 kJ/mol). Thermodynamic data for the rest of oxyanions was not possible to determine due to the presence of immiscible solid solutions (Zhang, 2000).

Calculation of distribution ratios

Figure 18 shows calculated kinetics and distribution ratios from solubility experiments carried out by Kindness et al. (1994). As can be observed, R_d resulted to be higher when higher molybdenum concentration has been used, and it increases with time in all the three cases, although the increase is more pronounced for the cases with higher Mo initial concentration.

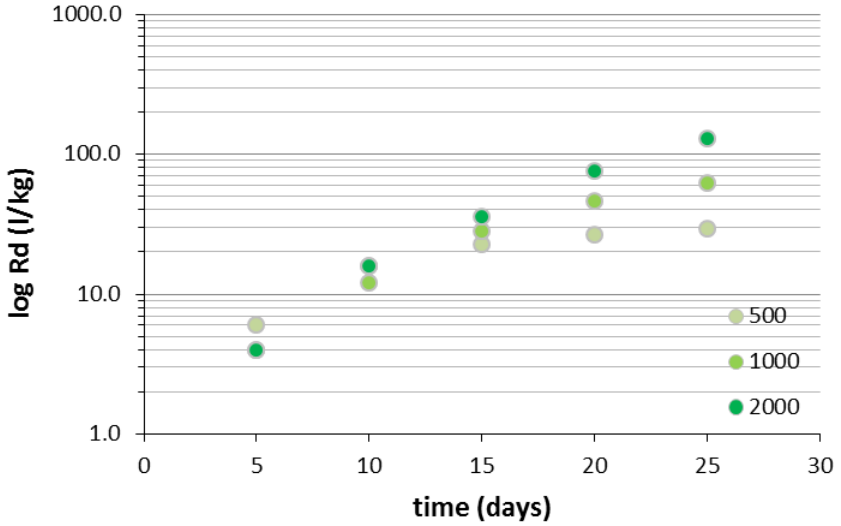

Figure 18. Molybdenum calculated R_d in cement versus contact time from data reported by Kindness et al. (1994). Circles correspond to initial Mo concentration in ppm.

At maximum contact time (25 days), calculated distribution ratios are 29, 62 and 129 l/kg for 500, 1000 and 2000 ppm Mo solutions, respectively. These data is in agreement with the results obtained by Kato et al. (2002) on hydrated Ordinary Portland Cement (OPC) for low Mo concentrations (Table 13).

Table 13. Comparison between R_d obtained by Kato et al. (2002) and calculated R_d from data reported by Kindness et al. (1994)

Distribution ratio - R_d (l/kg)	Calculated from Kindness et al. (1994)	Kato et al. (2002)
Initial [Mo] (ppm)		Low [Mo]
500	29	30-100
1000	62	
2000	129	

These values are higher than the ones attained by Ochs et al. (2016) (Table 8) and chosen by Skagius et al. (1999) in accordance with actual measurements made by Holgersson and Albinsson (1999), which are 3 and 6 l/kg respectively.

Zeta potential of cementitious systems

Surface charge of a solid phase may influence in a great extent the interactions that occur between the solid surface and the surrounding species in solution. Zeta potential (ζ) measurements are then of great importance for the study of surface properties and adsorption on solid materials. Cement produces a colloidal suspension when contacts

water, where electrostatic repulsion forces take place between electrically-charged cement particles. As a result of chemical cement composition in water, system charge is positive mainly due to Ca^{2+} ions located in the surface, which attract opposite charge ions forming a counter-ion layer around the particles called "Stern layer" (Figure 19). Counter-ion concentration is higher at the surface and decreases inwards the liquid. Inversely, co-ion concentration increases inwards the liquid and decreases at the surface. All these colloids are distributed at different levels forming the "Diffuse layer" (Figure 19). Both layers constitute the so-called "double layer" which thickness depends on type and concentration of ions in solution (Moreno, 2005). Solution ionic strength, pH and the concentration of adsorbed ionic species will determine particle superficial charge.

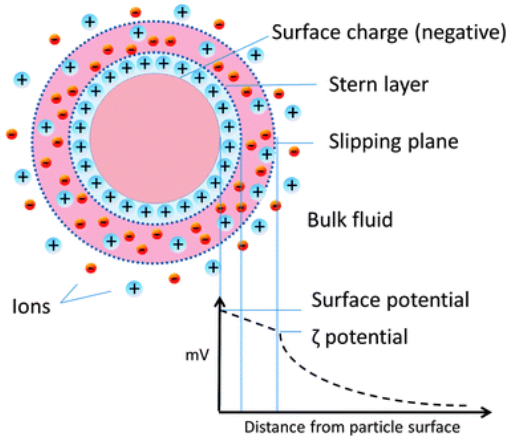

Figure 19. Representation of a charged particle and distribution of surrounding ions. Source: Liese and Hilterhaus (2013)

As the main phases of hydrate cement pastes, the ζ of calcium silicate hydrates (C-S-H) has been the focus of numerous studies (e.g. Nachbaur et al., 1998; Viallis-Terrisse et al., 2001; Pointeau et al., 2006). The ζ values of C-S-H decrease with the pH or calcium concentration of the equilibrium water, in fact, Nachbaur et al. (1998) reported an isoelectric point (IEP) for Ca ($2\text{-}4 \cdot 10^{-3}$ M) and observed no variation with increased NaOH concentration in solution, which pointed out the strong dependence of system ζ on Ca content. These results are in agreement with the ones obtained by Viallis-Terrisse et al. (2001), who found the same IEP for Ca and no modification of this point was observed for lithium and sodium chlorides (Figure 20). Only a slight displacement of the isoelectric point was evidenced with CsCl which resulted in a decrease in zeta potential for a given value of calcium activity.

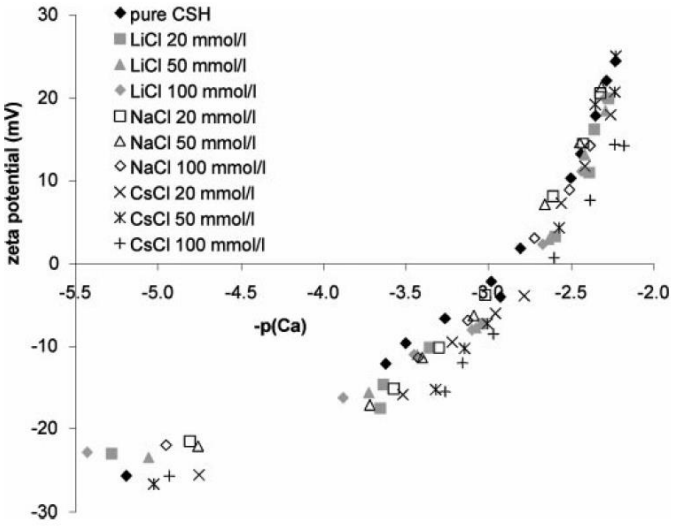

Figure 20. Evolution of the zeta potential as a function of calcium activity in the solution. Source: Viallis-Terrisse et al. (2001)

Two equilibria was proposed by Viallis-Terrisse et al. (2001) and Pointeau (2000) to represent the evolution of the C-S-H surface chemistry, and the surface charge of the C-S-H has been considered as the result of the ionization of silanol sites, mostly through deprotonation (eq. 12) as well as by the sorption of Ca^{2+} on the silanol sites (eq. 13):

$$>SiOH \rightarrow >SiO^{-} + H^{+} \qquad \text{eq. 12}$$

$$>SiOH + Ca^{2+} \rightarrow >SiOCa^{+} + H^{+} \qquad \text{eq. 13}$$

According to these authors, the speciation of the C-S-H silanol sites will be dominated by $>SiO^{-}$, >SiOH, and $>SiOCa^{+}$ surface complexes.

Experimental investigations on the potential of the cement surface were conducted by Pointeau et al. (2006) from fresh states (with high pH) to highly degraded states (with pH close to 11). They observed two different situations: (i) an increase of surface potential from negative to positive values at pH between 13.3 and 12.65 (pH buffered by portlandite) and (ii) a decrease of surface potential from positive to negative values when portlandite is totally dissolved and C-S-H phases begin to be leached out from the HCP (Figure 21). The ζ values obtained in this second pH range were in agreement with the ones reported by Viallis-Terrisse et al. (2001) for C-S-H (data included in the figure), which led them to conclude that, in this range of degradation state, the contribution of the surface charge of the C-S-H imposes the actual ζ values of the whole HCP system.

As a result, two IEPs were evidenced which coincided to pH close to 12.9 and 11.7 (Figure 21). These points define three areas of pH wherein different surface complexes dominate:

- $13.3 > pH > 12.9$ = **$>SiO^{-}$**
- $12.9 > pH > 11.7$ = **$>SiOCa^{+}$**
- $11.7 > pH > 11.0$ = **>SiOH** and **$>SiO^{-}$**

In general, no remarkable differences were observed between the two type of cement tested, the ζ evolution of CEM-V and CEM-I show both negative and positive zeta potential along the pH (degradation process). The main cement phases such as C-S-H and ettringite show a positive zeta potential over a wide range of pH which indicates these phases might fix to some extent molecules negatively charged (Figure 21).

Calcium concentration is controlled by portlandite or C-S-H solubility, and has a direct influence on the concentration of calcified surface sites of C-S-H ($>SOCa^+$), which can bring positive charge in addition of the deprotonated surface sites ($>SO^-$).

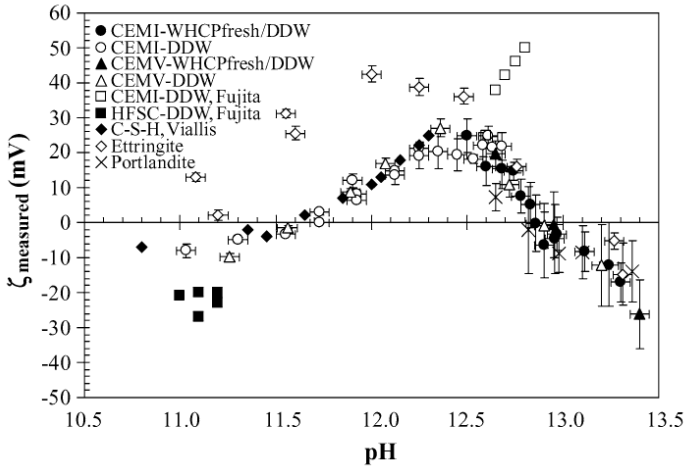

Figure 21. Evolution of the ζ potential of CEM-I and CEM-V HCP as a function of pH. The measured ζ values of portlandite (CH) and ettringite (AFt) show the possible contribution of secondary cementitious phases in the value of degraded HCP surface potentials. Source: Pointeau et al. (2006)

Selection of C/S ratios for C-S-H phases

The alteration of the cementitious materials has been repeatedly performed in laboratory experiments by several authors (e.g. Flint and Wells (1934); Greenberg and Chan (1965); Harris et al. (2002); Chen et al. (2004)). In general, there is a rather similar dependence between the pH of pore water and the C/S ratio of the hydrated calcium-silicate phases (Figure 22). The C/S ratio decreases as the C-S-H is progressively replaced by Si-enriched phases since C-S-H dissolution is clearly incongruent. In the initial stages, the cement alteration is limited to portlandite dissolution as pure phase or as a $Ca(OH)_2$ hypothetical end-member of C-S-H phases. In the latter case, the loss of calcium results in the formation of new C-S-H with lower Ca/Si ratio.

From the data reported by Harris et al. (2002) and taking into account the IEP at pH = 11.7 determined by Viallis-Terrisse et al. (2001) and Pointeau et al. (2006) for C-S-H, a range of calcium-to-silica ratio can be established in which zeta potential is close to zero. From this range, two C/S ratios can be defined so that to obtain two C-S-H phases controlled by different surface complexes and thus with different surface charge. According to this, and assuming this range of C/S ratio covering from ~0.87 to ~1.0 (Figure 22), two C-S-H phases are suggested to be studied as they will show clear opposite ζ values:

1. **C-S-H gel with C/S ratio of 0.8**
2. **C-S-H gel with C/S ratio of 1.1**

Once two C/S ratios has been acquired as a function of their apparent charge, the role of surface area with regards to molybdate retention in comparison with zeta potential in C-S-H phases can be investigated.

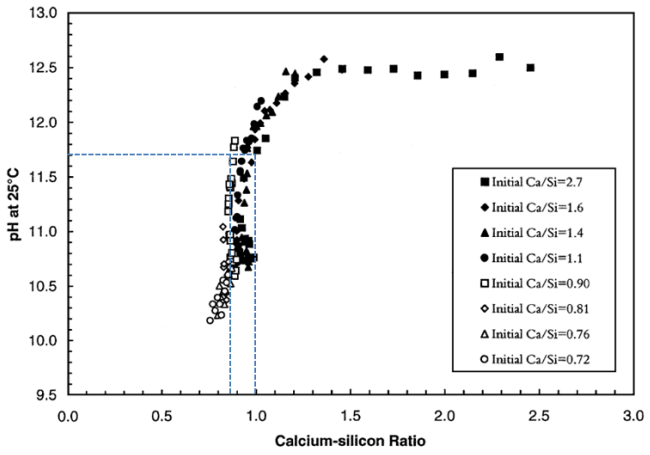

Figure 22. Evolution of the C-S-H composition with respect to pH variation from reported experimental data. Source: Harris et al. (2002). Dashed lines determine the C/S ratio range at given pH value of 11.7.

Concluding remarks

- Molybdenum has a strong capacity to form complex poly-anions, although it is assumed that the principal Mo species existing in alkaline solution is the simple molybdate anion (MoO_4^{2-}).
- Being negatively charged, this anion has been reported as non-sorbing in many studies which can be considered as solely conservative assumptions.
- The great thermodynamic stability of molybdate anion as well as its high mobility in alkaline waters makes its immobilization an avoidable challenge to pursue. Ettringite and monosulphate have been initially shown to be important cement constituents for the immobilization of oxyanions.
- Solid solution formation with ettringite in cement can be undergone through partial or full replacement of sulphates by anions of similar geometry and charge.
- Differences in size and charge between sulphate and substituting oxyanions are the major factors determining the extent of the uptake, so the incorporation of molybdate anion with dissimilar size (ionic radii of S is 0.29 Å while Mo is 0.62 Å) and electronegativity is reported to be low or non-existent.
- Ettringite-SO_4 formation is highly favored over other different oxyanion-substituted ettringites even when these ones have been already formed.
- Monosulphate (as a SO_4-hydrocalumite) has unique structural characteristics which enable it to accommodate anions of various sizes.
- The mechanism is similar to ettringite, i.e. sulphate in the interlayer of monosulphate can be replaced by oxyanions, however differences in ionic size between SO_4^{2-} and a substitution anion is not a controlling factor of the extent and preference for oxyanion incorporation.
- Although more scarcely studied than ettringite, several studies found in the literature point to monosulphate as the prevailing host mineral at pH > 12, indicating that it is capable to exert oxyanion solubility control to lower levels than substituted ettringite.

- While ettringite and monosulphate may serve as viable mechanisms for oxyanion immobilization, several factors have to be considered though when the formation of these phases is proposed to be the main immobilization factor of oxyanions as their stability depends on several physico-chemical conditions, such as pH, temperature, presence of sulphate and other competing anions, among others.
- There are studies showing that C-S-H phases can immobilize oxyanions (CrO_4^{2-} and AsO_4^{3-}) by replacing silicate in its structure, these experimental data suggest that these phases could also be an important sink for molybdate.
- Zeta potential can be an important factor limiting the extent and mechanism of molybdate-C-S-H binging. In this context, two C-S-H phases with C/S ratio of 0.8 and 1.1 has been suggested to be studied as they show clear opposite ζ values.
- There is a lack of thermodynamic parameters which difficult the development of efficient models to predict molybdenum behaviour at repository conditions.
- In order to feed geochemical databases with new relevant datasets, experimental activities must be conducted to provide reliable thermodynamic data from Mo analogues as well as to acquire information on sorption/desorption capacities under different but representative conditions.

References

Aguilera, J. 2003, *Efectos provocados por el ataque conjunto de los agentes atmosféricos CO2 y SO2. Condiciones termodinámicas que permiten la formación de taumasita y sus efectos destructivos en los morteros de cemento,* PhD thesis, Universidad Complutense de Madrid.

Aveston, J., Anacker, E. W., Johnson, J. S. 1964, *Hydrolyses of molybdenum(IV). Ultracentrifugation, acidity measurements, and raman spectra of polymolybdates*, Inorg. Chem., 3, 735-746.

Baes, C. F., Mesmer, R. E. 1976, *The hydrolysis of cations*, Wiley, New York.

Bard, J. A., Parsons, R., Jordan, J. 1985, *Standard potentials in aqueous solution*, IUPAC, Oxford, U.K.

Baur, I., Johnson, C.A. 2003, *Sorption of selenite and selenate to cement materials*, Environ. Sci.Technol. 37, 3442–3447.

Baur, I., Johnson, C.A., 2003, *The solubility of selenate Aft (3CaO Al2O3 3CaSeO4 637.5H2O) and selenate-AFm (3CaO Al2O3 CaSeO4 xH2O)*. Cement Concrete Res. 33, 1741–1748

Beaudoin, J.J., Ramachandran, V.S., Feldmann, R.F. 1990, *Interaction of chloride and C-S-H*, Cem. Concr. Res. 20 875-883.

Berner, R. A. 1964, *Stability fields of iron minerals in anaerobic marine sediments*, J. Geol., 72: 826- 834.

Berner, U. 2002, *Project Opalinus Clay: Radionuclide Concentration Limits in the Cementitious Near Field of an ILW Repository*, PSI Bericht Nr. 02-26, Paul Scherrer Institute, Villigen PSI, Switzerland and Nagra Technical Report NTB 02-22, Nagra, Wettingen, Switzerland.

Berner, U. 2014, *Solubility of radionuclides in a concrete environment for provisional safety analyses for SGT-E2*, Nagra.

Bertine, K. K. 1972, *The deposition of molybdenum in anoxic waters*, Marine Chemistry, 1(1), 43-53.

Blanc, P., Bourbon, X., Lassin, A. Gaucher, E. C. 2010, *Chemical model for cement-based materials: Thermodynamic data assessment for phases other than C-S-H*. Cement and Concrete Research, 40, 1360-1374.

Chen, J. J., Thomas, J. J., Taylor, H. F., Jennings, H. M. 2004, *Solubility and structure of calcium silicate hydrate*, Cem. Concr. Res., 34(9), 1499-1519.

Colàs, E., Grivé, M., Olmeda, J., Campos, I., Bruno, J. 2014, *Reduction of radionuclide uptake in hydrated cement systems by organic complexing agents: Selection of reduction factors and speciation calculations*. SKB report. R-14-22.

Cornelis, G., Johnson, C. A., Van Gerven, T., Vandecasteele, C. 2008, *Leaching mechanisms of oxyanionic metalloid and metal species in alkaline solid wastes: a review*. Applied Geochemistry, 23(5), 955-976.

Damidot, D., Glasser, F. P. 1995a, *Investigation of the CaO-Al 2 O 3-SiO 2-H 2 O system at 25 C by thermodynamic calculations*, Cem. Concr. Res., 25(1), 22-28.

Damidot, D., Glasser, F. P. 1995b, *Thermodynamic investigation of the CaO—Al2O3—CaSO4—CaCO3-H2O closed system at 25° C and the influence of Na2O*, Advances in Cement Research, 7(27), 129-134.

Dellien, I., Hall, F. M., Hepler, L. G. 1976, *Chromium, molybdenum, and tungsten: thermodynamic properties, chemical equilibriums, and standard potentials*, Chemical Reviews, 76(3), 283-310.

Engelsen, C. J., Van der Sloot, H. A., Wibetoe, G., Justnes, H., Lund, W., Stoltenberg-Hansson, E. 2010, *Leaching characterisation and geochemical modelling of minor and trace elements released from recycled concrete aggregates*, Cem. Concr. Res., 40(12), 1639-1649.

Flint, E. P., ells, L. S. 1934, *Study of the system CaO-SiO2-H2O at 30 ºC and of the reaction of water on the anhydrous calcium silicates*, Journal of Research of the National Bureau of Standards, 12, 751-783.

Gabrisova, A., Havlica, J., Sahu, S. 1991, *Stability of calcium sulphoaluminate hydrates in water solutions with various pH values*. Cem. Concr. Res., 21(6), 1023-1027.

Glasser, F.P. 1993, *Chemistry of cement-solidified waste forms. In: chemistry and microstructure of solidified waste forms*, Spence, R. D., Ed.; Lewis Publishers, Boca Raton, FL; pp 1-40.

Grangeon, S., Claret, F., Linard, Y., Chiaberge, C. 2013, *X-ray diffraction: a powerful tool to probe and understand the structure of nanocrystalline calcium silicate hydrates*, Acta Crystallographica Section B: Structural Science, Crystal Engineering and Materials, 69(5), 465-473.

Greenberg, S. A., Chang, T. N., Anderson, E. 1960, *Investigation of colloidal hydrated calcium silicates*, I. Solubility products. The Journal of Physical Chemistry, 64(9), 1151-1157.

Grivé, M., Montoya, V., Valls, A., Domenech, C., Colàs, E., Duro, L. 2012, Assessment of solubility limits for radionuclides and toxics under clay and cementitious conditions: Recommended solubility limits calculated with ThermoChimie v.8.0. ANDRA Report.

Hampson, C. J., Bailey, J. E. 1983, *The microstructure of the hydration products of tri-calcium aluminate in the presence of gypsum*, Journal of Materials Science, 18(2), 402-410.

Harris, A. W., Manning, M. C., Tearle, W. M., Tweed, C. J. 2002, *Testing of models of the dissolution of cements—leaching of synthetic CSH gels*, Cem. Concr. Res., 32(5), 731-746.

Hassett, D. J., McCarthy, G. J., Kumarathasan, P., Pflughoeft-Hassett, D. 1990, *Synthesis and characterization of selenate and sulfate-selenate ettringite structure phases*, Materials research bulletin, 25(11), 1347-1354.

Kaback, D. S., Runnells, D. 1980, *Geochemistry of molybdenum in some stream sediments and waters*, Geochim et Cosmochim. Acta, 44, 447-456.

Keller, I. R. B. 2002, *The Immobilisation of Heavy Metals and Metalloids in Cement Stabilised Wastes: A Study Focussing on the Selenium Oxyanions SeO3-2 and SeO4-2*, Doctoral dissertation, Universität Zürich.

Kindness, A., Lachowski, E. E., Minocha, A. K., Glasser, F. P. 1994, *Immobilisation and fixation of molybdenum (VI) by Portland cement*, Waste management, 14(2), 97-102).

Kumarathasan P., McCarthy G. J., Hassett D. J., and Pflughoeft-Hassett D. F. 1990, *Oxyanion substituted ettringites: synthesis and characterization; and their potential role in immobilization of As, B, Cr, Se and V*, In Materials Research Society Symposium, 83-104.

Liese, A., Hilterhaus, L. 2013, *Evaluation of immobilized enzymes for industrial applications*, Chemical Society Reviews, 42(15), 6236-6249.

Lindgren, M., Pettersson, M., Wiborgh, M. 2007, *Correlation factors for C-14, Cl-36, Ni-59, Ni-63, Mo-93, Tc-99, I-129 and Cs-135*, In operational waste for SFR 1. Swedish Nuclear Fuel and Waste Management Co.

Linklater, C.M. 1998, *A natural analogue study of cement-buffered, hyperalkaline porewaters and their interaction with a repository host rock. Phase II. Maqarin Natural Analogue site study group*, Science report. Nirex safety assessment research programme. Nirex Report, S/98/003.

Lothenbach, B., Ochs, M., Hager, D. 1999, *Confinement of radioactive waste in cementitious barriers for surface and deep geological disposal*, Andra 2005 report 1999, C. RP.0BMG.99-001.

Martínez-Ramírez, S., Blanco-Varela, M. T. 2009, *Thermodinamically stable phases in the CaO-SiO 2-Al 2 O 3-CaSO 4-H 2 O closed system at 25 °C*, Application to cementitious systems. Materiales de Construcción, 59(294), 31-39.

Matschei, T., Glasser, F. P. 2010, *Temperature dependence, 0 to 40 ºC, of the mineralogy of Portland cement paste in the presence of calcium carbonate*. Cem. Concr. Res., 40(5), 763-777.

Moreno, R. 2005, *Reología de suspensiones cerámicas*, Colección Biblioteca de Ciencias, Ed. CSIC.

Möschner, G., Lothenbach, B., Winnefeld, F., Ulrich, A., Figi, R., Kretzschmar, R. 2009, *Solid solution between Al-ettringite and Fe-ettringite (Ca 6 [Al1− xFex (OH)6]2(SO4)3·26H2O)*, Cem. Concr. Res., 39(6), 482-489.

Muidrow, C. N. Jr., Hepler L. G. 1958, *Heats of Precipitation and Formation of Lead and Calcium Molybdates*, J. Phys. Chem., 62 (8), 982.

Myneni S. C. B. 1995, *Oxyanion-Mineral Surface Interactions in Alkaline Environments: AsO4 and CrO4 Sorption and Desorption in Ettringite*, Dissertation, The Ohio State University, 250 p.

Nachbaur, L., Nkinamubanzi, P. C., Nonat, A., Mutin, J. C. 1998, *Electrokinetic properties which control the coagulation of silicate cement suspensions during early age hydration*, Journal of Colloid and Interface Science, 202(2), 261-268.

Naumov, G. B., Ryzhenko, B. N., Khodakovskii, I. L. 1971, *Handbook of Thermodynamic Values*. Atomizdat, Moscow, in Russian; Engl. Transl: Report USGS-WRD-74-001 (Solimani, G.J., Barnes, I., Speltz, V., eds.), U.S. Geological Survey, Menlo Park, California, USA, 1974, 328.

Ochs, M., Lothenbach, B., Talerico, C. 2001, *Support of Kd models and datasets for the retention of radionuclides in cementitious repositories*, Andra 2005 report C.RP.0BMG.01-001, Andra 2005, France.

Ochs, M., Mallants, D., Wang, L. 2015, *Radionuclide and Metal Sorption on Cement and Concrete*, Vol. 9999, Springer.

O'Hare, P. A. G., Kenneth, J. J., Hoekstra, H. R. 1974, *Thermochemistry of molybdates IV. Standard enthalpy of formation of lithium molybdate, thermodynamic properties of the aqueous molybdate ion, and thermodynamic stabilities of the alkali-metal molybdates*, J. Chem. Thermodynamics, 6, 681-691.

O'Hare, P. A. G. 1974, *Thermochemistry of molybdates III. Standard enthalpy of formation of barium molybdate, and the standard entropy and standard Gibbs energy of formation of the aqueous molybdate ion*, J. Chem. Thermodynamics, 6, 425-434.

O'Hare, P. A. G. Hoekstra, H. R. 1973, *Thermochemistry of molybdates I. Standard enthalpy of formation of caesium molybdate (Cs2MoO4)*, J. Chem. Thermodynamics, 5, 851-856.

O'Hare, P. A. G. Hoekstra, H. R. 1974, *Thermochemistry of molybdates II. Standard enthalpies of formation of rubidium molybdate and the aqueous molybdate ion*, J. Chem. Thermodynamics, 6, 117-122.

Palmer, C. D. 2000, *Precipitates in a Cr (VI)-contaminated concrete*, Environmental science & technology, 34(19), 4185-4192.

Papadokostaki, K. G. and A. Savidou 2009, *Study of leaching mechanisms of caesium ions incorporated in Ordinary Portland Cement*, J. Hazard Mater. 171(1-3): 1024-1031.

Parker, V. B., Wagman, D. D., Evans, W. H. 1971, *Selected Values of Thermodynamic Properties*, NBS Technical Note 270-6, US government printing office, Washington.

Perkins, R. B. 2000, *The solubility and thermodynamic properties of ettringite, its chromium analogs, and calcium aluminum monochromate (3CaO· Al2O3· CaCrO4· nH2O)*, Doctoral dissertation, Portland State University.

Poellman H., Auer S., Kuzel H. J., Wenda R. 1993, *Solid solution of ettringites, Part II: incorporation of B(OH)4- and CrO42- in Ca6Al2O6(SO4)3·32H2O*, Cem. Concr. Res., 23, 422-430.

Pointeau, I. 2000, *Etude Mechanistique et modelisation de la retention de radionucliedes par les silicates de calcium hydrates (CSH) des ciments*, Doctoral dissertation.

Pointeau, I., Landesman, C., Giffaut, E., Reiller, P. 2004, *Reproducibility of the uptake of U (VI) onto degraded cement pastes and calcium silicate hydrate phases*, Radiochimica Acta/International journal for chemical aspects of nuclear science and technology, 92(9-11/2004), 645-650.

Pointeau, I., Reiller, P., Macé, N., Landesman, C., Coreau, N. 2006, *Measurement and modeling of the surface potential evolution of hydrated cement pastes as a function of degradation*, Journal of colloid and interface science, 300(1), 33-44.

Richardson, I.G., Groves, G.W. 1993, *Models for the composition and structure of Calcium Silicate Hydrate (C-S-H) gel in hardened tricalcium silicate pastes and the incorporation of minor and trace-elements into Calcium Silicate Hydrate (C-S-H) gel in hardened cement pastes - Reply*, Cem. Concr. Res. 23 999-1000.

Robbie, R. A., Hemingway, B. S. 1995, *Thermodynamic properties of minerals and related substances at 298.15 K and 1 bar (105 pascals) pressure and at higher temperatures*, Washington and Denver, CO, U.S. G. P. O.

Robbie, R. A., Hemingway, B. S., Fisher, J. R. 1979, *Thermodynamic properties of minerals and related substances at 298.15 K and 1 bar and at higher temperatures*, Geol. Sur. Amer. Bull, 1452.

Sasaki, Y., Sillén, I. G. 1968, *Equilibrium studies of polyanions. 16. Equilibria of molybdates in 3 (M) Na(ClO4) medium at 25 °C*, Ark,. Kemi., 29, 253

Sasaki, Y., Sillén, I. G., Ark, K. 1968, *Spectrophotometric investigation of the protonation of monomeric mollybdic acid in sodium perchlorate medium*, In: Cruwage, J. J., Heyns, J. B. B. Rohwer, E. F. C. H. 1976, *Spectrophotometric investigation of the protonation of monomeric molybdic acid in sodium perchlorate medium*, J.Inorg. Nucl. Chem., 38(11), 2033-2036.

Scadden, E. M., Ballou, N. E. 1960, *The radiochemistry of Molybdenum*, Vol. 3009, National Academies.

Short, R. J., Hand, R. J., Hyatt, N. C. 2002, *Molybdenum in Nuclear Waste Glasses-Incorporation and Redox state*, In MRS Proceedings (Vol. 757, pp. II5-4). Cambridge University Press.

Short, R., Hand, R. J. 2004, *Incorporation of molybdenum in nuclear waste glasses*, University of Sheffield.

Skagius, K., Pettersson, M., Wiborgh, M., Albinsson, Y., Holgersson, S., 1999, *Compilation for the analysis of radionuclide migration from SFL 3-5*, SKB Report R-99-13, SKB, Sweden.

SKB, 2014a, *Data report for the safety assessment SR-PSU*. SKB TR-14-10.

SKB, 2014b, *Waste form and packaging process report for the safety assessment SR-PSU*. SKB TR-14-03.

Staudt, W. J., Reeder, R. J., Schoonen, M. A. A. 1994, *Surface structural controls on compositional zoning of SO42− and SeO42− in synthetic calcite single crystals*, Geochim. Cosmochim. Acta 58, 2087–2098.

Taylor, H. F. 1986, *Proposed structure for calcium silicate hydrate gel*, Journal of the American Ceramic Society, 69(6), 464-467.

Taylor, H. F. 1997, *Cement chemistry*. Thomas Telford ed.

Taylor, H. F. 2002, *Sulfates in Portland clinker and cement*, International RILEM TC Workshop on Internal Sulfate Attack and Delayed Ettringite Formation. London, Thomas Telford.

Thorium: Reduce, Reuse, Recycle. n.d., Available at http://energyfromthorium.com

Tits, J., Iijima, K., Wieland, E., Kamei, G. 2006, *The uptake of radium by calcium silicate hydrates and hardened cement paste*, Radiochimica Acta, 94(9-11), 637-643.

Viallis-Terrisse, H., Nonat, A., etit, J. C. 2001, *Zeta-potential study of calcium silicate hydrates interacting with alkaline cations*, Journal of colloid and interface science, 244(1), 58-65.

Vollpracht, A., Brameshuber, W. 2016, *Binding and leaching of trace elements in Portland cement pastes*, Cem. Concr. Res., 79, 76-92.

Wagman, D. D., Evans, W. H., Parker, V. B., Schumm, R. H., Halow, I., Balley, S. M., Churney, K. L. Nuttal, R. L. 1982, *NBS Tables of Chemical Thermodynamic Properties: Selected Values for Inorganic and C1 and C2 Organic Substances in SI Units*, Journal of Physical and Chemical Reference Data, 11, 1-392.

Weller, W. W., Kingm E. G. 1963, *Bureau of Mines Report of Investigations No. 6147*, US. Government Printing Office, Washington, D.C.

Wenda, R., Kuzel, H. J. 1986, *B3+ in calcium aluminate hydrates*, In: Proceedings of 8th International Congress on the Chemistry of Cement (2nd edn), Vol. III, Rio de Janeiro (pp. 307-313).

Ziegler, F., Gieré, R., Johnson, C.A. 2001, *Sorption mechanisms of zinc to calcium silicate hydrate: sorption and microscopic investigations*, Environ. Sci. Technol. 35. 4556-4561.

Characterization of Hydrated Cement Paste (CEM II) by Selected Instrumental Methods and a Study of ^{85}Sr Uptake (CTU)

Barbora Drtinová, Jana Kittnerová, Dušan Vopálka

Affiliation: Department of Nuclear Chemistry, Czech Technical University in Prague, Czech Republic

barbora.drtinova@fjfi.cvut.cz

Abstract

In relation with the Czech program of radioactive waste disposal the two cements of CEM II grade were chosen for studying. Both materials have been evaluated by standard and also advanced methods. The obtained characteristics of selected cements are quite different. All methods used for characterization of cements have not been applied to both materials yet. A system consisting of crushed hydrated cement paste (CEM II / A-S 42.5), its leachate obtained at the phase ratio m/V = 0.2 kg/L (with the natural concentration of Sr 3.5×10^{-4} mol/L), and a radioactive tracer ^{85}Sr was studied in order to understand the interaction of hydrated cement with Sr as an analog of Ra. In a wider range of phase ratio, the equilibrium of tracer, described by means of distribution coefficient K_d, was reached after approx. 2 days. The value of distribution coefficient for m/V ratio in the interval of (0.01, 0.1) kg/L was constant, while for higher values of m/V K_d increased linearly. This effect may be connected with the fact that the hydrated cement paste contains strontium and that the equilibrium concentration of Sr in both liquid and solid phases belonging to this "exchangeable Sr" could be influenced by conditions of the experiments.

Introduction

A significant part of low and intermediate radioactive wastes containing radium is stored in Czech Republic in the repository Bratrství. This repository is running out of space and will be closed in the near future. It is important to provide safety studies, collect necessary parameters and check safety of the repository before its closure. As barriers in this repository are based on cementitious materials and ^{226}Ra is there the main contaminant of interest, SURAO (the Czech Radioactive Waste Repository Authority) aims to study systems radium – hydrated cement materials.

As there are not many studies available dealing specifically with radium and all the necessary techniques are not at hand yet, we decided to perform an introductory methodological study with strontium, which could be considered chemically similar to radium. This approach corresponds with that of other laboratories (e.g. Berner 2002, Tits et al. 2006). Our aim is to gain experience and knowledge about optimal experimental conditions and procedures while working with hydrated cement pastes and about the description of interaction of radionuclides with cementitious materials, which is necessary in modeling of radium transport in the repository environment.

Two cements of CEM II grade, A: CEM II / A-S 42.5 R (produced by Lafarge Cement, a. s.) and B: CEM II / B-M (S-LL) 32.5R (produced by Českomoravský cement, a. s. - HeidelbergCement Group) were chosen for the study, based on recommendations of SURAO. The first cement (A) is made, according to an information of the producer, by grinding together silicate clinker, blast furnace granulated slag and gypsum. Slag adjusts the cement blend and decreases hydration heat and its cement content is max.

20%. Gypsum acts as a regulator preventing cement flash setting. The second cement (B) is Portland composite cement of the strength class made of clinker, granulated blast furnace slag (approx. 15 %), of limestone (approx. 12 %) with low TOC content and anhydrite as retarder.

Both materials have undergone testing by instrumental methods available in our laboratory (determination of density and specific surface area, FTIR, XRD, AAS) and part of the results of this work became the basis for a bachelor thesis (Kittnerová 2015). With the hydrated cement paste of cement A, a preliminary study of the interaction using ^{85}Sr tracer was carried out.

Experimental

Materials and methods

Preparation of cement pastes

Cement A was used for preparation of cement blocks with water/cement ratio $w = 0.667$ with time of hydration 19 days in co-operating laboratory in ÚJV Řež. A relatively short time used for hydration was chosen according to the demands of other types of experiments that were planned to be accomplished. Blocks of cement paste from cement B were prepared with water/cement ratio $w = 0.667$ (a mixture of water and ice was used), time of hydration in humid atmosphere was almost 3 months.

For some experiments performed in our laboratory the blocks of hydrated cement paste were crushed and sieved. The fraction < 0.71 mm was used for interaction experiments and for some characterizations (determination of density and specific surface), larger pieces and blocks were applied by leaching and IR spectroscopy.

Characteristics of cement pastes

Simple methods

Values of density of hydrated cement determined by pycnometric method on crushed materials were 2177 ± 44 kg/m^3 for cement A and 1998 ± 29 kg/m^3 for cement B (the presented uncertainty represents in the all text an estimate of the standard deviation).

The rapid dynamic flow method for determinations of single-point B.E.T. (Quantachrome Monosorb MS-22 device) was utilized to measure specific surface areas of both materials. Obtained values were 20.1 ± 0.3 m^2/g and 48.5 ± 0.3 m^2/g for cements A and B, respectively. Significant differences between studied cement materials in both characteristics need a thorough check of the laboratory procedures and further discussion that will include a comparison with literature data.

Instrumental methods

FTIR spectra were measured by Nicolet iS 50 FT-IR spectrometer by Attenuated Total Reflection (ATR) technique in the scan range of $400 - 4000$ cm^{-1} for two blocks of cement B. One of these blocks (sample W) was placed for 3 months in a closed vessel submerged in distilled water (cement-to-water ratio was 0.1 kg/L), the second one (reference sample R) was left dry in sealed flask with no contact with liquid phase. From results on Figure 1 it can be seen that leaching of hydrated cement caused only very small change of FTIR spectrum.

An attempt of the interpretation of the character of obtained spectra, based on the database of the device, is presented in Table 1.

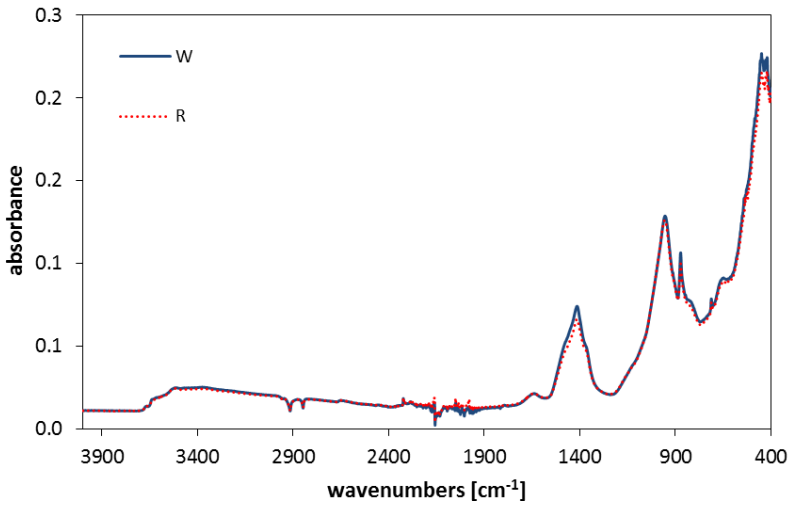

Figure 1 FTIR spectra of two cement blocks (cement B),
W: contact with water for 3 months, R: no contact with water

Table 1 Possible assignment to some peaks observed in FTIR spectra

Wave number [cm^{-1}]	Vibration	Compound
3600 – 3300	(OH)	H_2O or $Ca(OH)_2$
1414	$(CO_3)^{2-}$	$CaCO_3$
1100 – 950	(OH) and (Si-O)	$Ca(OH)_2$ and SiO_2
870, 420, 300, 250	$(CO_3)^{2-}$	$CaCO_3$
650	(Si-O)	SiO_2
450	Ca-Si	x

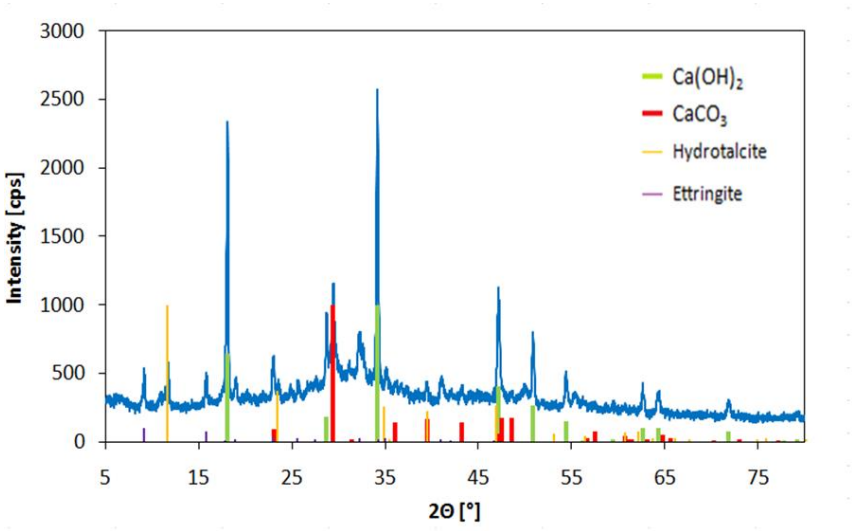

Figure 2 XRD spectrum of the hydrated cement A

Both cementitious materials (cement A and cement B) were tested by X-ray diffraction (Rigaku Mini Flex 600). As an illustration, XRD spectrum of cement A is presented on Figure 2. The comparison of measured spectrum with database ICDD PDF-2 (version 2013) of the measuring system enabled to identify four mineral phases, namely calcite

$CaCO_3$, portlandite $Ca(OH)_2$, hydrotalcite $Mg_6Al_2CO_3(OH)_{16}\cdot 4(H_2O)$ and ettringite $Ca_6Al_2(SO_4)_3(OH)_{12}\cdot 26H_2O$.

It should be noted here that in XRD spectra of cement B (samples W and R) only calcit and portlandite were identified. From a comparison of spectra of samples R and W could be proved that the content of $Ca(OH)_2$ (portlandite) decreased significantly in the bulk of the cementitious block by leaching of hydrated cement in water.

Sorption experiments with ^{85}Sr

Preparation of working solution

With the aim to prepare a working solution the influence of which on solid phase by sorption experiments would not be important the crushed hydrated cement A was contacted with distilled water for 1 month (solid-to-liquid ratio equaled to 0.2 kg/L). The concentrations of important cations determined by AAS (Varian AA 240 FS) in this leachate (pH = 12.8) are presented in Table 2. In comparison, there are also presented concentrations of cations in leachate of hydrated cement B (pH = 12.2) that originated during the preparation of the sample W mentioned above.

Table 2 Concentrations of important cations in leachates of hydrated cements A and B

cation	cement A, V/m = 0.2 kg/L, contact time 1 month		cement B, V/m = 0.1 kg/L contact time 3 months	
	C [mmol/L]	σ_C [mmol/L]	C [mmol/L]	σ_C [mmol/L]
Na^+	5.88	0.01	1.37	0.04
K^+	23.8	0.3	4.08	0.05
Ca^{2+}	13.5	0.1	3.1	0.2
Mg^{2+}	0.0016	0.0002	< 0.001	
Sr^{2+}	0.350	0.002	n.d.	

Kinetic experiments

Crushed hydrated cement A (diameter of grain ≤ 0.71 mm) was contacted with cement leachate in a set of kinetic experiments. Monitored element was strontium traced by radioactive isotope ^{85}Sr (added as $SrCl_2$, its activity measured by Na(I)Tl detector, of molar concentration equal to $1\cdot 10^{-7}$ mol/L). The change of ^{85}Sr activity caused by the radioactive decay was eliminated in the way of evaluation of results of experiments. Solid-to-liquid ratio (m/V) was in the range from 0.033 (1:30) to 0.33 (1:3) kg/L. As the total Sr concentration was not measured during the experiments, the uptake of ^{85}Sr is presented in Figure 3, in which the results of this study is described.

The observed kinetics of ^{85}Sr uptake was relatively fast – after 2 days equilibrium for all phase ratios was reached. So the duration of each experiment in the subsequent set of equilibrium experiments was set to 4 days.

Equilibrium experiments

A broad set of equilibrium experiments was performed in which the initial total concentration of strontium in the liquid phase was changed from 0.35 to 1 mmol/L,

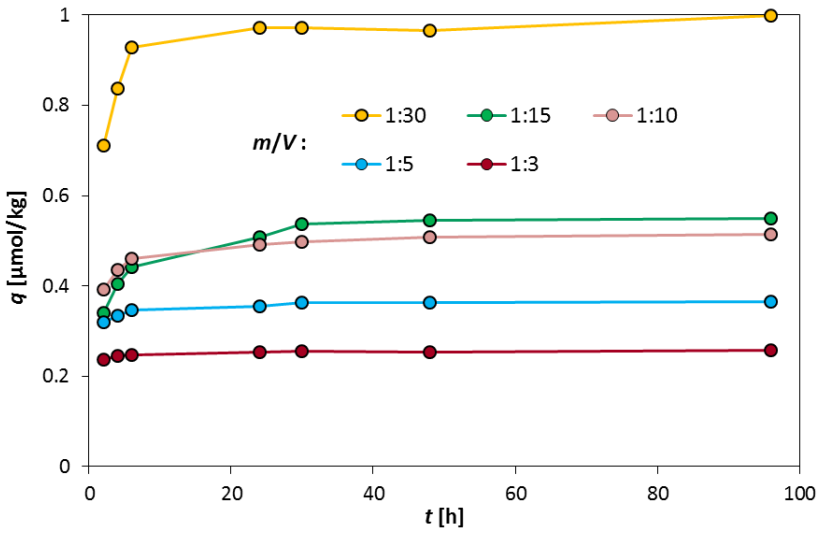

Figure 3 Kinetics of the ^{85}Sr uptake on the hydrated cement A

while the concentration of Sr in the leachate used as the basic component of the working solution was taken into account. Experiments were carried out for 6 different *m*/*V* ratios (from 1:100 to 1:3). The distribution coefficient K_d, obtained from the balance evaluation of ^{85}Sr activity in the liquid phase, as the measure of the ^{85}Sr, uptake was used. No influence of the total initial concentration on the ^{85}Sr uptake was observed, but the spread of results obtained for different initial concentrations enabled to describe the uncertainty of determined K_d values by standard deviation.

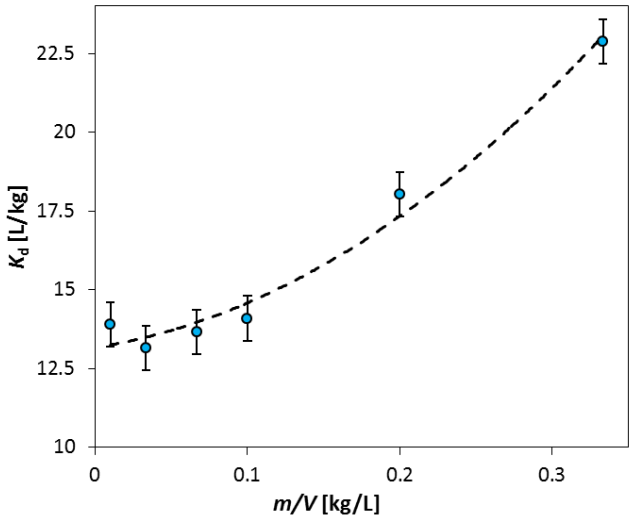

Figure 4 Dependence of determined K_d values describing ^{85}Sr uptake on hydrated cement A on the phase ratio *m*/*V*

The obtained results are presented in Figure 4. The increase of K_d values with increasing phase ratio *m*/*V* is evident. This trend is unexpected if the ion-exchange would be taken into account as an important mechanism of the uptake, as stated e.g. Wieland et al. 2008. In our last study (Vopálka et al. 2015) we reported, for the description of Cs sorption on bentonite, the opposing trend and the description of sorption equilibrium with the use of ion-exchange mechanism was successful in this case. The presence of Sr in both working solution and solid phase at the beginning of sorption experiment changes the standard procedure of sorption experiments evaluation. The so-called exchangeable Sr in the solid phase could be dependent on the

composition of the liquid phase that varies with m/V ratio. We expect that the determination of the exchangeable Sr in a further research will help with the interpretation of the observed trend of K_d.

Conclusions

Hydrated cement pastes from two different cements considered in the Czech program of disposal of ILW were tested by techniques available in the laboratory of Department of Nuclear Chemistry, CTU in Prague. One of the cement, namely CEM II / A-S 42.5 R was selected for an introductory study of ^{85}Sr uptake on crushed hydrated cement. The leachate of hydrated cement (m/V = 0.2 kg/L, pH 12.8) containing Sr in a significant concentration was used as the base for both kinetic and equilibrium experiments. The equilibrium was attained in approx. 2 days in kinetic experiments. An unexpected trend of measured distribution coefficient K_d of ^{85}Sr, in which the K_d values were higher for higher values of m/V ratio, was supposed to be connected with the influence of m/V and initial composition of liquid phase on the equilibrium concentrations in both liquid and solid phases. As Sr and Ra are similar to some extent, the performed study of Sr uptake will help us with the planned study of Ra uptake on the same material.

References

Berner, U. 2002, *Project Opalinius Clay. Radionuclide concentration limits in the cementitious near-field of an ILW repository*. PSI Report Nr. 02-26, Paul Scherrer Institut, Villigen, Switzerland, 61 p.

Kittnerová, J. 2015, *Cementitious materials in barriers of radioactive waste repositories.* Thesis, Department of Nuclear Chemistry, CTU in Prague, 77 p. (in Czech)

Tits, J., Wieland, E., Möller, C.J., Landesman, C., Bradbury, M.H. 2006, *Strontium binding by calcium silicate hydrates*. Journal of Colloid and Interface Science 300, 78-87.

Vopálka, D., Gondolli, J., Drtinová, B., Klika, Z. 2015, *Cesium uptake by Ca/Mg bentonite: evaluation of sorption experiments by a multicomponent two-site ion-exchange model*. Journal of Radioanalytical and Nuclear Chemistry 304, 429-434.

Wieland, E., Tits, J., Kunz, D., Dähn, R. 2008, *Strontium uptake by cementitious materials*. Environmental Science and Technology 42, 403-409.

^{14}C and ^{226}Ra sorption on hardened cement paste and mortars (RATEN-ICN)

Crina Bucur

Affiliation: Institute for Nuclear Research Pitesti (RATEN ICN)

crina.bucur@nuclear.ro

Introduction

In Romania, the long-lived radioactive waste (LL-ILW) and CANDU spent fuel are foreseen to be disposed of in a future geological repository.

The main source of Carbon-14 in the LL-ILW to be disposed of in the Romanian geologic repository is the spent ion exchange resins generated mainly in the Moderator System and in the Primary Heat Transport System of the two CANDU units of Cernavoda NPP. The dominant Carbon-14 species in spent ion exchange resins is inorganic carbonate $^{14}CO_3^{2-}$ and more than 90% of Carbon-14 is bound on the anion resin fraction (Park et al., 2008).

Other LL-ILW to be geological disposed of consists in the pressure tubes and calandria tubes that could contain Carbon-14 both as inorganic and organic species.

^{226}Ra is one of the major daughter nuclides of the ^{238}U that could be found in the fuel-contact spent ion exchange resins but also in other waste streams.

In form of dissolved carbonate or bicarbonate, inorganic Carbon-14 is strongly immobilized in cemented waste forms. Under strongly alkaline conditions, the dominant species of inorganic Carbon-14 is $^{14}CO_3^{2-}$. The carbonate ions can either precipitate as $CaCO_3$ or sorb onto cement phases.

Information on the speciation of Carbon-14 associated with organic compounds which might be released from the various waste forms, and their potential immobilization by cementitious materials is limited.

Literature data regarding Ra(II) sorption on fresh and aged HCP show that distribution coefficient is less than 0.1 m^3/kg for fresh HCP and less than 0.4 m^3/kg for aged HCP. The uptake of Ra by HCP could be interpreted in terms of Ra binding to C-S-H phases.

There is reported in the literature results of numerous studies on C-14 sorption on hardened cement paste and mortars and some on Ra-226 sorption. Experimental data regarding the effect of the cement degradation in the disposal conditions on radionuclide sorption are scarce and the experiments to be carried out in RATEN ICN in the frame of CEBAMA WP2 will be specifically oriented to assess the influence of HCP degradation on C-14 and Ra-226 sorption.

^{14}C sorption on hardened cement paste and mortars

A number of studies have investigated the sorption of Carbon-14 (both in inorganic and organic forms) in cementitious materials.

In its review article Evans (Evans, 2008) states that inorganic C-14 sorption by cementitious materials can be roughly divided into two reactions; (i) adsorption onto a positive site and (ii) precipitation.

Isotopic exchange with solid $CaCO_3$ in cement paste is expected to control the $^{14}CO_3^{2-}$ retention in cement paste (Bradbury and Sarott, 1994) but the extent of removal of $^{14}CO_3^{2-}$ is very dependent on the particular cement/concrete system in question. Wieland (Wieland, 2014) noted that $CaCO_3$ precipitation also occurs at the interface between the cementitious near field and the host rock due to diffusion-controlled mixing of Ca rich pore water emanating from the alkaline near field and CO_3^{2-} rich pore water intruding from the host rock formation.

The experimental results obtained by batch sorption experiments and zeta potential measurements (Noshita et al, 1995) suggested that inorganic Carbon-14 (CO_3^{2-}) is adsorbed onto the cement surface by an electrostatic force, due to the reaction between SiO_2 and CaO contained in the cementitious composition. The $^{14}CO_3^{2-}$ distribution coefficient (Kd) was increased from 2,000 to 7,000 ml/g by adding SiO_2 to the Ordinary Portland Cement (OPC).

In a study performed by Matsumoto et al. (Matsumoto et al., 1995) on inorganic and organic Carbon-14 sorption on mortar the authors concluded that in the mortar-sodium carbonate system, the sorption ratio of inorganic Carbon-14 is high until mortar is completely carbonated because of the high Ca^{2+} content in the mortar and the low solubility of calcite. In the mortar-organic carbon system ($CH_3{}^{14}COONa$ and $^{14}CH_3{}^{14}CHO$ were used as organic Carbon-14), the soluble organic Carbon-14 is hardly sorbed on the mortar surface, and consequently the cementitious material may not inhibit the release of organic radiocarbons from low-level radioactive waste.

Sorption experiments were carried out by Matsumoto et al. (Matsumoto et al., 1999) on various types of cementitious mortars and organic Carbon-14 in form of acetic acid, formaldehyde, acetaldehyde and arginine. This study showed that aqueous organic Carbon-14 was not sorbed to any great extent on mortar at high pH. The authors concluded that organic carbon is mainly electrostatically adsorbed onto the surface of mortar via silanol groups, and the extent of sorption depend on the ionic speciation of the organic carbon in aqueous solution.

Notshita et al. (Notshita et al., 2001) tried to provide a categorization of cement components from the viewpoints of their chemical constituents and sorption behaviours. In this study, the authors assumed that the cement components are categorized into four groups: calcium silicate compounds, hydroxides, calcium aluminate compounds, and others. The authors compared the sorption behaviours among the four groups of cement components by batch sorption experiments carried out for 12 kinds of cement components using the radionuclides cesium, iodine, inorganic carbon, and nickel as different chemical species. For inorganic Carbon-14 they found that $^{14}CO_3^{2-}$ is sorbed onto calcium silicate compounds with lower Ca:Si ratios if the bulk solution was in NaOH, but that sorption was less in $Ca(OH)_2$ solution. This indicated that formation of $CaCO_3$ may affect Kd values, although the initial carbonate concentration was adjusted to below its maximum solubility. In $Ca(OH)_2$

solution, the order of sorption was gibbsite > brucite > portlandite, which may reflect the tendency of $CaCO_3$ to flocculate and precipitate as colloids.

In a recent publication, Wieland et al. (Wieland et al., 2016) reported experimental data obtained for the uptake of methanol, ethanol, formaldehyde, acetaldehyde, formic acid and acetic acid by cement paste. These data show that the uptake the organic compounds investigated exhibit very weak interaction (either specific electrostatic interaction) or non-specific (hydrogen bonding adsorption) with the hydrate assemblage of cement paste except formate for which strongly sorbing sites exist in the cement matrix, e.g. by SO_4^{2-}/$HCOO^-$ replacement in the ettringite structure.

^{226}Ra sorption on hardened cement paste and mortars

Available data on radium sorption on cementitious materials indicate that Ra (II) sorption is significant with Kd values ranging from $5x10^{-2}$ to $5x10^{-1}$ m^3/kg.

The Ra(II) sorption kinetics and reversibility, as well as the effect of the solid to liquid ratio and the CaO/SiO_2 ratio on the Ra(II) uptake on fresh and degraded hardened cement pastes (HCP) were investigated by Tits et al. (Tits et al., 2006a). Their results show that the uptake of Ra(II) by the degraded Hardened Cement Paste is fast (sorption equilibrium was attained within one day) with a Kd value at equilibrium of $14x10^{-2}$ m^3/kg. A clear dependence on the CaO/SiO_2 ratio was observed.

For fresh HCP a two-step process was used to explain the Ra(II) uptake: fast sorption occurred within one day, giving rise to a Kd value of $26x10^{-2}$ m^3/kg. In a second step the Ra(II) appears to increase slowly to an Kd value of $40x10^{-2}$ m^3/kg over a period of 60 days. Nevertheless, the authors noted that the significance of the slow increase in the Kd value can be questioned due to the high uncertainties on the data.

It is assumed that Ra(II) only sorbs on the C-S-H fraction in HCP and that the aqueous Ra(II) speciation is dominated by the Ra^{2+} species. In these conditions, the cation-exchange model developed by Tits et al. (Tits et al., 2006a) for the Ra(II) sorption on C-S-H phases in the absence of alkalis can be used to estimate the Kd value for the Ra(II) sorption on degraded HCP.

Even chemical analogues of Ra(II), such as Sr(II) and Ba(II), are often recommended to be used in sorption databases for the cementitious near-field (Wieland and Van Loon, 2002), the experiments performed by Tits et al. (Tits et al., 2006a, Tits et al., 2006b) show that sorption values for Ra are almost 5 times greater than those obtained for Sr.

Ra uptake is higher in stages I and III compared to stage II of the cement degradation (Wieland, 2014). Competition with alkalis leads to weaker uptake in stage I compared to stage II of the cement degradation while decreasing Ca concentrations results in increasing Ra uptake in stage I compared to stage II of the cement degradation.

References

Park, S. D., Kim, J. S., Han, S. H., Jee, K. Y. , 2008, *Distribution characteristics of ^{14}C şi ^{3}H in spent resins from the Canada deuterium uranium-pressurized heavy water reactors (CANDU-PHWRs) of Korea*, Journal of Radioanalytical and Nuclear Chemistry, Vol. 277, No.3, 503-511

Bradbury, M.H., Sarott, F.A., 1994, *Sorption databases for the cementitious near-field of a L/ILW repository for performance assessment*, PSI Bericht 95-06, Paul Scherrer Institut, Villigen PSI, Switzerland and Nagra Technical Report NTB 93-08, Nagra, Wettingen, Switzerland.

Wieland, E, 2014, Sorption Data Base for the Cementitious Near Field of L/ILW and ILW Repositories for Provisional Safety Analyses for SGT-E2, Nagra Technical Report NTB 14-08, Nagra, Wettingen, Switzerland.

Matsumoto, J., Banba, T., Muraoka, S., 1995, *Adsorption of C-14 on mortar.* Mat.Res.Soc.Symp.Proc. 353, 1029-1035.

Evans, N.D.M., 2008, *Binding mechanisms of radionuclides to cement*, Cem. Concr. Res. 38, 543-553.

Tits, J., Iijima, K., Wieland, E., Kamei, G., 2006 a, *The uptake of radium by calcium silicate hydrates and hardened cement paste*, Radiochim. Acta 94, 637–643.

Tits, J., Wieland, E., Müller, C.J., Landesman, C., Bradbury, M.H., 2006 b, *Strontium* binding *by calcium silicate hydrates*, Journal of Colloid and Interface Science 300, 78-87.

Wieland, E., Van Loon, L., 2002, *Cementitious near-field sorption database for performance assessment of an ILW repository in Opalinus Clay*, PSI Report Nr. 03-06, Paul Scherrer Institut, Villigen, Switzerland, and Nagra Technical Report, NTB 02-20,

Nagra, Wettingen, Switzerland.

State-of-the-art report for BRGM contribution to WP2 of the European Cebama project (BRGM)

Sylvain Grangeon (BRGM) & Nicolas Marty (BRGM)
e-mail: s.grangeon@brgm.fr & n.marty@brgm.fr

Abstract
This report reviews currently available studies of AFm interaction with various anions, and discuss the workplan for BRGM contribution to WP2 of the Cebama project.

Introduction
AFm are layered double hydroxides found in cementitious environments. They are foreseen to play a pivotal role on the fate of anion, through sorption/incorporation mechanisms. Retention and incorporation capacities are certainly driven by AFm crystallographic structure, including crystal size, and nature of the layer charge (e.g., isomorphic substitutions, vacancies).

BRGM contribution to the Work Package 2 (WP2) of the European project Cebama will focus on various aspects of AFm behavior in cements, with the global aim of better understanding the role played by this phase in retaining anions from migrating. In this view, exchange constants for a set of anions of interest will be determined, and structure of the resulting phase will be studied. The first point is a prerequisite to the thermodynamic modeling of anion migration in cements, and the second will both allow for a better understanding of the mechanisms of interaction between AFm and anions at the atomic scale, information which is crucial to our capacity to model retention phenomena, and will facilitate further structural studies. In parallel, to mimic the probably compositional variability of AFm occurring cements, samples having various nature and density of layer charge will be synthesized, and the effect of this parameter on anion retention capacities will be studied. Finally, to an effort to contribute to a better description of the behavior of anions in clay/cement interfaces, the kinetics and mechanisms of AFm degradation will be studied, and their influence on anion retention capacities will be discussed. Generally speaking, BRGM plans to focus on the Mo/Se/Cl anion chemical system, although other anions might be included if relevant (for example if partners from the cluster which so). Indeed, BRGM will combine its efforts into a "cluster" (INE, PSI, Amphos21, BRGM) aiming to better understand the sorption properties of relevant RN on cement phases, i.e. AFm and C-S-H (Calcium Silicate Hydrate). Among others, BRGM will synthesized AFm phase for the "joint cluster" and better described AFm structure using state of the art technics, but will also provide a realistic description of AFm anion retention capacity and link it to a realistic kinetic model for AFm degradation.

Anion exchange and structure studies

State of the art

Because AFm probably are the most efficient anion-sorbing phases in cements, their structure and their capacity to sorb anions have been extensively studied, and many results are available in the literature. Relevant literature on this topic is given in *Table 14*.

Table 14. Literature data concerning AFm interaction with anions. Both experimental and predictive (ab initio) studies are reported.Data taken from previous studies (Aimoz et al., 2012a; Aimoz et al., 2013; Aimoz et al., 2012b; Baur and Johnson, 2003; Birnin-Yauri and Glasser, 1998; Bonhoure et al., 2006; Cornelis et al., 2012; Glasser et al., 1999; Hirao et al., 2005; Johnson et al., 2000; Kalinichev and Kirkpatrick, 2002; Kirkpatrick et al., 1999; Mesbah et al., 2012; Motzet and Pollmann, 1999; Moulin et al., 2000; Ochs et al., 2015; Pollmann et al., 2006; Qiu et al., 2015; Segni et al., 2006; Wu et al., 2010)

Authors	**Studied material**	**Nature of exchange reaction**	**Main results**
Qiu *et al.* (2015)	Hydrocalumite (AFm-OH)	$OH^-/B(OH)_4^-$	Langmuir and Freundlich isotherm
Birnin-Yauri and Glasser (1998)	Friedel's salt (AFm-Cl)	OH^-/Cl^-	Exchanges effect on solubility constants
Aimoz *et al.* (2012a)	AFm-I_2 and AFm-SO_4	I^-/SO_4^{2-}	Thermodynamics of AFm-(I_2,SO_4) solid solution
Aimoz *et al.* (2012b)	AFm-I_2 and AFm-SO_4	I^-/SO_4^{2-}	Structural model
Aimoz *et al.* (2013)	AFm-I_2 and AFm-SO_4	I^-/SO_4^{2-}	Exchanges effect on solubility constants
Baur and Johnson (2003)	Monosulfate (AFm-Cl)	SeO_3^{2-}/SO_4^{--} SeO_4^{2-}/SO_4^{--}	Distribution ratios (Rd=0.38 m^3 kg^{-1}) for selenite and selenate (Rd=2.06 m^3 kg^{-1})
Bonhoure *et al.* (2006)	Hardened cement paste	SeO_3^{2-}/? SeO_4^{2-}/?$^-$	Freundlich isotherm. Distribution ratios (0.2<Rd<0.02 m^3 kg^{-1}) for selenite and selenate (0.002<Rd<0.02 m^3 kg^{-1})
Johnson *et al.* (2000)	27 cementitious formulations were investigated	SeO_3^{2-}/?	Freundlich isotherms Experimental Kd values ranging from 250 to 930 l kg^{-1}
Cornelis *et al.* (2012)	AFm-Sb and AFm-SO_4	$Sb(OH)6-/SO_4^{--}$	Formation of a pillared structure, with Sb forming inner-sphere complex with 6 O.

Glasser *et al*. (1999)	This paper is a review	OH, CO3, SO4, Cl	A large range of compositional variation within binary and ternary systems occurs. Anions can have both ordered and disordered configuration in the interlayer space.
Hirao *et al*. (2005)	Cl interaction with cement phases, including AFm	Cl^-/?	Cl sorption into AFm surfaces was fitted with a Freundlich isotherm.
Kalinichev and Kirkpatrick (2002)	Molecular dynamics simulation of Cl interaction with cement phases, including AFm	Cl^-/?	Cl outer-sphere complexation is favored as compared to inner-sphere complexation.
Kirkpatrick *et al*. (1999)	NMR study of $^{35}Cl^-$ intercalated hydrotalcite and Friedel's salt	Cl^-/?	Interlayer Cl and water are ordered. Cl has uniaxial or almost uniaxial symmetry above ~0 °C and triaxial at lower temperatures.
Mesbah *et al*. (2012)	Synthesis of SO_4^{2-} and Cl^--rich AFm phases, structural characterization and experiments focusing on competition between the two anions, as well as between SO_4^{2-} and CO_3^{2-}	Cl^-/SO_4^{2-} SO_4^{2-}/CO_3^{2-}	AFm-SO_4 has a better potential for insolubilizing CO_3^{2-} than Cl^-. Lattice parameters depend on the extend of anion exchange.
Motzet and Pollmann (1999)	Synthesis of AFm-SO_3/OH solid solution. Carbonation processes were also investigated.	SO_3^{2-}/OH^- /CO_3^{2-}	The thermal stability and the hydration stages were investigated.
Moulin *et al*. (2000)	Hydration of C_3A were performed. Four different AFm-type phase samples were also synthesized (AFm-OH, AFm-CO_3, AFm-Cr and AFm-NO_3)	CrO_4^{2-} /$Zn(OH)_4^{2-}$/OH^-	Chromium ions substitute Al in structures. Adsorption of CrO_4^{2-} and $Zn(OH)_4^{2-}$ ions at the interlamellar or external surfaces of

			the AFm phases.
Ochs *et al.* (2015)	Review on cementitious materials and their sorption properties	Radionuclide and metal sorption on cement and concrete	AFm structure is tolerant of substitution and can sorb many contaminants through ion substitution.
Pollmann *et al.* (2006)	Synthesis of CEM I pastes and AFm-sulfonates	Sulfonates/OH^-	Formation of AFm phases with aliphatic sulfonate anions.
Segni *et al.* (2006)	Incorporation of Cr, V and Si oxoanions into hydrocalumite	$CrO_4^{2-}/V_2O_7^{4-}$ /$SiO_3^{2-}/Cl^-/NO_3^-$	Anion uptake was examined in terms of the structural characteristics
Wu *et al.* (2010)	Sorption of selenite by Friedel's salt	SeO_4^{2-}/Cl^-	Exchange of Se with Cl is efficient. The formed product is stable over a wide range of pH values (4-13, as reported by the authors). Sorption is reversible, thus supporting outer-sphere complexation
Yuan *et al*. (2009)	Review of studies focusing on Cl binding with cement materials, including C3a.	Cl^-/?	C3a is found to be the most efficient Cl-binding phase, followed by C3s, C2s and C4AF, thus suggesting that AFm may be the most efficient Cl-sorbing phase in cements.
Zhang *et al*. (2003)	Interaction between hydrocalumite (naturally-occuring AFm) and B, Cr, Mo and Se. Coprecipitation experiments.	Coprecipitation, but final products contain OH which compete	All elements are very efficiently uptaken, although affinity for B is lower. The necessity to take into account the competition with OH is highlighted. It is empathized

			that pH must remain above ~10.7.

From this compilation of data, it becomes clear that although many relevant data exists, many fundamental information are still missing, thus preventing a sound understanding of (and thus capacity to model) AFm interaction with anions. For example, in the case of Se, it has both been reported that Se can form outer-sphere and inner-sphere complexes. However, these two interaction modes are very different, and have profound implications for the mobility of Se. Indeed, if Se is to be sorbed as inner-sphere complex, then it will be strongly bound to AFm structure, and likely irreversibly trapped as long as AFm is stable. Contrastingly, if Se is sorbed as an outer-sphere complex, it will be subject to competition with other anions present in the pore water, and is thus susceptible of being released to the solution if another anion(s) having a high affinity for AFm surface occurs in the pore water in significant concentration.

In addition, while many sorption data are presented for a large number of different anions, experimental studies are often conducted at very high anion concentration, and often fail to report parameters that are mandatory to a reproduction (and modeling) of the experiment. For instances, few studies report solid-to-liquid ratio, ionic background (and ionic strength), or pH/Eh conditions at the end of the experiment. All these problems prevent the use of most of currently available data for inclusion in a thermodynamic modeling code.

Finally, when modelled, data are often interpreted in terms of isotherms, with a Freundlich model, which cannot be transposed to other chemical conditions and is usually limited to low-concentration solutions. For example, if chemical composition of water changes with time – as expected in any natural system – present modelling cannot be reused.

Methods

To contribute to a better description of AFm/anions interactions, BRGM will perform batch experiment in controlled conditions (e.g., in the glove-box, with well-characterized AFm samples. In particular, BRGM will use AFm samples having varying reactivity (e.g., several samples having different nature and density of layer charge). Different anion of interest will be studied, in the Se/Mo/Cl competition system.

Such experiments will require first to establish synthesis protocols for AFm samples. For this, we will use protocols available in the open literature (*Table 14*). Once synthesized, samples will be carefully characterized, for example for their properties (including nature and density of the layer charge). Then, several tests will be performed to determine the best experimental conditions required for experiments focusing on anion retention.

Finally, batch experiments will be conducted in the glove box, using different protocols. Amongst them, it is envisioned that experiments consisting in varying the concentration of an anion of interest in different solutions in contact with AFm saturated with another anion. Same solid/liquid ratios will be considered for experiments. Concentrations of both anions, as well other parameters of interest (e.g., pH), will be then measured at the end of experiments. Another type of experiment could consist in flowing a solution having a fixed concentration of an anion of interest through a pellet built of AFm saturated of anion, and measuring the output

concentrations of the two anions while strictly controlling all instrumental parameters (including flow rate).

Kinetics study: Dissolution kinetics of AFm-Cl as a function of pH at room temperature

General context of the study

In the most design of deep underground radioactive waste disposal, cementitious materials will be used to build access structures, galleries, vaults and packages for some radioactive wastes. In such context, cement materials have essentially mechanical function (e.g. low permeable barriers that retard radionuclide migration). However cement phases have also a sorptive potential for radionuclides. Indeed, several studies report cationic and anionic sorptions on concretes, cements as well as on isolated cement phases (Aimoz *et al.*, 2012a; Aimoz *et al.*, 2013; Aimoz *et al.*, 2012b; Atkinson and Nickerson, 1988; Baur and Johnson, 2003; Birnin-Yauri and Glasser, 1998; Bonhoure *et al.*, 2006; Cornelis *et al.*, 2012; Gougar *et al.*, 1996; Iwaida *et al.*, 2001; Johnson *et al.*, 2000; Kindness *et al.*, 1994; Miller *et al.*, 2000; Moulin *et al.*, 2000; Pointeau *et al.*, 2008; Pollmann *et al.*, 2006; Segni *et al.*, 2006; Tits *et al.*, 2011). Some authors highlight a possible long-term stabilization of sorbed elements (Cornelis *et al.*, 2012). However, part of these cement materials will be in physical contact with the surrounding rock formation. The chemical gradient between the cement material and horst rock will induce mineralogical transformations whose impact must be evaluated in the framework of repository long-term evolution. Therefore, the stability of cement phases, both from a thermodynamic and kinetic point of view, is a fundamental importance in the determination of radionuclide migration, and more generally, for nuclear safety assessments.

The present study is focused on AFm (hydrated calcium aluminate phases) stability, one of the main product formed in hydrated cement paste. The AFm phase belongs to the layered double hydrate (LDH) family having positively charged layers and water plus charge-balancing anions in the interlayer (Aimoz *et al.*, 2012a; Baquerizo *et al.*, 2015; Birnin-Yauri and Glasser, 1998; Matschei *et al.*, 2007; Moulin *et al.*, 2000; Pollmann *et al.*, 2006; Segni *et al.*, 2006). The presence of an anionic exchanger confers interesting properties to the concrete for retention of radionuclides negatively charged in basic conditions (e.g. I, Se, Mo, Cl etc.). Moreover, the stability study of AFm, such as the Friedel's salt, is of great significance due to its capacity for releasing chloride which increase the steel corrosion in concrete (Glass *et al.*, 2000; Goñi and Guerrero, 2003).

Aims of dissolution experiments are twofold: first, kinetics law for the dissolution of AFm-Cl will be determined. Second, the evolution of AFm structure during dissolution will be monitored in order to better understand the structural mechanisms of phase dissolution. In this view, the initial material will be first carefully examined using a combination of chemical and physical techniques. Dissolution experiments will be done in flow-through reactors at various basic conditions (pH 9.2 to 13) at room temperature. Alteration products will be carefully examined at the end of experiments.

Methods

Dissolution experiments will be carried out on AFm-Cl using flow-through reactors at room temperature (Fig. 23). The total volume of reactors available in the BRGM laboratory is about 83 mL. An input buffer solution will circulate at a constant flow rate of about 0.5 mL min^{-1} through the reactors using a peristaltic pump (Watson Marlow,

205U). The input solution will be continuously cooled under a N_2 flux. The objective here was to suppress the CO_2 partial pressure in order to avoid carbonation during dissolution experiments (e.g. Goñi and Guerrero, 2003). The magnetic stirrer rotates on an axle in order to avoid any grinding of AFm particles between the bar and the bottom of the reactor (Metz and Ganor, 2001).

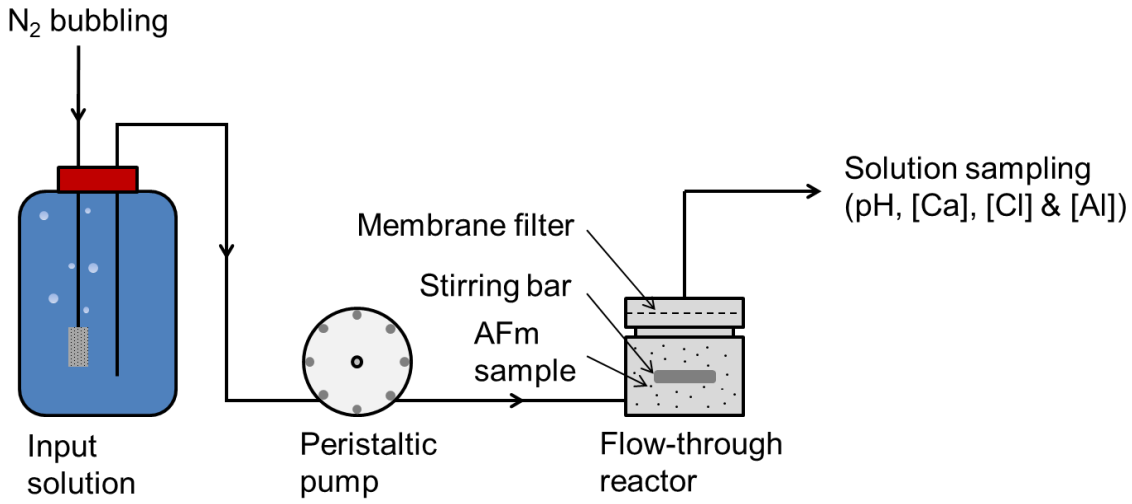

Fig. 23. The experimental apparatus. Figure modified from Marty et al. (2015).

Output concentrations of Ca, Cl and Al will probably not match a steady state due to the high reactivity of the dissolved material. Indeed, the decrease of output concentrations is expected due to the mass loss during alteration process. It will be therefore particularly relevant to take mass variation into account in our calculations.

The BET surface areas will be used for the rate normalization. However, BET surfaces do not necessary correspond to reactive surface areas, i.e. really involved in the dissolution process. For example, several authors report a clay dissolution from edge surface areas (ESA) in basic conditions (e.g. Marty *et al.*, 2011); reported ESA by the authors are significantly lower than BET areas (e.g. ESA = 11.2 m^2 g^{-1} and BET = 104 m^2 g^{-1} for a synthetic montmorillonite). Therefore, both mass and surface normalized rates will be studied as function of pH.

References

Aimoz, L., Kulik, D.A., Wieland, E., Curti, E., Lothenbach, B., Mäder, U., (2012a) Thermodynamics of AFm-(I2, SO4) solid solution and of its end-members in aqueous media. Applied Geochemistry, 27, 2117-2129.

Aimoz, L., Wieland, E., Kulik, D.A., Lothenbach, B., Glaus, M.A., Curti, E., (2013) Characterization and Solubility Determination of the Solid-Solution Between AFm-I2 and AFm-SO4, in: Bart, F., Cau-di-Coumes, C., Frizon, F., Lorente, S. (Eds.), Cement-Based Materials for Nuclear Waste Storage. Springer New York, New York, NY, pp. 57-65.

Aimoz, L., Wieland, E., Taviot-Gueho, C., Dahn, R., Vespa, M., Churakov, S.V., (2012b) Structural Insight into Iodide Uptake by AFm Phases. Environmental Science & Technology, 46, 3874-3881.

Atkinson, A., Nickerson, A.K., (1988) Diffusion and sorption of cesium, strontium, and iodine in water-saturated cement. Nuclear Technology, 81, 100-113.

Baquerizo, L.G., Matschei, T., Scrivener, K.L., Saeidpour, M., Wadsö, L., (2015) Hydration states of AFm cement phases. Cement and Concrete Research, 73, 143-157.

Baur, I., Johnson, C.A., (2003) Sorption of selenite and selenate to cement minerals. Environmental Science & Technology, 37, 3442-3447.

Birnin-Yauri, U.A., Glasser, F.P., (1998) Friedel's salt, Ca2Al(OH)6(Cl,OH)·2H2O: its solid solutions and their role in chloride binding. Cement and Concrete Research, 28, 1713-1723.

Bonhoure, I., Baur, I., Wieland, E., Johnson, C.A., Scheidegger, A.M., (2006) Uptake of Se(IV/VI) oxyanions by hardened cement paste and cement minerals: An X-ray absorption spectroscopy study. Cement and Concrete Research, 36, 91-98.

Cornelis, G., Etschmann, B., Van Gerven, T., Vandecasteele, C., (2012) Mechanisms and modelling of antimonate leaching in hydrated cement paste suspensions. Cement and Concrete Research, 42, 1307-1316.

Glass, G.K., Reddy, B., Buenfeld, N.R., (2000) The participation of bound chloride in passive film breakdown on steel in concrete. Corrosion Science, 42, 2013-2021.

Glasser, F.P., Kindness, A., Stronach, S.A., (1999) Stability and solubility relationships in AFm phases - Part 1. Chloride, sulfate and hydroxide. Cement and Concrete Research, 29, 861-866.

Goñi, S., Guerrero, A., (2003) Accelerated carbonation of Friedel's salt in calcium aluminate cement paste. Cement and Concrete Research, 33, 21-26.

Gougar, M.L.D., Scheetz, B.E., Roy, D.M., (1996) Ettringite and C□S□H Portland cement phases for waste ion immobilization: A review. Waste Management, 16, 295-303.

Hirao, H., Yamada, K., Takahashi, H., Zibara, H., (2005) Chloride binding of cement estimated by binding isotherms of hydrates. Journal of Advanced Concrete Technology, 77-84.

Iwaida, T., Nagasaki, S., Tanaka, S., (2001) Sorption behavior of strontium onto C-S-H (calcium silicate hydrated phases), in: Yasuhiro Iwasawa, N.O., Hironobu, K. (Eds.), Studies in Surface Science and Catalysis. Elsevier, pp. 901-904.

Johnson, E.A., Rudin, M.J., Steinberg, S.M., Johnson, W.H., (2000) The sorption of selenite on various cement formulations. Waste Management, 20, 509-516.

Kalinichev, A.G., Kirkpatrick, R.J., (2002) Molecular dynamics modeling of chloride binding to the surfaces of calcium hydroxide, hydrated calcium aluminate, and calcium silicate phases. Chemistry of Materials, 14, 3539-3549.

Kindness, A., Lachowski, E.E., Minocha, A.K., Glasser, F.P., (1994) Immobilisation and fixation of molybdenum (VI) by Portland cement. Waste Management, 14, 97-102.

Kirkpatrick, R.J., Yu, P., Hou, X.Q., Kim, Y., (1999) Interlayer structure, anion dynamics, and phase transitions in mixed-metal layered hydroxides: Variable temperature Cl-35 NMR spectroscopy of hydrotalcite and Ca-aluminate hydrate (hydrocalumite). American Mineralogist, 84, 1186-1190.

Marty, N.C.M., Cama, J., Sato, T., Chino, D., Villiéras, F., Razafitianamaharavo, A., Brendlé, J., Giffaut, E., Soler, J.M., Gaucher, E.C., Tournassat, C., (2011) Dissolution kinetics of synthetic Na-smectite. An integrated experimental approach. Geochimica et Cosmochimica Acta, 75, 5849-5864.

Marty, N.C.M., Grangeon, S., Warmont, F., Lerouge, C., (2015) Alteration of nanocrystalline calcium silicate hydrate (C-S-H) at pH 9.2 and room temperature: a combined mineralogical and chemical study. Mineralogical Magazine, 79, 437-458.

Matschei, T., Lothenbach, B., Glasser, F.P., (2007) The AFm phase in Portland cement. Cement and Concrete Research, 37, 118-130.

Mesbah, A., Cau-dit-Coumes, C., Renaudin, G., Frizon, F., Leroux, F., (2012) Uptake of chloride and carbonate ions by calcium monosulfoaluminate hydrate. Cement and Concrete Research, 42, 1157-1165.

Metz, V., Ganor, J., (2001) Stirring effect on kaolinite dissolution rate. Geochimica et Cosmochimica Acta, 65, 3475-3490.

Miller, W., Alexander, R., Chapman, N., Mckinlely, I., Smellie, J., (2000) Chapter 4: Analogues of repository materials, Waste Management Series. Elsevier, pp. 65-152.

Motzet, H., Pollmann, H., (1999) Synthesis and characterisation of sulfite-containing AFm phases in the system CaO-Al2O3-SO2-H2O. Cement and Concrete Research, 29, 1005-1011.

Moulin, I., Stone, W.E.E., Sanz, J., Bottero, J.Y., Mosnier, F., Haehnel, C., (2000) Retention of zinc and chromium ions by different phases of hydrated calcium aluminate: A solid-state Al-27 NMR study. Journal of Physical Chemistry B, 104, 9230-9238.

Ochs, M., Mallants, D., Wang, L., (2015) Radionuclide and metal sorption on cement and concrete. Springer.

Pointeau, I., Coreau, N., Reiller, P.E., (2008) Uptake of anionic radionuclides onto degraded cement pastes and competing effect of organic ligands. Radiochimica Acta, 96, 367-374.

Pollmann, H., Stefan, S., Stern, E., (2006) Synthesis, characterization and reaction behaviour of lamellar AFm phases with aliphatic sulfonate-anions. Cement and Concrete Research, 36, 2039-2048.

Qiu, X., Sasaki, K., Takaki, Y., Hirajima, T., Ideta, K., Miyawaki, J., (2015) Mechanism of boron uptake by hydrocalumite calcined at different temperatures. Journal of Hazardous Materials, 287, 268-277.

Segni, R., Vieille, L., Leroux, F., Taviot-Guého, C., (2006) Hydrocalumite-type materials: 1. Interest in hazardous waste immobilization. Journal of Physics and Chemistry of Solids, 67, 1037-1042.

Tits, J., Geipel, G., Macé, N., Eilzer, M., Wieland, E., (2011) Determination of uranium(VI) sorbed species in calcium silicate hydrate phases: A laser-induced luminescence spectroscopy and batch sorption study. Journal of Colloid and Interface Science, 359, 248-256.

Wu, Y.Y., Chi, Y., Bai, H.M., Qian, G.R., Cao, Y.L., Zhou, J.Z., Xu, Y.F., Lu, Q., Xu, Z.P., Qiao, S.Z., (2010) Effective removal of selenate from aqueous solutions by the Friedel phase. Journal of Hazardous Materials, 176, 193-198.

Diffusion properties of inorganic ^{14}C species (dissolved and gaseous) through unsaturated hardened cement paste : Influence of water saturation (SUBATECH)

Catherine Landesman, Bernd Grambow

SUBATECH/ARMINES (Ecole des Mines, University de Nantes, CNRS), landesman@subatech.in2p3.fr

This report aims at giving a rapid overview of some scientific and experimental basis necessary to tackle the main topics of the project: water saturation of cement paste, carbonation process, aqueous and gas diffusion in cement, reactivity of inorganic carbon-14 in cementitious environment.

INTRODUCTION

The existence of unsaturated states in rocks, materials (engineered barriers, backfill materials) and surface environments is a common situation to all disposal sites. In France, this concerns either the current surface waste disposal facilities (very-low-level waste repository, low and intermediate-level short lived waste repository) or the future deep or sub-surface geological repositories such as CIGEO project for high-level waste (HLW) and intermediate-level long-lived waste (IL-LL waste) and FAVL project for low-level long-lived wastes. The unsaturated conditions are very variable depending on the type of disposal (surface or underground) and also on the origin of the gas which substitute water inside the materials.

Under surface and sub-surface conditions or during the construction and the operation phase of a deep geological repository, the ventilation of underground galleries or shafts would induce, by gas exchanges with the atmosphere, a partial dehydration of the different materials of the storage. In porous media, partially saturated conditions (or unsaturated conditions) denote the co-presence of an aqueous phase and a gaseous phase within the network of pores. The degree of saturation (S) macroscopically defines the ratio between the pore volume filled with water to the total pore volume. Unsaturated terms denote situations where the degree of saturation is less than 100% [DRO10]

For example, in the Callovo-Oxfordian claystones (CIGEO project), during the operation phase, the saturation will range from 70-95% in the excavation damaged zone (EDZ) around the galleries to over 95% in the intact clay rock. In a repository, cement materials play also an important role either as engineered barriers or confinement matrices for some IL-LL wastes. Depending on their use, saturation values of cement materials may range from 30-40% (backfill) to 80-90% (sealings). Moreover, some IL-LL wastes may produce gases such as H2, CO_2 and CH_4 that will be diluted and discharged by ventilation (operation period). Nevertheless, during the post-closure period, Hydrogen release due to the corrosion of metal components (HLW overpack or IL-LL metallic wastes,…) and the radiolysis of some IL-LL wastes (polymers, bitumen) and/or of water (cemented wastes, salts) constitutes the main sources of gas. This means that wastes in disposal cells may remain partially unsaturated for many thousands of years before the completed resaturation by water of the repository (after 100 000 years) [AND14].

Carbon-14 has been identified as one of the important radionuclide in the inventory of radioactive waste due to its pretty long half-live (5730 years) [AND05]. Results from previous and current European collaborative projects such as CARBOWASTE and CAST show that carbon-14 could be released by the corrosion of irradiated metals (zirconium alloys or stainless steels) and by the degradation of irradiated graphite and ion exchange materials. The issue of carbon-14 in wastes is then common to all the disposal facilities (HLW, IL-LLW, LL-LLW). The speciation of carbon-14 covers various chemical forms: organic and/or inorganic species dissolved or gaseous. Under his volatile form, carbon-14 may be present as CO_2 (inorganic species) or CH_4 and C_2H_6 (organic species) [CAR13, CAS15]. It is well know that the speciation of an element influences its sorption and transport properties. For carbon-14, inorganic species (CO_2/CO_3^{2-}) are the most reactive species toward cement materials is inorganic species due to their ability to enter in the carbonation process.

The carbonation process has been intensively studied for decades due to its importance in civil engineering [SUZ85, GRO90, COW92, THI05, BOR10]. Depending on water saturation conditions, the reactivity of inorganic carbon with cement is basically due to the diffusion of either dissolved carbonate ions (saturated condition) or gaseous CO_2 (unsaturated condition) [DRO10]. The main consequences are: i) a decrease of pH in the cement pore water, ii) a change in cement mineralogy (dissolution of Portlandite, progressive decalcification of C-S-H phases) and iii) a precipitation of in the open porosity (clogging) [AUR15]. The formation of calcium carbonate inside the porosity may have an impact on the transfer properties of carbon gaseous species including $^{14}CO_2$ and thus contributes to the potential entrapment of carbon-14 species released from wastes.

Thus, the objective of this work is to investigate the behaviour of inorganic carbon-14 species (dissolved and gaseous) by describing their diffusion properties (diffusion coefficients) in hardened cement paste (HCP) for different saturation conditions and different water degradation stages (presence of absence of alkali ions).

CARBON REACTIVITY IN CEMENT MATERIALS UNDER UNSATURATED CONDITIONS

DESCRIPTION OF THE CARBONATION PROCESS

Numerous studies describe the carbonation process of cement materials as a two-step diffusive process: diffusion of gaseous species (CO_2) in the unsaturated open porosity of the cement matrix and diffusion of aqueous carbonate ions in solution [BAR04, DRO10, AUR15 and references inside]. Carbon dioxide dissolves in alkaline solution with the following acid-base reaction:

$$CO_2(g) + 2OH^- \leftrightarrows CO_3^{2-} + 2H_2O \qquad (1)$$

The pK_a values of the two acid-base couples are 6.37 and 10.33 (T = 298K) [COW92].

This dissolution leads to the neutralization of the cement pore water and induces reactions with cement hydrated minerals.

- Portlandite

Portlandite ($Ca(OH)_2$) is the most sensitive hydrates for this reaction. The neutralization of hydroxide ions in solution leads to the precipitation of calcium carbonate following the reaction 2

$$Ca(OH)_2(s) + CO_2(g) \leftrightarrows CaCO_3(s) + H_2O \qquad (2)$$

Due to the strong buffering effect of Portlandite, the pH value of the pore water is stabilized around 12.5 until complete dissolution of $Ca(OH)_2$.

❖ Calcium silicate hydrated (C-S-H)

C-S-H minerals also react with carbon dioxide following a specific mechanism [SUZ85] (reaction 3).

$$CaO_xSiO_{2y}H_2O_z + xCO_2(g) \leftrightarrows xCaCO_3(s) + ySiO_2.tH_2O + (z-t)H_2O \quad (3)$$

- The precipitation of calcium carbonate is concomittant to a noncongruente dissolution of C-S-H leading to a progressive decrease of the calcium to silica ratio (C/S) in the C-S-H.
- This decalcification induces the release of silicate ions in solution and in case of a complete carbonation, leads to their polymerization into silica gel.

Other cement hydrates such as hydrated calcium sulfoaluminate (ettringite, AFm phases) may react with carbon dioxide and form calcite, gypsum and hydrated alumina following reaction 4 for ettringite as an example:

$$3CaO.Al_2O_3.3CaSO_4.32H_2O + 3H_2CO_3 \leftrightarrows 3CaCO_3 + 3(CaSO_4.H_2O) + Al_2O_3.xH_2O + (26-x)H_2O \quad (4)$$

Complete carbonation of cement hydrates may modify the cement microstructure. Due to their different molar volumes, the transformation of one mole of portlandite (V_{molar} = 33 $cm^3.mol^{-1}$) into one mole of calcite (V_{molar} = 35 $cm^3.mol^{-1}$) induces an increase of the solid phase and as a consequence a decrease of the porous space [AUR15]. The porous distribution is then strongly affected by the carbonation process. Many studies report a decrease of the microporosity (< 100 nm) and a formation of a macroporosity (> 100nm). The changes in porosity are reported to be much more important for Portland cement (CEM I) than for Blast Furnace Slag cement (CEMV) [HOU94, THI05].

INFLUENCE OF RELATIVE HUMIDITY (RH)

Because of the carbonation process is based on the diffusion of both gaseous (CO_2) and dissolved (carbonate ions) species, water saturation of the cement material has an impact on the process. Indeed, capillary porosity (open porosity) controls the rate of CO_2 transfer and as far as it is not saturated, carbon dioxide transfer is mainly due to a gas transfer. In these conditions, the diffusion rate of $CO_2(g)$ is 10 000 times higher than that of carbonate species [BOU13]. Auroy reports a synthesis of the evolution of the carbonation rate for different cement materials as a function of relative humidity.

This evolution shows that the carbonation rate is maximal for a relative humidity ranged between 55-65% of RH depending on the materials (cement paste, concrete,…) and the carbonation protocol (natural or accelerated carbonation). This range is a compromise between the transfer of CO_2 in the gas phase (existence of a continuous unsaturated path in the material) and the presence of water (as a continuous liquid phase) in the pore network which allows that the carbonation reactions can take place.

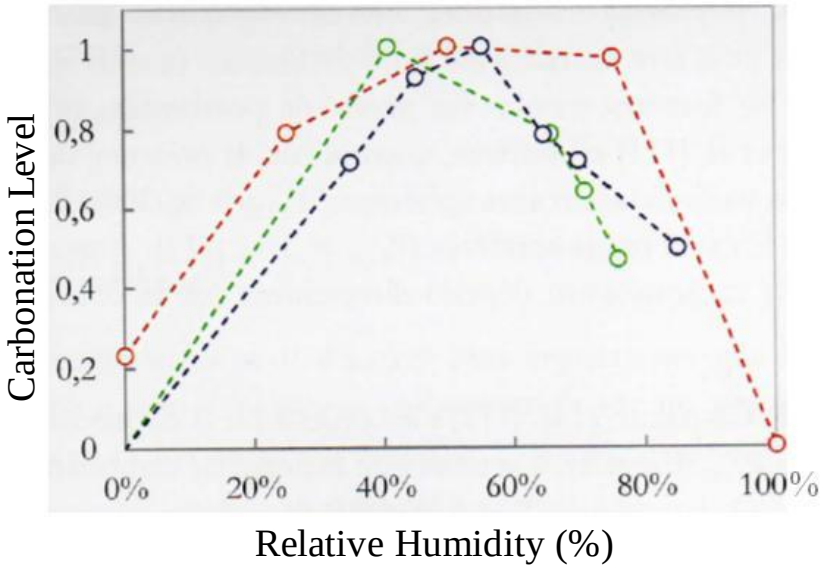

Figure 1: Evolution of the carbonation rate *vs* relative humidity for different cement materials (from [AUR15] and references herein: red [VER58], blue [PAP91], green [THI05])

Moreover, at high saturation condition (> 80%), the percolation of the gaseous phase in the porous network is more and more difficult and the effective diffusion coefficient of gaseous species diminish drastically in order to achieved very low value 10^{-14}-10^{-13} m^2s^{-1} similar to those of aqueous species[SER07]. It means that there is probably a transition from a gas diffusion process to an aqueous diffusion process at high saturation conditions. Nevertheless, very few experimental data are available for these conditions.

REACTIVITY OF INORGANIC CARBON-14 IN CEMENT ENVIRONMENT

Inorganic carbon-14 released from waste is expected to behave like stable carbon. Results of wet chemistry experiments (batch) performed on non carbonated hardened cement pastes show that Rd(^{14}C) value (distribution ratio defined as the ratio of ^{14}C activity in the solid to ^{14}C activity in the corresponding equilibrium solution) ranges from 1 to 10 m^3/kg with a very slow kinetic [ALL84, BAY88].

These results were interpreted as a coupling of two mechanisms: first, co-precipitation of $^{14}CO_3^{2-}$ with calcium carbonate and second isotopic exchange of $^{14}CO_3^{2-}$ with $^{12}CO_3^{2-}$ and $^{13}CO_3^{2-}$ species.

For more complex cement materials (mortar, concrete) containing calcareous aggregates, Bradbury and Sarott [BRA95] have developped a retention model based on the assumption that $^{14}CO_3^{2-}$ uptake is only rely on the accessible quantity of (stable) carbonate in the solid and the solubility of calcite in solution. Rd expression is then:

$$Rd = \alpha \times [Carbon]_{solid}/[Carbon]_{solution} \ (m^{-3}/kg^{-1}) \quad (5)$$

with

α : accessibility factor taking in account the fraction of accessible carbonate in aggregates.

α equals $0.17\times(1- \log\phi)$, where ϕ is the mean diameter of calcareous aggregate [POI02].

DIFFUSION IN CEMENT MATERIALS IN UNSATURATED CONDITIONS

As explained previously, transfer properties of carbon (and so of carbon-14) in cement materials are dominated by diffusion processes in aqueous or gas phases. Nevertheless, in literature very few studies are dedicated to the acquisition of transfer parameters in unsaturated conditions because of experimental difficulties. In the following paragraphs, basis of diffusion mechanism both in aqueous and gaseous phases will be described with a focus on the results obtained in unsaturated conditions.

Generally speaking, diffusion process refers to the transport of species (molecular or ion) in a environment (solid, liquid or gas) due to a gradient of chemical potential. A proportional relationship exists between this gradient and the transfer of the species expressed by the first Fick laws. The proportionality coefficient is then the diffusion coefficient (D_0). This description is particularly true for the diffusion process applied to (radioactive) tracers in which the gradient of chemical potential correspond to the concentration (or activity) gradient.

Based on Powers, initially developped for CEM I cement, the microstructure of cement paste can be described with two distinct classes of porosity:

Capillary porosity (> 125-150 nm): It is a vestige of the inter granular space in the initially hydrated paste.

Hydrate porosity (<125 nm): porosity forms inside the hydrated phases mostly C-S-H phases

The microstructure depends on the nature of the cement, on the water/cement ratio (W/C) used for the hydration of the cement and on the aged of the paste. Classically, the capillary porosity tends to diminish with a decrease of W/C and with time (ageing). The jointly increase of the total porosity and of the capillary porosity leads to the increase of the porous volume accessible to the diffusion process. Moreover, the microstructure of a BFS paste contains less capillary porosity than in an OPC paste. For a given W/C ratio, the total porosity value is similar but the pore diameters are smaller in a CEM V paste than in a CEM I one.

For the diffusion process, the most important parameter is not the total porosity but the interconnectivity of the capillary porosity. Results from Bentz and Garboczi show that, below a certain limit (percolation threshold), the interconnectivity of the capillary porosity falls to zero. The value is around 18% for a CEM I paste and do not depend on W/C ratio (figure 2) [BEN91].

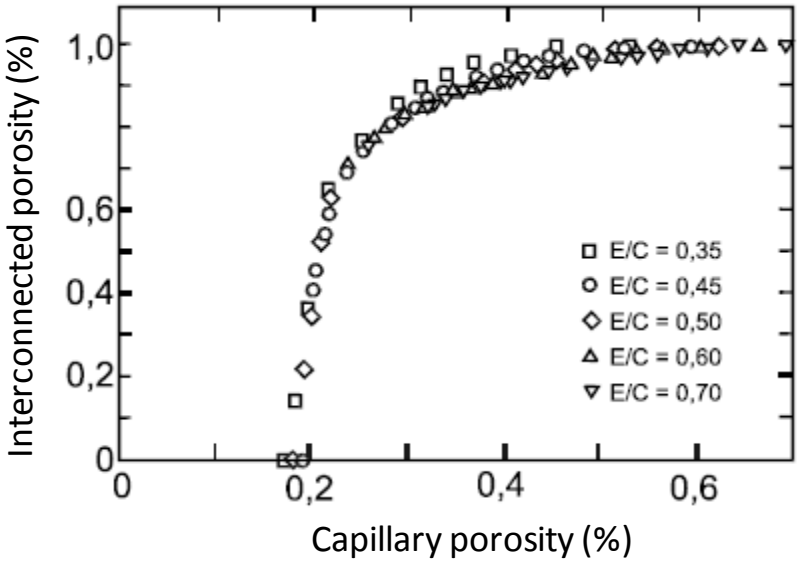

Figure 2: Evolution of the fraction of interconnected porosity *vs* the fraction of capillary porosity

AQUEOUS DIFFUSION

In a porous media such as a cement paste, the aqueous diffusion of molecular or ion species (solute) takes place in the cement pore water through a volume of porous material. In saturated conditions, solute diffusion in cement-based materials is entirely described by the mass-balance equation. Thus, the first Fick law can be expressed by the following relation:

$$J_e = -D_e\left(\frac{\partial c}{\partial x}\right) \quad (6)$$

with

J_e : flux of species through the surface ($mol.m^{-2}.s^{-1}$)
D_e : effective diffusion coefficient ($m^2.s^{-1}$)
$\delta c/\delta x$: gradient of concentration ($mol.m^{-4}$)

In a fully saturated material, the effective diffusion coefficient of a species can be related to its diffusion coefficient in solution (D_0) and to the geometry of the porous network (constrictivity and tortuosity) by the relation

$$D_e = D_0 \times \chi/\tau^2 \quad (7)$$

with χ and τ are the constrictivity and the tortuosity of the pores respectively. Unfortunately, these parameters are not experimentally accessible.

If the species has no interaction with the material, it is considered as a “non reactive species”. In cement material, this is often the case for tritiated water (HTO) which a tracer of water behaviour, even if results shows that isotopic exchange with water takes place during the diffusion process [TIT03].

On contrary, reactive tracers are species which can interact with the materials by different chemical or physical processes (sorption, incorporation, precipitation, isotopic exchanges,…). These interactions are expressed by the rock capacity factor, *a*. For those species, the diffusion process is described by the second Fick law (8)

$$\frac{\partial C(x,t)}{\partial t} = \frac{D_e}{a} \times \frac{\partial^2 C}{\partial x^2}$$

with

a :rock capacity factor ; $a = \varepsilon + \rho \times \frac{\partial [species]_{solid}}{\partial [species]_{solution}}$ (-)

$\frac{\partial [species]_{solid}}{\partial [species]_{solution}}$ stands for the chemical interaction of the species with the material. If this term is constant, it is equal to the distribution ratio, Rd. If not, it could be described by isotherm (Langmuir or more complex) for sorption).

ε : water accessible porosity (-)
ρ : bulk material density (kg.m^{-3})
R_d: distribution ratio (m^{-3}.kg)

The ratio D_e/a expresses the apparent diffusion coefficient, D_a.

Classically, the effective diffusion coefficient of a solute (tracer) is measured with a through-diffusion set-up in which a water saturated cement sample is sandwiched between two cells. In the upstream cell, the solute is injected and maintained at a constant concentration. The diffusion process through the sample is then driven by the gradient created by the difference of solute concentration in the two cells. The measurement of the solute in the downstream cell allows determining the steady state and calculating the effective coefficient diffusion by applying the first Fick law.

INFLUENCE OF WATER SATURATION (S_w)

There are very few studies dealing with the influence of water saturation (S_w) on the aqueous diffusion in cement materials and none dealing with radioactive tracers in HCP. A precise review of this topic has been done by Bourbon [BOU13]. The main results of this study are reported below.

First of all, as the aqueous diffusion takes place in the pore water, transfer of species is possible only if the pore water constitutes a continuous phase meaning that water saturation should be higher than a critical threshold (S_c). Based on data obtained from impedance spectroscopy on concrete samples, Bourbon concluded that the effective diffusion coefficients for chloride ions tend to zero for S_w values below 0.36. This value is then considered as the critical threshold S_c for concrete materials.

A recent study from Dridi and Lacour performed with a new specific experimental set-up (half-cell) confirm these results for CEM I paste (drastic decrease of D_e below S_w= 0.3-0.5) [DRI14]. The principle of this method consists in placing two samples of the material (source and target) into contact with one another in a sealed cell (Figure 3). The source sample is uniformly pre-doped with tracer (here lithium ions), while the

target sample is tracer free. Bonding with fresh cement paste improves the continuity of the porous network between the source and the target during the diffusion test.

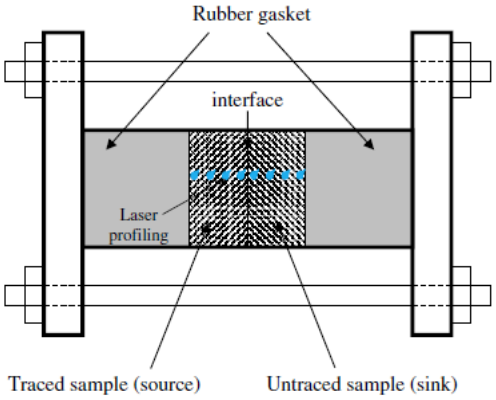

Figure 3: Sketch of a halfcell diffusion test (from [DRI14])

After a certain diffusion time, concentration profiles of lithium within the samples are measured by elemental mapping (Laser Induced Breakdown Spectroscopy technique, LIBS). Diffusion profile of Li ions are ajusted by the analytical solution of a 1D problem in a semi-infinite environment [CRA75] and lithium effective diffusion coefficients are then calculed by inverse analysis. Figure 4 summarizes the results obtained for different S_w values.

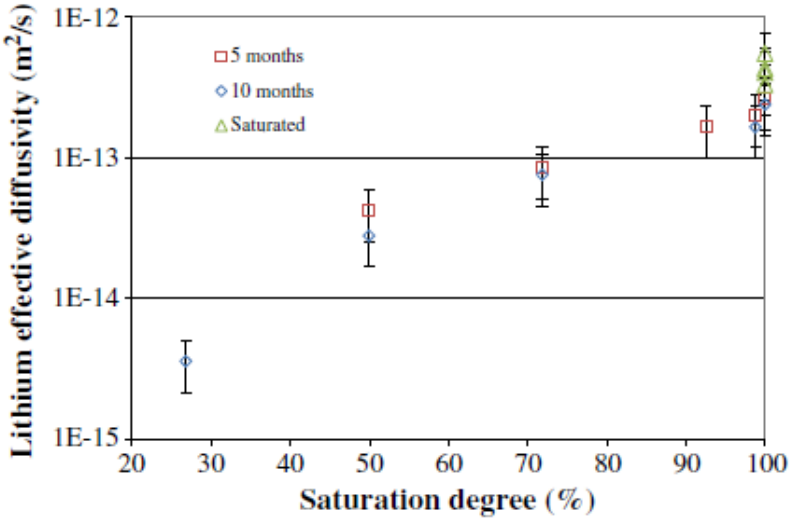

Figure 4: Evolution of the effective diffusion coefficient *vs* water saturation in a CEM I paste with W/C = 0.4 (from [DRI14])

The authors interpret the drop of D_e(Li) values for S_w values ranged between 0.3 and 0.5 as the disappearance of connected liquid phase in the capillary pores as well as in hydrates. This confirms previous interpretation [BOU13].

Bourbon reports a comparison between CEM I and CEM V concretes based on impedance spectroscopy data (figure 5) [BOU13, MER12]. For CEM I concrete, the results show that, at high water saturation ($S_w > 0.75$), the decrease of D_e values is very limited but becomes more important for $S_w < 0.75$ while for CEM V concrete, the D_e values are continuously decreasing on the all range of S_w values. Below 0.75, the two materials seem to follow the same trend. These different behaviours have been interpreted as due to the difference in the microstructure of the materials. The evolution of D_e value at high saturation in CEM I material, is due to the presence of capillary pores which are progressively drained while those pores being absent in CEM V material, smaller pores (from hydrates) are drained. Below 0.75 (S_w), in both material, the same type of porosity (from hydrates) is concerned by the draining process.

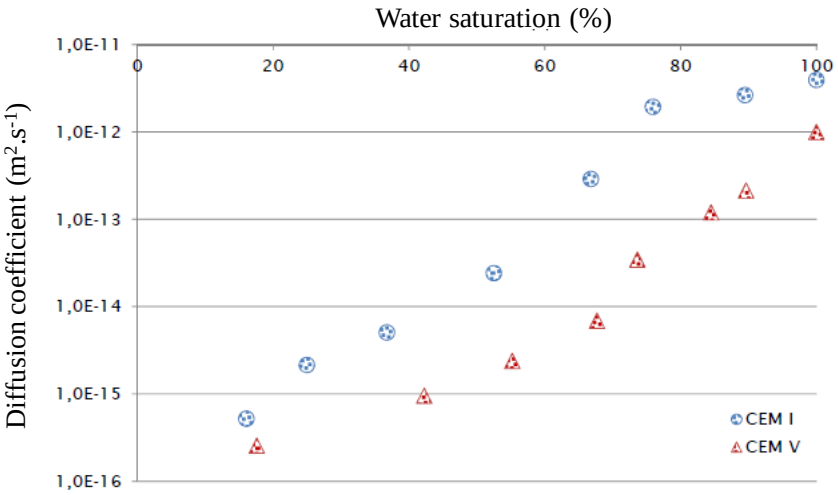

Figure 5: Evolution of diffusion coefficient *vs* water saturation for CEM and CEM V concretes

From the experimental point of view, Dridi and Lacour have reported several technical difficulties (*eg*: contact between the two samples) which can easily have impact on the results. They have even proposed some important changes in the set-up (removal of the diffusion cell and use of a desiccator with constant RH). This means that even if this experimental set-up seems to be very attractive for acquiring data in unsaturated conditions, its realization appears to be touchy and has never been used for radioactive tracers.

Due to these experimental difficulties, we have chosen to test, in this project, another experimental set-up for acquiring aqueous diffusion coefficient at high S_w value. This new experimental set-up is based on Savoye *et al* work dedicated to the study of diffusion of radioactive tracers through unsaturated argillite clay stone [SAV10]. In this study, the diffusion parameters are determined using modified through-diffusion cells in which the water saturation of samples is generated by the osmosis process. In fact, osmosis allows for the control of the water suction in a sample while maintaining contact with a chemical solution. This technique which is used by soil scientist and geotechnical engineering is an alternative to the classical supersaturated salt solution technique [ZUR66, DEL98]. The suction is then generated by an osmosis process between the pore water and a highly concentrated solution of polymer (polyethylene glycol, PEG). The clay sample is separated from the PEG-solution by a semi-permeable membrane, which is permeable to all dissolved species except PEG. The exclusion of

the PEG from the clay sample results in a chemical-potential imbalance between the porewater and the water in the reservoirs chambers of the diffusion cell. This osmotic suction has the effect of keeping the clay sample unsaturated. The value of the imposed suction depends on PEG concentration in solution. Delage *et al* reported the evolution of the suction *vs* PEG concentration (Figure 6). All data under 4 MPa fit the following parabolic

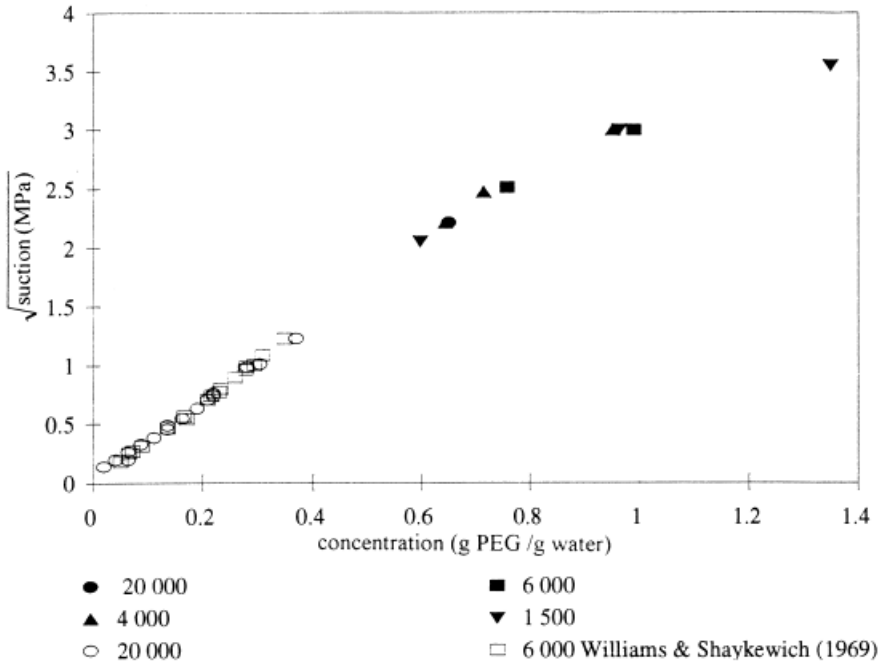

Figure 6: Evolution of the suction *vs* PEG concentration with various molar mass (from [DEL98])

relation between the suction (in MPa) and the concentration of PEG (g of PEG/g of water)

$$\Psi = 11 \times [PEG]^2 \quad (9)$$

Above 4 MPa, suction values are lower than those expected from equation (9). Nevertheless, suctions up to about 10 MPa can be reached by using very highly concentration PEG solution (> 1g of PEG/g of water). Previous geomechanical studies on Callovo-Oxfordian clay stone showed that suctions up to 10 MPa lead to a water saturation of about 80%. It is clear that the relation between suction and water saturation strongly depends on the nature of the material and more precisely on the microstructural properties (porosity, geometry of the pore network, permeability,…). The application of this technique to cement pastes will need first to definite such a relationship for these materials.

A schematic view of the modified through-diffusion cell used for the diffusion experiments is given in Figure 7.

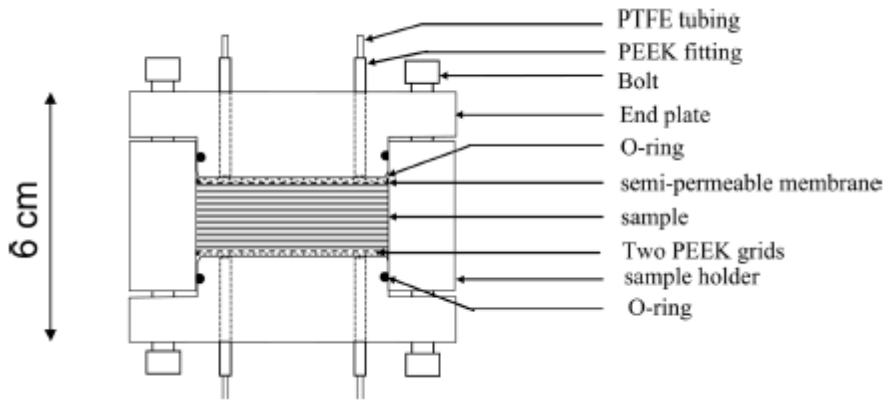

Figure 7: Schematic cross-section of a modified through-diffusion cell (from [SAY10])

The cut-off of the membrane has to be adapted with the molar mass of PEG molecule. For example, with PEG (6 kDa), a membrane with a cut-off of 3.5 kDa has been used. With this set-up, Savoye *et al* succeeded in measuring effective diffusion coefficients of molecular (HTO) and ionic radionuclides (Na^+, Cs^+, Sr^{2+} and I^-) for water saturation ranged from 0.8 to 1 in unsaturated clay stone samples [SAV12].

For application to cement pastes, the resistance of the semi-permeable membrane to highly alkaline solution will have to be tested.

In conclusion, literature review shows that the osmosis technique is probably the easiest technique which can be adapted for the measurement of diffusion parameters of radionuclides in unsaturated conditions. Nevertheless, preliminary specific studies have to be done before performing experiments with cement pastes (checking the Ψ = f[PEG] relationship, testing the resistance of the membrane to high alkaline solutions,..).

GASEOUS DIFFUSION

The paragraph deals with the diffusion of gas molecule (in air) contained in the pore of an unsaturated porous media. Two diffusion mechanisms have then to be considered [SE07, BOU13]:

- Molecular (or ordinary) diffusion) occurs predominantly when molecule-molecule collisions dominate over molecule-pore wall collisions. The molecule of different species move under the influence of concentration gradients and the diffusive transfer follows the Fick law.
- Knudsen (or free-molecule) diffusion occurs predominantly when molecule-molecule collisions can be ignored compared to molecule-pore wall collisions. The molecule of different species move entirely independently from each other.

The prevalence of ordinary of Knudsen diffusion depends firstly on the mean free path of the gas molecule (approximately 100 nm for a gas molecule at atmospheric pressure and T = 293K) depending itself on global parameters (total pressure, temperature, nature of the gas)as and secondly, on the geometry of the porous media (pores size, degree of connectivity of the unsaturated pores). As the pore sizes in cement pastes are widely distributed from nm to mm scale, it is difficult a priori to state which is the relevant mechanism for a given paste.

Experimental set-ups designed for studying gas diffusion in cement paste as a function of water saturation are scarce and experiments are performed with hydrogen or inert gas (helium or xenon). For these light gases (H_2 or He), the effective diffusion coefficient value is around 7.10^{-7} $m^2.s^{-1}$. Classically, it consists on a diffusion cell, vacuum pumps, pressure sensors, gas flow lines and a gas chromatography system. As an example, the set-up used by Sercombe et al is showed Figure 8.

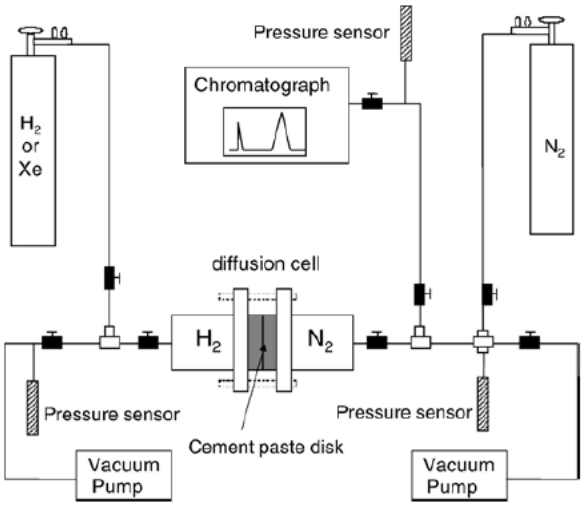

Figure 8: Sketch of the experimental gas diffusion set-up (from [SER07])

To our knowledge, no use of gas diffusion of set-up has been already reported for radioactive gas experiment.

For CEM I paste, the evolution of effective diffusion coefficient *vs* water saturation is reported in figure 9 [BOU13].

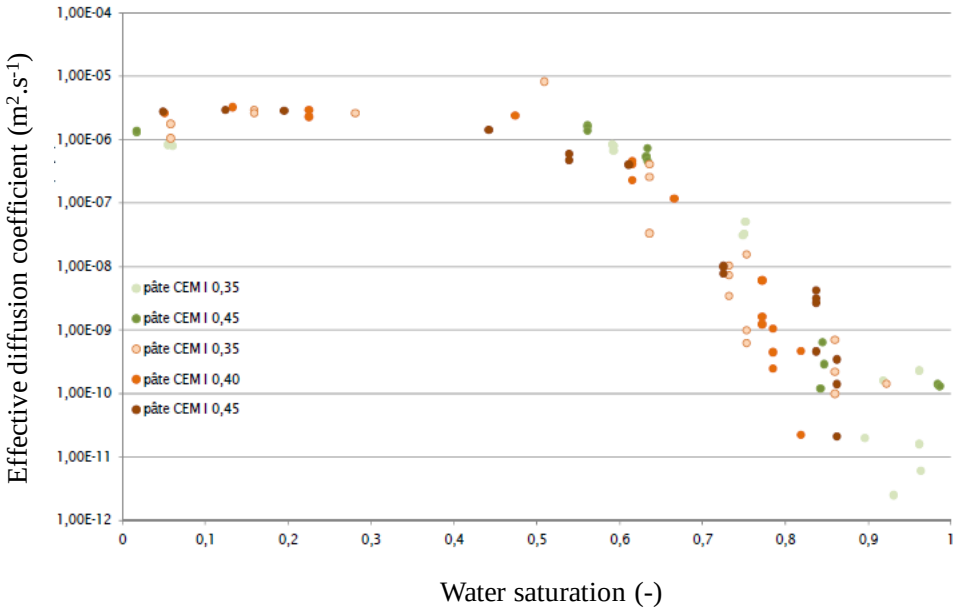

Figure 9: Evolution of effective diffusion coefficient *vs* water saturation for CEM I pastes at different W/C ratio (from [BOU13])

For S_w < 0.4, D_e(He) values are constant at 10^{-6} $m^2.s^{-1}$. The interpretation is that the continuity of the gaseous phase is such that even great variations of water saturation have no impact on the diffusion. For 0.4 < S_w < 0.75, D_e(He) values decrease linearly of almost four orders of magnitude (D_e(He) = 5. 10^{-10} $m^2.s^{-1}$) and do not depend on W/C ratios. This linear drop is interpreted as the progressive closure of the percolation path due to the filling of the porosity by water and then the apparition of a continuous aqueous phase which prevents the progression of gas in the porosity. For S_w> 0.75, the dispersion of experimental is such that is not really to give a trend.

These results have been macroscopically modelled with a simplified formalism taking into account the microstructure of the cement paste and the water saturation [BOU13]. The relationship is the following:

$$De = \frac{De^{\circ}}{p^b}(1 - S_w)^a$$

(

with

p : total porosity (-) with p= 0.35±0,05
D_e^0: He diffusion coefficient at dry state with D_e^0 = (3.0±1.5)10^{-6} $m^2.s^{-1}$
S_w : water saturation (-)

The best fit of the experimental data has been obtained with a = 5.25±1.25 and b =2 and it' reported figure 8.

$$De = \frac{De^{\circ}}{p^b}(1 - S_w)^a$$

(

with
p : total porosity (-) with p= 0.35±0,05
D_e^0: He diffusion coefficient at dry state with D_e^0 = (3.0±1.5)10^{-6} $m^2.s^{-1}$
S_w : water saturation (-)

The best fit of the experimental data has been obtained with a = 5.25±1.25 and b =2 and it' reported figure 10.

The same fitting approach can be done with data acquired on CEM V based material with the following parameters
p : total porosity (-) with p= 0.35±0,05
D_e^0: He diffusion coefficient at dry state with D_e^0 = (1.1±0.5)10^{-7} $m^2.s^{-1}$
S_w : water saturation (-)

The best fit of the experimental data has been obtained with a = 3.1±1.0 and b =1.67 (figure 11).

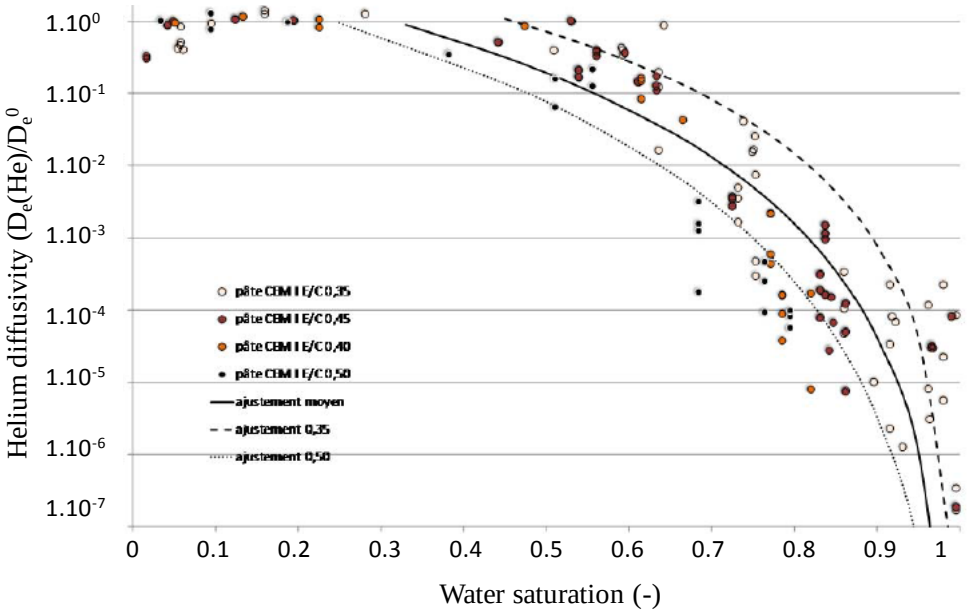

Figure 10: Fit of Helium diffusivity (D_e/D_e^0) *vs* water saturation for CEM I paste with various W/C ratio

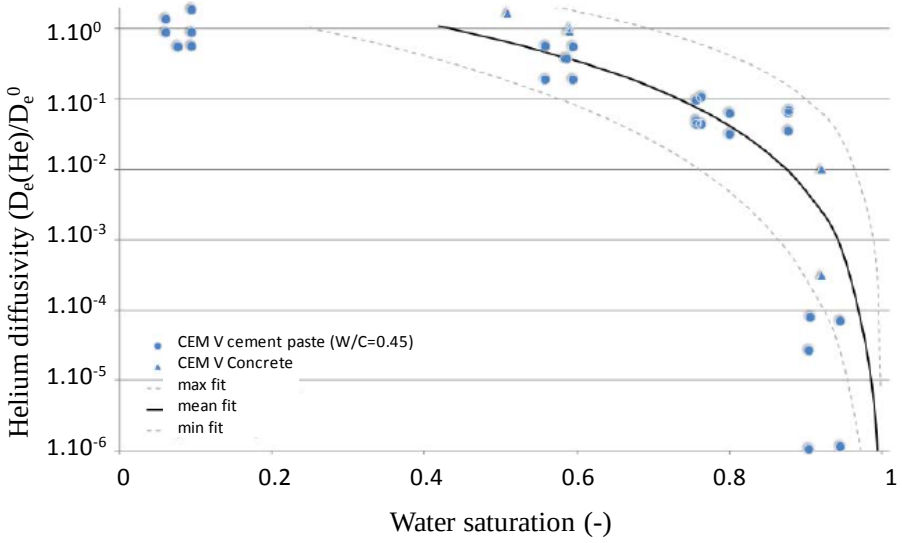

Figure 11: Fit of Helium diffusivity (D_e/D_e^0) *vs* water saturation for a CEM V paste (W/C =0.45) and CEM V concrete

In this type of material (CEMV), the presence of a very dense porosity due to the hydrates smoothes the difference between paste and concrete samples. Moreover, Sercombe *et al* have compared hydrogen diffusion coefficient data obtained for CEM I and CEM V pastes (figure 12). The behaviour of CEM V paste is different from this of CEM I sample. First, the hydrogen diffusion coefficient, for S_w values ranges from 0.1 to 0.6 is one order of magnitude lower than this of CEM I paste ($D_e(H)$ = 2 to 8 10^{-8} $m^2.s^{-1}$). Second, the evolution of the diffusion coefficient *vs* water saturation shows two steps:

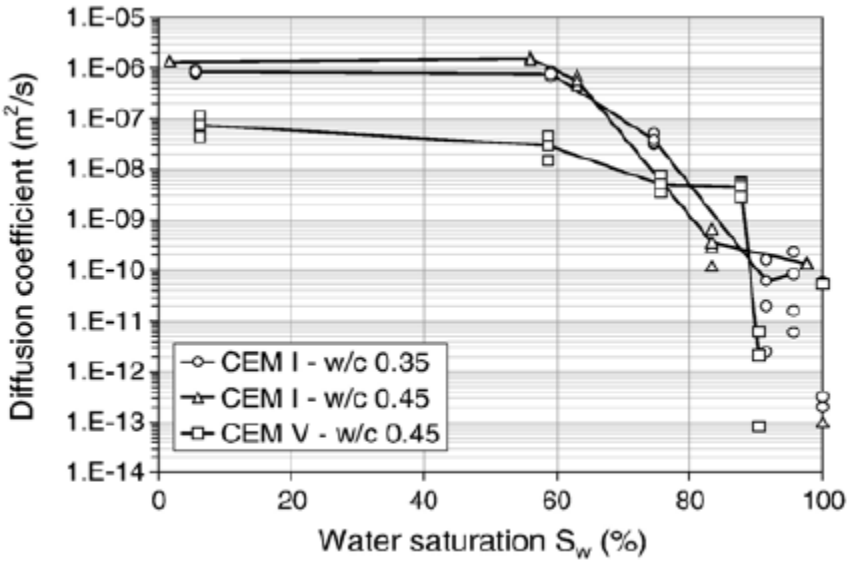

Figure 12: Hydrogen diffusion coefficient vs water saturation for CEM I (W/C=0.35 and 0.45) and CEM V (W/C=0.45) cement paste

For $0.6<S_w<0.85$, a very slow decrease (by one order of magnitude), then for $S_w>0.85$, a sharp decrease (three orders of magnitude) is registered. This sharp decrease of the diffusion coefficient indicates a discontinuity (like a percolation threshold) of the capillary pore system in the CEM V cement paste. It shows that above a given saturation (here 0.9), the pore network of the CEM V paste accessible to gas species becomes highly discontinuous. This beviour is not observed on CEM I paste which presents a continuous evolution of the diffusion coefficient in the same range of S_w. This difference probably originates from a more uniform pore size distribution in CEM V paste, centered on smaller pore diameters. The diffusion threshold would then be related to the saturation of an important fraction of pores of similar diameter. The wider pore size distribution in CEM I paste lead to a smoother evolution of the diffusion coefficient since the saturation (or desaturation) of the porosity occurs progressively [SER07].

CONCLUSION

Unsaturated conditions will prevail in surface and/or underground waste disposal for a very long period of time (100 000 years) due to the interaction of materials with atmospheric condition during the operation phase or to the release of gas from wastes during the post-closure phase. Cement materials which are used for several purposes in a storage (engineered barriers, matrix for IL-LL wastes,…) will then be affected. Due to its relatively long half life, carbon-14 is a radionuclide of interest for studying the long-term behaviour of a repository. It is now well established that carbon-14 can be released from wastes with a complex speciation (organic or inorganic, dissolved or gaseous species). As inorganic carbon species ($^{14}CO_2$ and its bases) is very reactive in saturated cementitious environment. Nevertheless, in unsaturated conditions, the presence of two phases (gas/solution interface) in the pore network may have an impact of the diffusive properties of carbon-14.

This rapid overview shows that if some (scarce) studies describe the diffusion properties of gas in unsaturated cement materials as a function of water saturation, none is related to CO_2. Moreover, due to its strong reactivity in cement pore water, carbonate ions are not studied as a potentially diffusive species. In conclusion, as far as we know, no data is available on the diffusive properties of carbon-14 in unsaturated cement materials.

From the experimental point of view, only few experimental set-ups are available for studying the diffusive parameters of radionuclides (or tracers) under unsaturated conditions. Depending on water saturation (S_w), either a modified through-diffusion set-up (high Sw >0.8) [SAV10] or a more classical gas diffusion set-up (intermediate Sw, 0.5-07) [SER07] will be then tested in our project.

REFERENCES

[ALL84] B. Allard, L. Eliasson, S. Hoglund, K. Anderson, Sorption of Cs I and actinides in concrete systems, 1984, SKB Technical report 84-15, Stockholm, Sweden

[AND05] Dossier 2005 Argile – tome Evolution phénoménologique du stockage géologique, juin 2005, www.andra.fr (site accessed 15 april 2016)

[AND14] Programme détaillé du Groupement Laboratoires 'Comportement chimique et transfert dans des environnements / ouvrages insaturés', rapport DRD Z.NT.ASTR.14.0017.A, juin 2014

[AUR15] M. Auroy, Impact of the carbonation on the water transport properties in cementitous material, PhD thesis, may 2015, Paris Est University

[BAR04] B. Bary, A. Sellier, Coupled moisture-carbon dioxide –calcium transfer model for carbonation of concrete, 2004, Cem. Concr. Res, 34, 1859-1872

[BAY88] S. Bayliss, F.T. Ewart, R.M. Howse, J.L. Smith-Briggs, H.P. Thomason, H.A. Willmott, 1988, The solubility and sorption of lead-210 and carbon-14 in a near-field environment, Material Research Society Symposium Proceedings 35-42

[BEN91] D.P Bentz, E.J. Garboczi, P.E. Stutzman, Computer modeling of the interfacial zone in concrete, 1992, RILEM Proceedin: Interfaces in cementitious composites, Ed J.C Maso, 18, 107-116

[BOR10] P.H.R. Borges, J.O. Costa, N.B. Milestone, C.J. Lynsdale, R.E. Streatfield (2010) Carbonation of CH and C–S–H in composite cement pastes containing high amounts of BFS. Cem. Concr. Res., 40, 284-292.

[BOU13] X. Bourbon, Référentiel des matériaux d'un stockage de déchets de haute activité et de moyenne activité à vie longue – Tome 2 : les matériaux cimentaires, rapport Andra CG.RP.ASCM.12.0014, février 2013

[BRA95] M.Bradbury and F.A. Sarott, Sorption databases for the cementious near-field of L/ILW repository for performance assessment, 1995, PSI report 95-06, Paul Scherrer Institut, Villigen, Switzerland

[CAS15] N. Toulhoat, E. Narkunas, B. Zlobenko, D. Diaconu, L. Petit, S. Schumacher, S. Catherin, M. Capone, W.von Lensa, G. Piña, S. Williams, J. Fachinger, S. Norris, Carbon-14 Source Term (CAST) project, 2015, Work Package 5, Review of Current Understanding of Inventory and Release of C14 from Irradiated Graphite (D5.5)

[CAR13] B. Grambow, S. Norris, L. Petit, L. Petit, V. Blin, J. Comte, E. de Visser-Tynova, CARBOWASTE Project, 2013, Work Package 6, Disposal Behaviour of Irradiated Graphite & Carbonaceous Wastes -Final Report

[COW92] J. Cowie, F.P. Glasser, The reaction between cement and natural waters containing dissolved carbon dioxide, Advances inCement Research, 4, (1992) 119-134

[CRA75] J. Crank, The Mathematics of diffusion, Oxford Univ. Press

[DEL98] P. Delage, M. D. Howat, Y.J. Cui, The relationship between suction and swelling properties in a heavily compacted unsaturated clay, Eng. Geol, 1998, 50, 31-48

[DRO10] E. Drouet, Impact of temperature on the carbonation process of hardened cement paste, PhD nov 2010, Ecole Normale Supérieure de Cachan

[GRO90] G.W. Groves, D.I. Rodway, I.G. Richardson, The carbonation of hardened cement pastes, Advances in Cement Research, 3, (1990), 117-125

[HOU94] Y.F.Houst, F.H. Wittmann, Influence of porosity and water content on the diffusivity of CO_2 and O_2 through hardened cement paste, Cement and Concrete Research, 24 (1994) 1165-1176

[MER12] H. Mercado, S. Lorente, X. Bourbon, Chloride diffusion coefficient: a comparaison between impedance spectroscopy and electrokinetic test, 2012, Cem. Concr. Compos, 34, 68-75

[PAP91] V.G. Papadakis, C.G. Vayenas, M.G. Fardis, Fundamental modeling and experimental investigation of concrete carbonation, 1991, ACI Mater. J. 83, 363-373

[POI02] I. Pointeau, N. Coreau, P. Reiller, C-14 carbonate uptake by limestone in concrete buffer environments, Nagra Workshop, september 2003

[POW58] T.C. Powers, Structure and physical properties of hardened cement paste, 1958, J. Am. Ceram. Soc. 41, 1-6

[SAV10] S. Savoye, J. Page, C. Puente, C. Imbert, D. Coelho, New experimental approach for studying diffusion through an intact and unsaturated medium: a case study with Callovo-Oxfordian argillite, Environ. Sci. Tech, 2010, 44, 3608-3704

[SAV12] S. Savoye, C. Beaucaire, A. Fayette, M. Herbette, D. Coelho, Mobility of Cesium through the Callovo-Oxfordian claystones under partially saturated conditions, Environ. Sci. Tech, 2012, 46, 2633-2641

[SER07] J. Sercombe, R. Vidal, C. Gallé, F. Adenot Experimental study of gas diffusion in cement paste, Cement and Concrete Research, 37 (2007), 579-588

[SUZ85] K. Suzuki, T. Nishikawa, S. Ito, Formation and carbonatation of C-S-H in water, Cement and Concrete Research, 15 (1985) 213-224

[THI05] M. Thiery,Modelling of the atmospheric carbonation process in cement material : influence of kinetic effects and microstructural and hydric changes, PhD thesis, september 2005, Ecole Nationale des Ponts et Chaussées

[TIT03] J. Tits, A. Jakob, E. Wieland, P. Spieler, Diffusion of tritiated water and $^{22}Na^{+}$ through non-degraded hardened cement pastes, 2003, Journal of contaminant Hydrology, 61, 45-62

[VER58] G. Verbeck, Carbonation of hydrated Portland cement, ASTM Special Publication, 205, (1958) 17-36

[WIE15] E. Wieland and W. Hummel, Formation and stability of ^{14}C-containing organic compounds in alkaline iron-water systems: preliminary assessment based on a literature survey and thermodynamic modeling, 2015, Mineralogical Magazine, DOI: 10.1180/minmag.2015.079.6.0

[ZUR66] B. Zur, Osmotic control the matrix soil water potential, Soil Sci., 1966, 102, 394-398